INFORMATION TO USERS

The most advanced technology has been used to photograph and reproduce this manuscript from the microfilm master. UMI films the original text directly from the copy submitted. Thus, some dissertation copies are in typewriter face, while others may be from a computer printer.

In the unlikely event that the author did not send UMI a complete manuscript and there are missing pages, these will be noted. Also, if unauthorized copyrighted material had to be removed, a note will indicate the deletion.

Oversize materials (e.g., maps, drawings, charts) are reproduced by sectioning the original, beginning at the upper left-hand corner and continuing from left to right in equal sections with small overlaps. Each oversize page is available as one exposure on a standard 35 mm slide or as a 17" × 23" black and white photographic print for an additional charge.

Photographs included in the original manuscript have been reproduced xerographically in this copy. 35 mm slides or 6" × 9" black and white photographic prints are available for any photographs or illustrations appearing in this copy for an additional charge. Contact UMI directly to order.

Accessing the World's Information since 1938

300 North Zeeb Road, Ann Arbor, MI 48106-1346 USA

Order Number 8821065

Studies in covariant soliton dynamics

Bannur, Vishnu Mayya, Ph.D.

City University of New York, 1988

U·M·I
300 N. Zeeb Rd.
Ann Arbor, MI 48106

STUDIES IN COVARIANT SOLITON DYNAMICS

by

VISHNU MAYYA BANNUR

A dissertation submitted to the Graduate Faculty in Physics in partial fulfillment of the requirements for the degree of Doctor of Philosophy, The City University of New York.

1988

This manuscript has been read and accepted for the Graduate Faculty in Physics in satisfaction of the dissertation requirement for the degree of Doctor of Philosophy.

Date	Chair of Examining Committee
April 14, 1988	
Date	Executive Officer

C.M. Shakin

L.S. Celenza

H. Lancman

M.K. Liou

M. Lax

Supervisory Committee

The City University of New York

Abstract

STUDIES IN COVARIANT SOLITON DYNAMICS

by

Vishnu Mayya Bannur

Adviser: Distinguished Professor Carl M. Shakin

We have studied various mesons: ρ, ρ', ω, φ, φ', charmonium and bottomonium, using covariant soliton dynamics. Both baryons and mesons are described as a nontopological solitons in this model, which is a simple, unified, covariant model for the description of the structure of all hadrons. The model describes quarks coupled to a scalar field, which plays the role of an order parameter of the QCD vacuum.

We develop an effective Lagrangian for low-momentum QCD. Various parameters of the model can be related to the dynamics of the gluon condensate. We find that flavor-dependent current quark masses and coupling constants are among the few parameters required to explain all energy levels below the open-flavor threshold. (There are also some high-momentum cutoffs needed in this formalism.)

In order to explain the energy levels above the open-flavor threshold, we have included a covariant model of confinement through the use of a phenomenological form for the quark self-energy. This form results in a quark propagator which has no on-mass-shell poles.

[The various spectra we obtained in this extended model are in good agreement with the experimental data.] Recently, we have considered a self-consistent approximation for the self-energy of a quark in the presence of a gluon condensate. We found chiral symmetry breaking and the absence of a fermion pole in the quark propagator. In fact, the self-energy we calculated is in very good agreement with the phenomenological form we had used previously.

We have also studied the wave functions of various mesons. Leptonic widths and radiative transition rates were calculated in a covariant formulation using these wave functions. We have also included "one-gluon-exchange" effects and generally satisfactory results were obtained for decay widths.

Thus far, we have kept one constituent on mass shell, as an approximation. Recently, we have developed a formalism where this approximation is avoided; we have also included a model of confinement in this new formalism. These developments lead to coupled nonlinear equations in two variables. Numerical analysis is underway.

Acknowledgements

To Professor Carl M. Shakin, my thesis advisor, I wish to express my deepest gratitude for his valuable guidance and constant encouragement throughout this thesis work.

I would also like to express my special gratitude to Professor Louis S. Celenza of Brooklyn College of CUNY for the help given to me during the course of this work.

I would also like to express my sincere thanks to Dr. Ramesh Babu Thayyullathil for his help in computer programming and for explaining his work in covariant soliton dynamics.

I would like to express another special thanks to Professor Shakin and Mrs. Shakin for providing 'Math Text' software and for printing this thesis on their laser printer.

I wish to acknowledge with gratitude the Department of Physics of Brooklyn College and the Research Foundation of CUNY for financial support during the course of this work, and the CUNY Computer Center for allowing me to use their facilities.

CONTENTS

List of Tables

List of Figures

Glossary

B-S equation. The Bathe-Salpeter equation is a relativistic equation describing two-particle dynamics.

Center-of-gravity (C.O.G). Spin-weighted average of energy levels having similar radial wave functions but different total spin.

Channel-coupling effect. Above the open-flavor threshold states of charmonium or bottomonium can decay into two open-flavor mesons. (This process can influence the calculation of meson spectra.)

Constituent quark mass. The mass parameter which appears in potential models of hadron structure is called the constituent quark mass. (For example, for up and down quarks the constituent mass is approximately equal to one-third of the proton mass.)

Current quark mass. This quantity is the flavor-dependent quark mass which appears in the Lagrangian of quantum chromodynamics.

EMC. European Muon Collaboration - an experimental group which studies the interaction of high-energy muons with matter.

Flux-tube model. A model of hadron structure in which the quarks or quarks and antiquarks are connected by tubes of chromoelectric flux.

GSI. Gesellshaft für Schwerionenforschung - an accelerator facility in Darmstadt, Federal Republic of Germany.

N_c. The number of colors in a gauge theory. (For QCD, we have $N_c=3$.)

QCD. Quantum chromodynamics - the gauge theory of strong interaction based on the SU(3) color group.

QED. Quantum electrodynamics - the quantum theory of the electromagnetic interaction.

Running coupling constant. In a gauge theory the coupling constant depends upon the renormalization scale (or the momentum scale) leading to the designation of a "running" coupling constant, $g(\mu^2)$ or $g(Q^2)$.

Standard model. The theory of strong interactions (quantum chromodynamics) taken together with the electroweak theory of Glashow, Weinberg and Salam is called the standard model [60].

CHAPTER 1

General Survey

1.1 Introduction :

The standard model, which encompasses electroweak theory and quantum chromodynamics (QCD), is now believed to be the fundamental theory in the low-energy regime (<1 TeV). Even though many aspects of electroweak theory, such as mass parameters and fields related to gauge symmetry breaking (Higgs fields) are unexplained, many predictions of the standard model have been experimentally verified. It is believed that the understanding of mass parameters and the Higgs fields will require a more fundamental theory than the standard model.

QCD is the theory of strong interaction. Current quark masses are parameters of the theory. (Current quark masses are related to a more comprehensive theory than QCD, as noted above.) There is also a parameter Λ which sets a scale for the running coupling constant. From the analysis of deep-inelastic lepton scattering one obtains a value of Λ which lies somewhere between 100 MeV and 500 MeV.

In principle, it should be possible to explain hadron spectroscopy using QCD. However, related to the non-Abelian nature of the theory,

the coupling constant becomes strong (>1) at the energy scale associated with hadron structure. Thus one cannot use perturbation theory in the study of the structure of hadrons. One can also question the use of perturbation theory in situations involving confined particles. For example, quarks and gluons are confined objects. They do not have asymptotic states. The existence of such asymptotic states is necessary to construct the rules for perturbation theory. (A similar situation might arise in QED in the strong coupling limit. For example, it has been conjectured that recently observed $e^+ e^-$ peaks in GSI experiments are believed to represent phenomena associated with a new confined phase of strong coupling QED [1]. If that is indeed the case, ordinary perturbative methods of analysis are not useful.)

There are methods, such as lattice simulations [2] of QCD and QCD sum-rule studies [3, 4], which are nonperturbative in character. Lattice simulations involve a great deal of computer time and there are other limitations as well. In lattice simulations, there are problems associated with putting fermions on the lattice and also with taking the lattice spacing to zero (the continuum limit). QCD sum-rule studies tell us little about confinement and applications are limited to only certain low-lying states of hadrons.

A large number of studies of hadron structure are based on

phenomenological models. There are two main categories : (1) potential models [5-8], (2) field-theoretic models [9-11].

1.2 Potential Models :

These are very simple models, either motivated by QCD or inspired by experimental facts. The methods of analysis used are similar to those used in atomic physics, where one uses either nonrelativistic or relativistic quantum mechanics. Let us note some of the potentials which have been extensively discussed in the literature.

(a) Cornell potential [12] : The potential is

$$V(r) = -\frac{4}{3}\frac{\alpha_s}{r} + kr \ , \qquad (1.2.1)$$

where α_s and k are the strong coupling constant and spring constant, respectively. This potential is motivated by the fact that the theory of strong interactions (QCD) has asymptotic freedom at small distances and confinement at large distances. Here distance means the separation between the quarks, r. At small r "one-gluon-exchange" is dominant and is represented by the first Coulombic term. For large r, according to the flux tube model (or the string model), the potential increases linearly and hence the second term. This form is also obtained in lattice calculations, in the quenched approximation, for heavy quarks [13, 14]. The constants α_s, k and the so called "constituent quark

masses" are fixed by fitting experimental data. One then predicts other properties.

(b) Martin's (or power law) potential [15] :

$$V(r) = A \left[\frac{r}{1\ GeV^{-1}}\right]^{\nu} + B \ , \qquad (1.2.2)$$

where A, ν and B are constants. This model is inspired by experimental facts. For example, the energy-level spacing between radially excited levels is the same in charmonium and bottomonium. This can be easily explained using a power-law potential or a logarithmic potential. The parameters and constituent quark masses are fixed by fitting experimental data. The best fit was obtained for the parameters A = 5.82 GeV , B = -6.377 GeV and ν = 0.104 .

(c) Quigg-Rosner (logarithmic) potential [7] :

$$V(r) = C \ln(r/r_0) \ , \qquad (1.2.3)$$

where C and r_0 are constants, to be fit from experimental data. The best fit was obtained for the parameters C = 0.71 GeV, r_0= 0.89 GeV^{-1}.

(d) Richardson potential [16] : This is another form of the Cornell potential but with a running coupling constant :

$$V(r) = \int \frac{d^3Q\ e^{i\vec{Q}\cdot\vec{r}}}{(2\pi)^3}\left(-\frac{4}{3}\right)\frac{12\pi}{(33-2n_f)\vec{Q}^2\ln\left(\frac{\vec{Q}^2}{\Lambda^2}+1\right)}. \quad (1.2.4)$$

This potential has only one parameter, Λ. To see its connection to Cornell potential, let us take the limiting cases of $\vec{Q}^2\to\infty$ and $\vec{Q}^2\to 0$.

As $\vec{Q}^2 \to \infty$,

$$V(\vec{Q}^2) \to -\frac{4}{3}\frac{12\pi}{(33-2n_f)\vec{Q}^2\ln\left(\frac{\vec{Q}^2}{\Lambda^2}\right)} = -\frac{4}{3}\frac{\alpha_s(\vec{Q}^2)}{\vec{Q}^2}. \quad (1.2.5)$$

This represents a Coulomb potential with "running" α_s.

As $\vec{Q}^2 \to 0$,

$$V(\vec{Q}^2) \to -\frac{4}{3}\ \frac{12\pi\ (-\Lambda^2)}{(33-2n_f)\vec{Q}^4}\ , \quad (1.2.6)$$

which is a linear confining potential.

Buchmüller and Tye [17] introduced a model which is numerically equivalent to the Richardson potential. They made use of the β function of QCD, which is related to the running coupling constant, with two-loop corrections. The parameters are the Regge slope α' (α'=1 GeV^{-2}) and the QCD scale parameter, Λ ($\Lambda_{\overline{MS}}$ =0.5 GeV). These parameters are related in the model. (The Regge slope is the slope of Regge trajectory, which is a straight line obtained by plotting spin versus

the squared mass of light mesons.)

(e) Relativistic potential models [18-20] : The potential models we discussed before are all non-relativistic and are applicable only to non-relativistic systems such as charmonium, bottomonium and toponium. For charmonium,

$$\left\langle \frac{p^2}{m^2} \right\rangle \approx O\left(\frac{\Delta M}{M}\right) \approx \frac{0.6}{3.0} = 0.2 \ ,$$

and for bottomonium

$$\left\langle \frac{p^2}{m^2} \right\rangle \approx \frac{0.6}{9.0} \approx 0.07 \ .$$

However, in order to explain fine and hyperfine spin splittings, one must use relativistic models. Alternatively, one can add spin-spin potentials, spin-orbit potentials, tensor potentials, and other relativistic corrections, to nonrelativistic models as perturbations. The general form of relativistic corrections is

$$V_{rel}(r) = V_{SI}(r) + V_{SD}(r) \qquad (1.2.7)$$

where SI denotes spin-independent and SD denotes spin-dependent. The general form for $V_{SD}(r)$ is

$$V_{SD}(r) = \left(\frac{\vec{S}_1 . \vec{L}}{2m_1^2} + \frac{\vec{S}_2 . \vec{L}}{2m_2^2} \right) \frac{1}{r} \left(\frac{d\epsilon(r)}{dr} + \frac{dV_1(r)}{dr} \right)$$

$$+ \frac{(\vec{S}_1 + \vec{S}_2).\vec{L}}{m_1 m_2} \frac{dV_2}{rdr} + \frac{2\vec{S}_1 . \vec{S}_2}{3m_1 m_2} \nabla^2 V_2(r)$$

$$+ \frac{1}{m_1 m_2} \left(\vec{S}_1 . \hat{r}\, \vec{S}_2 . \hat{r} - \frac{1}{3} \vec{S}_1 . \vec{S}_2 \right) V_3(r) \qquad (1.2.8)$$

$$= V_{SO}(r) + V_{SS}(r) + V_T(r) \ ,$$

where m_1 and m_2 are masses of the two constituents and $V_1(r)$, $V_2(r)$ and $V_3(r)$ are functions of r. These potentials transform either as Lorentz vectors or scalars; $\epsilon(r)$ is the Cornell (or nonrelativistic) potential. These corrections are called "Breit-Fermi corrections". In principle they can be obtained from QCD. However, at present, most researchers use phenomenological potentials.

Gupta et al. made use of a perturbative potential that they derived to order α_s^2. This potential included spin-dependent terms. In addition to a phenomenological linear potential, they also added spin-orbit terms to the confining part of the potential and treated the spin-dependent term perturbatively in their analysis.

A discussion of potential models should not end without mentioning the work of Godfrey and Isgur [21]. They made an extensive study of

many meson states using a Coulomb-plus-linear potential, with all relativistic corrections and calculated many energy levels and various decay properties. Their results are in good agreement with experiment, however, their model has about 10 parameters besides the quark masses. (Six parameters are used in "smearing" functions, which are used to "smear" the singularities in Breit-Fermi term.)

There are also other potential models which are variants of the models we have mentioned.

All the models we have discussed provide a very good fit to the spectra of heavy quarkonia ($c\bar{c}$ and $b\bar{b}$ systems). The reason is that all the above potentials coincide, apart from an arbitrary constant, in the region $0.1<r<1$ fm. That is the region of r which is important in the calculation of the spectra of these systems. Therefore, from the properties of $c\bar{c}$ and $b\bar{b}$ quarkonia it is not clear whether the agreement between theory and experiment is a test of some aspects of QCD. It is hoped that the properties of t-quarkonium, whose radius is < 0.1 fm, may tell us something concerning QCD and the QCD scale Λ.

There are many questions which are unanswered in potential models. The relation of the mass parameter, the "constituent mass", to QCD is unknown. Different models use different mass parameters. For the charm quark, the choices for the constituent mass ranges from 1.1 GeV to 1.9

GeV. For the bottom quark, the range chosen is from 4.5 GeV to 5.2 GeV. Similarly, the linear potential, which is required to model confinement, is not yet strictly derived from QCD. It is mainly motivated by the flux tube model and also from lattice calculations with quarks of infinite mass [13]. We will have more to say concerning the problem of confinement in Chapter 4.

Another drawback of most of potential models is their inability to explain the spectrum, leptonic decays, radiative transitions and hadronic decays satisfactorily using the same model [12, 22]. When the parameters are adjusted so as to get the correct leptonic width, the radiative transition rates become worse and visa versa. Only the results of Godfrey and Isgur for the spectrum (and all other properties) are in good agreement with experiment. (They included an annihilation interaction term in their model, which they believe is important for light quarks. They did not include, however, the channel-coupling effect which may be important for excited states above threshold. Most of the authors of potential models believe that the channel-coupling effect is important in obtaining good results for the levels above threshold.) Gupta et al. obtained good leptonic widths below the open-flavor threshold, however, they did not calculate radiative transition rates.

1.3 Field-Theoretic Models :

There are three main categories : bag models, models based upon the Bethe-Salpeter equation and soliton models.

The MIT bag model was one of the first field-theoretic models to describe nucleons in terms of quarks. The model incorporates some aspects of asymptotic freedom and confinement. Quarks are confined inside a bag and they interact weakly. (This feature is motivated by the fact that in deep-inelastic lepton scattering leptons "see" quarks which appear to be interacting weakly.) The bag wall is a sharp confining boundary. Outward pressure on the wall due to the quarks is balanced by the pressure exerted by the vacuum on the wall. These simple assumptions are not sufficient to explain many quantitative properties of nucleons. For example, the MIT bag radius is about 1.6 fm, which is quite large compared to the generally accepted value of about 0.7 fm. Brown and Rho [23] introduced pion fields outside the bag so that the axial current, which otherwise would not be conserved at the bag wall, is carried by pions outside the bag. Existence of pions outside the bag leads to an additional pressure which reduces the size of nucleon to $\approx$ 0.5 fm in this generalized (chiral) bag model.

The bag model has not been useful in calculating the properties of hadrons containing heavy quarks or in calculating the energy levels of

excited hadron states.

The Bethe-Salpeter approach is often applied in the description of bound states in relativistic quantum field theory [24]. At present we do not know much concerning the appropriate kernel for that equation. In principle, it should be possible to derive such a kernel from QCD. However, almost all calculations use the "ladder approximation" to the exact kernel. In QCD the ladder approximation is based upon "one-gluon-exchange". The resulting potential has a spin-independent term (Coulomb) and spin-dependent terms (spin-spin, spin-orbit and tensor). One has to insert a confinement term (a linear or harmonic potential) in the B-S kernel in a somewhat arbitrary manner. One usually solves the B-S equation in the instantaneous approximation (i.e., one puts the time component of the relative momentum equal to zero and works in the c.m. frame.) The use of the B-S equation is questionable because of the strong potentials used. For example, in reference [25], it was shown that the ladder approximation (i.e., a perturbative analysis) is probably less satisfactory than the use of a nonperturbative nonlinear theory in the strong coupling regime.

It should be noted that, in our model, we work with a non-zero relative-time component. We also keep one constituent (quark or antiquark) on-mass-shell. In case both constituents are off-mass-shell, singularities in the kernels of our (nonlinear and covariant)

equations are avoided because of the special confining self-energy which appears in the most general form of our model. [These comments will be clarified in the following discussion.]

In the theory of solitons one can distinguish two types: topological and nontopological [26, 27, 9]. A form of topological soliton (skyrmion) was first studied by Skyrme in the early 60's. A renewed interest in this field began a few years ago because of the possible connection of the skyrmion to QCD in large N_c limit. Here baryons are made out of "mesons" and appear as topological solitons.

Nucleon observables calculated from skyrmion theory deviate about 20-30% from experimental values. Workers in this area believe that in order to get better results, more mesons, such as the ρ, ω, etc., should be included. They argue that, if confinement is assumed, and if N_c is large, QCD is equivalent to a meson theory in which the meson coupling constant is of order N_c^{-1}. Since in QCD $N_c = 3$, the validity of the large-N_c limit is questionable. Further, the form of the effective meson Lagrangian for QCD is not known. [Also, there is also some confusion as to whether these "mesons" are physical mesons or meson-like fields. We will discuss this question in Chapter 5.]

The nontopological soliton model was introduced by Friedberg and Lee and developed by several researchers. In this model the quark is

coupled to a scalar field. This model provides a framework for a dynamical calculation of hadron structure and hadronic processes. (If one is to have a renormalizable theory, the potential of the scalar field can have terms up to fourth order in the field.) We note that the scalar field in the Friedberg-Lee model is related to the dielectric function of the QCD vacuum. (Some researchers include one-gluon-exchange [28] in this model and treat such effects perturbatively.)

The models we have discussed above are usually solved in the static limit. One has to do lengthy calculations to restore Lorentz covariance of the description. Another important point to be noted is that potential models have been applied mainly to heavy mesons. (Even though some of potential models were applied to study the structure of light mesons, there is little theoretical justification for such calculations.) As we see in this work, the covariant soliton model provides a Lorentz covariant description, a description of confinement and of dynamical chiral symmetry breaking, as well as a symmetrical treatment of baryon and meson structure. We believe that these are quite general principles, which should be incorporated into a model of hadron structure.

1.4 Covariant Soliton Dynamics :

Inspired by the success of relativistic nuclear physics, which is largely based upon the use of the Dirac equation to describe nucleon motion, Celenza, Shakin and collaborators formulated the covariant soliton model for hadrons (both baryons and mesons) to investigate nuclear phenomena from a microscopic viewpoint [29]. They first explained many properties of the nucleon using this model. The properties of this soliton (nucleon) in nuclear matter were then considered in the study of several interesting phenomena in nuclear physics, such as the EMC effect and the quenching of the longitudinal response (seen in inclusive (e,e') reactions). There were also studies of the use of the Dirac equation to describe nucleon motion in nuclei [30, 31] from the point-of-view of covariant soliton dynamics.

The Lagrangian of the covariant soliton model appears similar to that of the Friedberg-Lee [26] nontopological soliton model, except for the fact that the potential for the scalar field is a simple, quadratic form. In the covariant soliton model the scalar field represents the deviation of an order-parameter field from its vacuum value. The interpretation of the vacuum is different in the covariant soliton model and in the Friedberg-Lee model. The physical picture of the covariant soliton model is somewhat analogous to that which appears in the theory of superconductivity, where one has an electron

condensate (Cooper pairs) characterized by a complex order parameter field. Recall that magnetic fields are expelled from the superconductor (Meissner effect). As we see in the next chapter, the QCD vacuum may contain a gluon condensate due to the self-interaction of gluons. This condensate can give rise to a chromo-electromagnetic Meissner effect. This effect, which leads to dynamical mass generation for gluons, can lead to the confinement of chromoelectric flux into flux tubes. (The order-parameter field describing this condensate must be a color singlet, scalar field.) Note that the description of various phenomena in QCD in terms of the gluon condensate is somewhat similar to the Landau-Ginzburg theory of superconductivity.

As noted above, the Friedberg-Lee and covariant soliton models differ in the physical interpretation of the vacuum. In the Friedberg-Lee model, the dielectric constant of the vacuum is taken as $\kappa = 0$. This quantity is then a function of x inside the hadron ($\kappa \rightarrow \kappa(x)$). This feature is motivated by the fact that when a source is introduced in the vacuum, the non-Abelian nature of QCD leads to antiscreening in contrast to the situation in QED (screening). When a hadron is formed, there will be less antiscreening when quarks are close and hence κ approaches 1 for zero separation. This specification of the behavior of κ in the Friedberg-Lee formalism is actually related to the perturbative analysis of QCD in the "asymptotic

freedom" regime. Nonperturbative effects such as confinement are not included in this model except through the dielectric description of the vacuum. In the dielectric formulation, the quark mass becomes infinite outside the hadron. In the covariant soliton model perturbative and nonperturbative effects are all included in a more rigorous fashion. As we see in Chapter 3, the quark dynamical mass becomes large because of confinement dynamics related to the presence of the gluon condensate. In our model, large dynamical masses are found at large separation of quarks where their momenta are timelike.

The Lagrangian of our model is,

$$\mathcal{L}(x) = \bar{q}(x)\left(i\gamma_\mu\partial^\mu - m_q\right)q(x) - g_\chi\,\bar{q}(x)\chi(x)q(x)$$
$$+ \frac{1}{2}\left(\partial_\mu\chi(x)\partial^\mu\chi(x) - m_\chi^2\,\chi^2(x)\right) \quad , \qquad (1.3.1)$$

where m_q and g_χ are the quark mass and the coupling constant respectively; $q(x)$ and $\chi(x)$ are the quark and scalar order-parameter fields, respectively. m_χ is the mass of the scalar field.

This model is very successful in describing the properties of the nucleon and of many meson states. (It may also be adapted to explain the $e^+\,e^-$ peaks seen in GSI experiments [1]. It has been suggested that the presence of strong fields (produced by heavy ions) causes a phase change from ordinary QED to confined phase of QED. As a result,

positrons and electrons become dressed "quasi-positrons" and "quasi-electrons". These quasi-particles can form hadron-like objects in the confined phase of QED and the decay of such objects can give rise to $e^+ e^-$ pairs.)

The organization of the thesis is as follows: In Chapter 2 we will discuss an effective Lagrangian for QCD. In Chapter 3 we discuss chiral symmetry breaking and confinement. The equations of the model are presented in Chapter 4. We will discuss the fully-off-shell problem in Chapter 5. Chapter 6 contains numerical results and conclusions.

CHAPTER 2

An Effective Lagrangian for QCD

In the last chapter we presented the Lagrangian of our model. Here we will discuss this Lagrangian as an effective Lagrangian for low-energy phenomena in QCD. We follow the procedures of Celenza and Shakin [32].

1.1 Description of the QCD Vacuum :

The description of the vacuum is a long-standing goal of scientists. Before the experiment of Michelson and Morley, people thought that the vacuum contained a so-called "ether". The negative result of the Michelson-Morley experiment and the development of theory of relativity led us to believe that there is no "ether" and that the vacuum is "empty". However, today researchers believe that there may be a gluon condensate and a quark condensate in the vacuum. The generally successful QCD sum-rule studies [3, 4] are based on the assumption that the vacuum contains gluon and quark condensates. The order parameters of the condensates are determined from a phenomenology which makes use of experimental data.

We will also assume that the vacuum contains a gluon condensate,

which is characterized by a vacuum order parameter ϕ. (As we pointed out in last chapter, our theory is somewhat analogous to the theory of superconductivity.) There are two types of vacuum specified in this kind of theory : the perturbative vacuum and the nonperturbative (or physical) vacuum. The former is assumed to have a higher energy density than the later. For example, let us consider the usual form chosen for the potential of an order-parameter field, ϕ:

$$V(\phi) = -a\phi^2 + b\phi^4 \ . \qquad (2.1.1)$$

This kind of potential is used in the Landau-Ginzberg theory of superconductivity [33] and in the theory of ferromagnetism near the critical temperature. It has the minimum at $\phi = 0$ for $a < 0$ and at $\phi = \phi_0 \equiv \sqrt{(a/2b)}$ for $a>0$. The perturbative vacuum has $\langle\phi\rangle = 0$; the physical vacuum is assumed to have $\langle\phi\rangle = \phi_0$. We denote the physical vacuum as $|vac\rangle$. Generally, the nonperturbative vacuum arises as a result of nonperturbative effects, and hence the name. One may, in some cases, represent a nonperturbative vacuum as a coherent state [34]. If one assigns a temperature or density dependence to the parameters 'a' and 'b', one can study the temperature and density dependence of various properties of the system. Phase transitions from the nonperturbative to the perturbative vacuum, and vice versa, can be studied. In QCD such transitions correspond to phase transitions

between confined and deconfined phases.

One essential assumption of our model is that the presence of quarks "digs a hole" in the condensate, that is $\phi_0 \to \phi(x) = \phi_0 + \chi(x)$. In this model a hadron is formed as a bubble in the condensate.

The second assumption we make is that the gluon condensate is made up of gluons with low momentum (≈ 0). We write $A^a_\mu(x) = A^a_\mu(x) + Q^a_\mu(x)$, with $A^a_\mu(x)$ the condensate field, which we assume can be treated as a semiclassical field. $Q^a_\mu(x)$ is the fluctuation field.

2.2 Equivalent Second Order Equation :

The QCD Lagrangian is

$$\mathcal{L}_{QCD}(x) = -\frac{1}{4} G^a_{\mu\nu}(x) G^{\mu\nu}_a(x) + \bar{q}(x)\left(i\not{\partial} - m^{cur}_q\right)q(x), \qquad (2.2.1)$$

where

$$i\not{\partial} = i\not{\partial} + g\frac{\lambda^a}{2}\not{A}^a$$

and

$$G^a_{\mu\nu}(x) = \partial_\mu A^a_\nu(x) - \partial_\nu A^a_\mu(x) + g f^{abc} A^b_\mu(x) A^c_\nu(x) \ .$$

Here m^{cur}_q is the current quark mass. At this point we may introduce $m^{q\bar{q}}_q = f_\pi g_\pi$, a dynamical quark mass arising from the coupling of a

quark to a "chiral condensate". Here f_π is the pion decay constant and g_π is a pion-nucleon coupling constant. This represents the original approach taken in this work with respect to chiral symmetry breaking and the generation of a mass, $m_q^{q\bar{q}}$. In Chapter 3 we will say more about chiral symmetry breaking and present a rather different and more fundamental viewpoint.

The role of the gluon condensate in modifying the equation of motion for q(x) is unclear. To exhibit that effect we use the equation of motion,

$$\left(i\not{\partial} - m_q^{cur} - m_q^{q\bar{q}}\right) q(x) = 0 \ . \qquad (2.2.2)$$

Then

$$q(x) = \frac{\left(i\not{\partial} - m_q^{q\bar{q}}\right)}{m_q^{cur}} q(x). \qquad (2.2.3)$$

We substitute the last expression back into the Lagrangian. Then we can exhibit a term, $\vec{A}^a.\vec{A}^a$, in the equation of motion for q(x). (There are other methods of exhibiting such a term, as discussed in [32], for example.) Once we express the QCD Lagrangian in terms of the condensate and fluctuating parts of $A_\mu^a(x)$, we will take the expectation value in the physical vacuum state $|vac>$. We write

$$\mathcal{L}_{QCD}(x) = -\frac{1}{4} G^a_{\mu\nu}(x) G^{\mu\nu}_a(x) + \bar{q}(x)\left(i\not{\partial} - m_q^{cur}\right)q(x)$$

$$= -\frac{1}{4} G^a_{\mu\nu}(x) G^{\mu\nu}_a(x) + \bar{q}(x)\left(i\not{\partial} + g\frac{\lambda^a}{2}\not{A}^a\right)q(x)$$

$$+ \bar{q}(x) g \frac{\lambda^a}{2} \not{\rho}^a(x) q(x) - \bar{q}(x)\left(m_q^{cur} + m_q^{q\bar{q}}\right)q(x). \qquad (2.2.4)$$

where we have, somewhat arbitrarily, introduced $m_q^{q\bar{q}}$ in the last expression. Substituting q(x) from Eq.(2.2.3) and rearranging various terms we get,

$$\mathcal{L}_{QCD}(x) = -\frac{1}{4} G^a_{\mu\nu}(x) G^{\mu\nu}_a(x) + \bar{q}(x) \frac{\left(-\partial^2 + g^2 \frac{\lambda^a \lambda^b}{4} A^a . A^b\right)}{m_q^{cur}} q(x)$$

$$+ \left(\frac{m_q^{cur} + m_q^{q\bar{q}}}{m_q^{cur}}\right) \bar{q}(x) g \frac{\lambda^a}{2} \not{\rho}^a(x) q(x) - \bar{q}(x) \frac{\left(m_q^{cur} + m_q^{q\bar{q}}\right)^2}{m_q^{cur}} q(x).$$

$$+ \bar{q}(x) g \frac{\lambda^a}{2m_q^{cur}} i\not{\partial}[\not{\rho}^a(x) q(x)] + [\ \ldots\ldots\ ], \qquad (2.2.5)$$

where $A^a_\mu(x)$ is taken to be independent of x. The symbol [.....] denotes terms which are linear in A^a and are zero if we take the vacuum expectation value of the Lagrangian. The expectation value, as developed here, will yield an operator in the space of the fluctuating fields.

We define the effective Lagrangian as

$$\mathcal{L}_{eff}(x) = \langle vac|\mathcal{L}_{QCD}(x)|vac\rangle \ . \qquad (2.2.6)$$

We also use the fact that

$$\langle vac|A^a_\mu|vac\rangle = 0,$$

$$\langle vac|\text{odd number of } A^a_\mu|vac\rangle = 0,$$

and

$$\langle vac|\text{even number of } A^a_\mu|vac\rangle \neq 0 \ . \qquad (2.2.7a)$$

We choose the temporal gauge, $A^a_0 = 0$, in our analysis and define

$$\langle vac|A^a_i\ A^b_j|vac\rangle = g^2\phi_0^2\ \frac{\delta_{ab}}{8}\ \frac{\delta_{ij}}{3} \ . \qquad (2.2.7b)$$

A description of a state, $|vac\rangle$, with the given properties in Eq.(2.2.7), is presented in [34]. There $|vac\rangle$ is constructed as a coherent state of zero-momentum gluons.

We find

$$\mathcal{L}_{eff}(x) = -\frac{1}{4}\langle vac|G^a_{\mu\nu}(x)G^{\mu\nu}_a(x)|vac\rangle + \bar{q}(x)\frac{\left(-\partial^2 - m_q^2\right)}{m_q^{cur}}q(x)$$

$$+\left(\frac{m_q^{cur}+m_q^{q\bar{q}}}{m_q^{cur}}\right)\bar{q}(x)g\frac{\lambda^a}{2}\not{Q}^a(x)q(x)$$

$$+\bar{q}(x)g\frac{\lambda^a}{2m_q^{cur}}i\not{\partial}[\not{Q}^a(x)q(x)]\ , \qquad (2.2.8)$$

where

$$m_q^2 = \left(m_q^{gl}\right)^2 + \left(m_q^{cur} + m_q^{q\bar{q}}\right)^2\ ,$$

with

$$\left(m_q^{gl}\right)^2 = \frac{1}{6}g^2\phi_0^2\ . \qquad (2.2.9)$$

To evaluate $\langle vac|G^a_{\mu\nu}(x)G^{\mu\nu}_a(x)|vac\rangle$ we expand $G^a_{\mu\nu}(x)$ as,

$$G^a_{\mu\nu}(x) = \mathbb{G}^a_{\mu\nu} + G^a_{\mu\nu}(x) + gf^{abc}\left(A^b_\mu Q^c_\nu(x) + Q^b_\mu(x)A^c_\nu\right)$$

with

$$G^a_{\mu\nu}(x) = \partial_\mu Q^a_\nu(x) - \partial_\nu Q^a_\mu(x) + gf^{abc}Q^b_\mu(x)Q^c_\nu(x)$$

and

$$\mathbb{G}^a_{\mu\nu} = gf^{abc}A^b_\mu A^c_\nu\ .$$

After some algebra,

$$\langle vac|G^a_{\mu\nu}(x)G^{\mu\nu}_a(x)|vac\rangle = -\frac{1}{4}G^a_{\mu\nu}(x)G^{\mu\nu}_a(x) + \frac{m^2_{gl}}{2}Q^a.Q_a + \left(\frac{-3\,g^2\phi_0^4}{52}\right).$$

Finally, the effective Lagrangian in the space of the fluctuating fields is,

$$\mathcal{L}_{eff}(x) = -\frac{1}{4}G^a_{\mu\nu}(x)G^{\mu\nu}_a(x) + \frac{m^2_{gl}}{2}Q^a.Q_a + V'(\phi_0) + \left(\frac{m_q^{cur} + m_q^{q\bar{q}}}{m_q^{cur}}\right)\bar{q}(x)g\frac{\lambda^a}{2}\not{Q}^a(x)q(x) + \bar{q}(x)\frac{\left(-\partial^2 - m_q^2\right)}{m_q^{cur}}q(x) + \bar{q}(x)g\frac{\lambda^a}{2m_q^{cur}}i\not{\partial}[\not{Q}^a(x)q(x)], \quad (2.2.10)$$

where

$$m^2_{gl} = \frac{1}{4}g^2\phi_0^2, \quad (2.2.11)$$

and

$$V'(\phi_0) = -\frac{3\,g^2\phi_0^4}{52}. \quad (2.2.12)$$

Thus the effect of the gluon condensate is to "dress" the gluon and the quark; these fields acquire dynamical masses. The gluon mass obtained in this procedure of Celenza and Shakin agrees with the mass obtained in lattice simulations of QCD [35-37]. (The values of various

masses we have defined will be given in the end of this chapter.)

The equation of motion for the quark is,

$$(\partial^2 + m_q^2)q(x) = 0 \ . \qquad (2.2.13)$$

Our assumption is that, when a hadron is formed, the gluon condensate is disturbed and $\phi_0 \to \phi(x) = \phi_0 + \chi(x)$. Here $\chi(x)$ represents the deviation of the order-parameter from the vacuum value. Therefore, $\chi(x)$ is zero outside the hadron. We also assume $m_q^{q\bar{q}} \to m_q^{q\bar{q}}(x) = m_q^{q\bar{q}}\left[1+ \frac{\chi(x)}{\phi_0}\right]$, for simplicity. That is, we use the same order-parameter field to describe the gluon condensate and chiral condensate. This is partly motivated by the fact that chiral symmetry restoration and deconfinement take place at the same temperature in lattice simulations of QCD. This assumption also reduces the number of parameters in the problem. We will see that this assumption is justified in a quite specific model of chiral symmetry breaking, which will be discussed in the next section.

We have, therefore,

$$m_q^2 \to m_q^2(x) = \left(m_q^{gl}(x)\right)^2 + \left(m_q^{cur} + m_q^{q\bar{q}}(x)\right)^2$$

$$= \left(m_q^{gl}\left\{1 + \frac{\chi(x)}{\phi_0}\right\}\right)^2 + \left(m_q^{cur} + m_q^{q\bar{q}}\left\{1 + \frac{\chi(x)}{\phi_0}\right\}\right)^2$$

$$= m_q^2 + 2\beta m_q g_\chi \chi(x) + g_\chi^2 \chi^2(x) \ , \qquad (2.2.14)$$

where

$$g_\chi \equiv \frac{m_q^{dyn}}{\phi_0} \ ,$$

and

$$\beta = \left(\frac{m_q^{dyn}}{m_q} + \frac{m_q^{cur}\ m_q^{q\bar{q}}}{m_q^{dyn}\ m_q} \right) \ , \qquad (2.2.15)$$

with

$$m_q^{dyn} = \sqrt{\left(m_q^{gl}\right)^2 + \left(m_q^{q\bar{q}}\right)^2} \ . \qquad (2.2.16)$$

The potential energy density for the order-parameter field also is modified to $V(\phi(x))$. The equation of motion for the quark field is then

$$[\partial^2 + m_q^2(x)]q(x) = 0,$$

or

$$[\partial^2 + m_q^2 + 2\beta m_q g_\chi \chi(x) + g_\chi^2 \chi^2(x)]q(x) = 0 \ . \qquad (2.2.17)$$

The corresponding Lagrangian is

$$\mathcal{L}'(x) = \frac{1}{m_q^{cur}}\bar{q}(x)[-\partial^2 - m_q^2(x)]q(x) + \frac{1}{2}\partial_\mu\chi(x)\partial^\mu\chi(x) - V[\phi(x)]$$

$$= \frac{1}{m_q^{cur}}\bar{q}(x)[-\partial^2 - m_q^2 - 2\beta m_q g_\chi \chi(x) - g_\chi^2 \chi^2(x)]q(x)$$

$$+ \frac{1}{2}\partial_\mu\chi(x)\partial^\mu\chi(x) - V[\phi(x)] \ . \qquad (2.2.18)$$

For simplicity, we further approximate the potential for the scalar field. Instead of using the "standard form",

$$V[\phi(x)] = -a\phi^2(x) + b\phi^4(x) \ ,$$

we use

$$\tilde{V}[\chi(x)] = -\frac{1}{2} m_\chi^2 \phi_0^2 + \frac{1}{2} m_\chi^2 \chi^2 \ . \qquad (2.2.19)$$

The first term in Eq.(2.2.19) is just an over-all constant which we can drop at this point. Therefore, we have

$$\mathcal{L}'(x) = \frac{1}{m_q^{cur}}\bar{q}(x)[-\partial^2 - m_q^2 - 2\beta m_q g_\chi \chi(x) - g_\chi^2 \chi^2(x)]q(x)$$

$$+ \frac{1}{2}\partial_\mu\chi(x)\partial^\mu\chi(x) - \frac{1}{2} m_\chi^2 \chi^2(x) \ . \qquad (2.2.20)$$

We tried to solve this second-order equation for q(x) using the same procedure as described in reference [32]. (Since it is a <u>second-order</u> equation for the quark field it does not generate the lower component.)

2.3 Effective First-Order Equation :

The linear version of Eq.(2.2.9) is

$$[i\gamma_\mu\partial^\mu - m_q]q(x) = 0 \ . \tag{2.3.1}$$

We again use the same assumption, $\phi_0 \to \phi(x)$, and use the following approximation for $m_q(x)$,

$$m_q(x) = \left(m_q^2 + 2\beta m_q g_\chi \chi(x) + g_\chi^2 \chi^2(x)\right)^{\frac{1}{2}}$$

$$= m_q\left(1 + \beta g_\chi \frac{\chi(x)}{m_q} + \frac{1}{2}(1-\beta^2)g_\chi^2 \frac{\chi^2(x)}{m_q^2} + \ldots\right), \tag{2.3.2}$$

$$\approx m_q + g_\chi^{eff}\chi(x) \ . \tag{2.3.3}$$

With this approximation, the equivalent first-order equation is

$$[i\gamma_\mu\partial^\mu - m_q - g_\chi^{eff}\chi(x)]q(x) = 0 \ . \tag{2.3.4}$$

The Lagrangian corresponding to above equation is

$$\mathcal{L}(x) = \bar{q}(x)[i\gamma_\mu\partial^\mu - m_q]q(x) - g_\chi^{eff}\,\bar{q}(x)\chi(x)q(x)$$

$$+ \frac{1}{2}\,\partial_\mu\chi(x)\partial^\mu\chi(x) - V[\phi(x)] \ . \tag{2.3.5}$$

This is the basic Lagrangian for our model of nontopological solitons. Approximating $V(\phi(x)) = \mathring{V}(\chi(x))$, [Eq.(2.2.19)], we get the final form

of our Lagrangian

$$\mathcal{L}(x) = \bar{q}(x)[i\gamma_\mu\partial^\mu - m_q]q(x) - g_\chi^{eff}\,\bar{q}(x)\chi(x)q(x)$$

$$+ \frac{1}{2}\,\partial_\mu\chi(x)\partial^\mu\chi(x) - \frac{1}{2}\,m_\chi^2\,\chi^2(x)\ . \qquad (2.3.6)$$

This is the Lagrangian used in previous studies of nucleon and meson structure. In those studies β=1 was used. From the expression for β, Eq.(2.2.11), we see that for $m_q^{cur} = 0$, $\beta = 1$. This is appropriate for u and d quarks, since $m_q^{cur} \approx 0$. For heavier quarks β is less than one and gives rise to an effective reduction in the coupling strength for heavier quarks in this model. This modification actually improves the results previously obtained for the $c\bar{c}$ and $b\bar{b}$ spectrum [38]. (We will describe our results in Chapter 6. An alternative scheme for deriving the Dirac equation from the second-order equation is discussed in Appendix A.)

2.4 Evaluation of Dynamical Masses :

Let us now evaluate various dynamical masses in terms of ϕ_0 or $g\phi_0$. To evaluate $g\phi_0$ we make use of the result obtained in (nonperturbative) QCD sum-rule studies [4],

$$\langle vac|:\frac{\alpha_s(\mu)}{\pi}G^a_{\mu\nu}(0)G_a^{\mu\nu}(0):|vac\rangle = 0.012\ GeV^4.$$

Here $\alpha_s(\mu)$ is the strong coupling constant renormalized at some mass scale μ. This expectation value is obtained by using dispersion relations for the vacuum polarization tensor and fitting the ground state mass of charmonium to the experimental value. We now write

$$\langle \text{vac} | \frac{g^2(\mu)}{4\pi^2} : G^a_{\mu\nu}(0) G^{\mu\nu}_a(0) : | \text{vac} \rangle = \langle \text{vac} | \frac{g^2(\mu)}{4\pi^2} : G^a_{\mu\nu}(0) G^{\mu\nu}_a(0) : | \text{vac} \rangle$$

$$\approx \langle \text{vac} | \frac{g^2(\mu)}{4\pi^2} f^{abc} f^{ade} A^b_i A^c_j A^i_d A^j_e | \text{vac} \rangle, \tag{2.4.1}$$

where we used the temporal gauge, $A^a_0 = 0$. Using Eq.(2.2.7b), we can put

$$\langle \text{vac} | A^a_i A^b_j A^k_c A^l_d | \text{vac} \rangle = \frac{\phi_0^4}{(24)(26)} \left(\delta_{ij}\delta_{kl}\delta_{ab}\delta_{cd} + \delta_{ik}\delta_{jl}\delta_{ac}\delta_{bd} + \delta_{il}\delta_{jk}\delta_{ad}\delta_{bc} \right) . \tag{2.4.2}$$

Using the properties of the structure constants given in Appendix B, we find

$$\langle \text{vac} | \frac{g^2(\mu)}{4\pi^2} : G^a_{\mu\nu}(0) G^{\mu\nu}_a(0) : | \text{vac} \rangle = \frac{6\, g^4 \phi_0^4}{4\pi^2 (24)} = 0.012 \text{ GeV}^4. \tag{2.4.3}$$

Therefore

$$\left(g^2 \phi_0^2 \right)^2 = 2.053 \text{ GeV}^4 ,$$

or

$$g^2\phi_0^2 = 1.433\ \text{GeV}^2 \ . \tag{2.4.4}$$

From Eq.(2.2.9) and Eq.(2.2.11), the dynamical masses of the gluon and of the quarks are found to be

$$\left(m_q^{gl}\right)^2 = \frac{1}{6}\, g^2\phi_0^2 = [489\ \text{MeV}]^2 \ , \tag{2.4.5}$$

and

$$m_{gl}^2 = \frac{1}{4}\, g^2\phi_0^2 \ = [599\ \text{MeV}]^2 \ . \tag{2.4.6}$$

We have $m_q^{q\bar{q}} = f_\pi g_\pi$. The phenomenological value generally used for f_π is 93 MeV and one usually takes $g_\pi \approx 4$. Thus, we find $m_q^{q\bar{q}} = 400$ MeV. Therefore, from Eq.(2.2.16), $m_q^{dyn} = 632$ MeV.

The value of m_χ also can be fixed by using its relation to $g\phi_0$. This is possible because of the approximation we made for the potential $V(\phi)$. We have

$$V[\phi(x)] = -a\phi^2(x) + b\phi^4(x) \ .$$

The minimum of this potential is at $\phi_0^2 = \frac{a}{2b}$ and

$$V[\phi_0] = -\, a\phi_0^2 + b\phi_0^4 \ ,$$

$$= - b\phi_0^4 \ .$$

In the "tree approximation", as shown in [32], 'b' can be related to $g(\mu)$ as

$$b = \frac{3}{52}\, g^2(\mu) \ .$$

Therefore

$$a = 2b\phi_0^2 = \frac{3}{26} g^2(\mu)\phi_0^2 \ .$$

The approximate potential, $\tilde{V}(\chi)$, is chosen so that it has the minimum value equal to $V(\phi_0)$. That is,

$$\tilde{V}(0) = V(\phi_0) \ ,$$

or

$$- \frac{1}{2}\, m_\chi^2 \phi_0^2 = - \frac{3}{52}\, g^2 \phi_0^4 \ .$$

Therefore

$$m_\chi^2 = \frac{3}{26}\, g^2 \phi_0^2 = [407 \text{ MeV}]^2. \qquad (2.4.7)$$

Hence, in the Lagrangian of Eq.(2.3.6) we have only two parameters, m_q^{cur} and g_χ. Note that g_χ and $g(\mu)$ are related:

$$g_\chi = \frac{m_q^{dyn}}{\phi_0} = \frac{g\, m_q^{dyn}}{g\, \phi_0} = \frac{632 \text{ MeV}}{\sqrt{1.433}\ \text{GeV}}\, g \ .$$

In our analysis we used $g_\chi = 7$, which corresponds to $g = 13.3$. The current quark masses are fixed by fitting the ground state of the corresponding family ($s\bar{s}$, $c\bar{c}$, and $b\bar{b}$) to experimental values. The value of $g\phi_0$ was originally fixed by the study of properties of nucleon. As we see in the Table A, the current quark masses are close to ones used in QCD sum-rule studies.

The Lagrangian of Eq.(2.3.6) does not contain gluons. Thus far, we have neglected the fluctuating fields in Eq.(2.2.10). We will take such fields into account by adding some gluon terms to Eq.(2.3.6). The Lagrangian with such terms is

$$\begin{aligned}\mathcal{L}(x) = {} & \bar{q}(x)[i\gamma_\mu\partial^\mu - m_q]q(x) - g_\chi^{eff}\,\bar{q}(x)\chi(x)q(x) \\ & + \tfrac{1}{2}\,\partial_\mu\chi(x)\partial^\mu\chi(x) - \tfrac{1}{2}\,m_\chi^2\,\chi^2(x) \\ & - \tfrac{1}{4}\,G^a_{\mu\nu}(x)G_a^{\mu\nu}(x) + \frac{m_{gl}^2}{2}\,Q^a(x).Q_a(x) + \bar{q}(x)g\,\frac{\lambda^a}{2}\,\not{Q}^a(x)q(x).\end{aligned} \tag{2.4.8}$$

The effective Lagrangian we derived from QCD is not invariant under local gauge transformations. Chiral symmetry is also broken in this Lagrangian. One can keep chiral symmetry in the model by introducing chiral fields $\sigma(x)$ and $\vec{\pi}(x)$. These are scalar and pseudoscalar fields, as given in reference [32]. The model then becomes more complicated.

At this point we also have not described confinement. In the next chapter we will discuss a somewhat different development of our model in which confinement and chiral symmetry breaking both occur as a consequence of the presence of the gluon condensate in the QCD vacuum.

CHAPTER 3

Chiral Symmetry Breaking and Confinement

In nature, chiral symmetry is broken and colored objects, such as quarks and gluons, are confined. Both these concepts underlie our understanding of many experimental facts. The dynamics giving rise to either of these phenomena is not understood, despite extensive efforts on the part of many researchers. We also note that, in most cases, these phenomena, chiral symmetry breaking [40-42] and confinement [43, 13, 14], are treated separately. However, there is some evidence from lattice simulations of QCD that the restoration of chiral symmetry and quark deconfinement take place at the same temperature. We further note that in the "bag" model, when a quark is reflected from a confining wall, its momentum direction is changed with no change in the quark spin. Hence, helicity is not conserved. That is, the breaking of chiral symmetry is related to confinement in a bag model description of hadron structure.

In this chapter we consider the propagation of a quark in the gluon condensate. We find that both chiral symmetry breaking and confinement are due to the presence of the condensate [44, 45]. To the best of

our knowledge, this appears to represent a completely new approach to understanding QCD.

3.1 Chiral Symmetry :

In the absence of current quark masses, the QCD Lagrangian is invariant under chiral transformation. That is,

$$\mathcal{L}_{QCD}(x) = -\frac{1}{4}G^{a}_{\mu\nu}(x)G^{\mu\nu}_{a}(x) + \bar{q}_L(x)i\not{\partial}q_L(x) + \bar{q}_R(x)i\not{\partial}q_R(x) \tag{3.1.1}$$

is invariant under the transformations U_L and U_R, such that

$$q'_L(x) = U_L q_L(x) \quad \text{and} \quad q'_R(x) = U_R q_R(x). \tag{3.1.2}$$

Here

$$q_L(x) = \tfrac{1}{2}(1-\gamma_5)q(x),$$

and

$$q_R(x) = \tfrac{1}{2}(1+\gamma_5)q(x),$$

are left-handed and right-handed quark fields and U_L and U_R are of the form,

$$U_L = \exp[-\tfrac{i}{2}T^f\theta^f_L] \quad \text{and} \quad U_R = \exp[-\tfrac{i}{2}T^f\theta^f_R].$$

Here T^f is a generator of the group under consideration. The absence of parity doubling in the observed hadron spectra (i.e., the absence

of an octet of scalar partners of the pseudoscalars and the absence of an octet of baryons with $J^P = \frac{1}{2}^-$) shows that chiral symmetry is broken by some dynamical mechanism. That is, the Lagrangian is invariant under chiral transformation [Eq.(3.1.2)], but the vacuum is not. From the Goldstone theorem, we know that spontaneous symmetry breaking leads to the existence of so-called Goldstone bosons: the pseudoscalar particles ($\vec{\pi}$, K etc.).

A model which is often used to describe spontaneous symmetry breaking is the σ-model. The Lagrangian of this model (when extended to include coupling to a gauge field) is

$$\begin{aligned}\mathcal{L}(x) = &-\frac{1}{4}G^a_{\mu\nu}(x)G_a^{\mu\nu}(x) + \bar{q}(x)i\not{\partial}q(x) \\ &- g\bar{q}(x)[\sigma(x)+i\vec{\tau}.\vec{\pi}(x)\gamma_5]q(x) + \frac{1}{2}\left([\partial_\mu\sigma(x)]^2+[\partial_\mu\vec{\pi}(x)]^2\right) \\ &- \frac{\lambda}{4}\left(\sigma^2(x)+\vec{\pi}^2(x) - f_\pi^2\right)^2 . \qquad (3.1.3)\end{aligned}$$

Choosing the non-trivial vacuum, $\sigma = f_\pi$, and expanding the σ and $\vec{\pi}$ fields about the vacuum values [$\sigma=f_\pi$, $\vec{\pi}=0$] leads to a massive σ mode and a massless $\vec{\pi}$ mode (Goldstone boson). A mass is also generated for the fermion field in this model.

Similar effects can be discussed from another point of view, that of "dynamical symmetry breaking". The above Lagrangian [Eq.(3.1.3)]

can be derived using the auxiliary-field formalism starting from the Nambu - Jona-Lasinio model [46]. The Nambu - Jona-Lasinio model is often used to study dynamical symmetry breaking [47]. (Chiral symmetry is broken dynamically in this model.) One also has a zero-mass $q\bar{q}$ pseudoscalar bound state, as can be seen by examining the pole of the $q\bar{q}$ scattering amplitude in this model. The Nambu - Jona-Lasinio model does not describe confinement and, hence, may not be good candidate for describing hadrons. It may, however, have some utility in studying the deconfined phase of QCD [48, 41].

3.2 Confinement :

The absence of colored objects in nature leads to the idea of confinement. No one has yet derived confinement from QCD. (There have been experimental searchs for free quarks. However, such searches have not been successful.)

The most physical phenomenological model of confinement may be the "flux tube" or "string model". (This model is consistent with the experimental observation of jet phenomena observed during hadron formation in $e^+ e^-$ collisions.) Consider a meson made up of a quark and an antiquark, which are connected by a flux tube of chromoelectric field. (In analogy to the formation of flux tubes in superconductors,

the nonperturbative vacuum is thought to lead to the formation of a flux tube between the sources.) Assuming a constant field in the flux tube, the energy for quarks separated a distance r is found to be

$$V(r) = \frac{E^2}{8\pi} Ar = \frac{E^2 A}{8\pi} r = kr \qquad (3.2.1)$$

where A is the cross-sectional area of the tube, r is the separation between the quarks and k is the spring constant. This form of confinement, (i.e., a linear potential) is used in potential models of hadron structure. As the quark and antiquark move apart, the energy increases linearly. As the separation increases, the energy may be sufficient to create a light quark-antiquark pair from the vacuum. For example, in the charmonium ($c\bar{c}$) spectrum one sees a threshold (the open-flavor threshold). Above this threshold, levels have relatively large widths due to their decay to D mesons($c\bar{u}$ and $u\bar{c}$). [This is also the threshold for Zweig-rule allowed decays. The Zweig-rule (or the Okubo-Zweig-Iizuka (OZI) rule) states that the strong processes in which the final states can only be reached through $q\bar{q}$ annihilation are suppressed. For charmonium the open-flavor threshold energy is twice the mass of the D meson.] We remark that the flux tube model may also be used to explain Regge trajectories. In this case one considers the rotation of the flux tube about its midpoint to understand how a sequence of hadron states with increasing angular momentum may be

generated.

As we mentioned earlier, lattice simulation of QCD with infinitly massive sources gives rise to linear confining potentials, when calculations are made in the quenched approximation.

3.3 A Phenomenological Covariant Confinement Model:

The confinement models we discussed above are static. Thus, they cannot be used in our covariant analysis. Our model, introduced in an earlier chapter, did not describe confinement. (The scalar field just binds the quarks and does not confine them.) Therefore, we are only able to describe the spectrum below the open-flavor threshold. Above the open-flavor threshold we have a continuum of solutions. As can be seen from Figure 1, charmonium has two levels below, while Υ has three levels below this threshold. Other excited levels, 3S, 4S in charmonium and 4S, 5S, 6S in Υ, lie in the continuum of our model.

In order to introduce confinement in our formalism, we require a specification of the quark self-energy for time-like momenta. Since little is known concerning that quantity, we chose a phenomenological form suggested by the results obtained for the fermion self-energy in an Abelian theory(with strong coupling) by Fukuda and Kugo[43]. These authors have solved an (approximate) Schwinger-Dyson equation and obtained a fermion propagator which is confining in the sense that

there is no fermion pole.

As a first step, we replaced the mass term in the propagator for a single quark or an antiquark by a self-energy $\Sigma(q^2)$ of the form [49],

$$\Sigma^2(q^2) = m_q^2 + (1+C)(q^2-m_0^2)\ \theta(q^2-m_0^2). \qquad (3.3.1)$$

Here C is taken to be a universal constant and m_0 is a flavor-dependent constant with the dimension of mass. The parameters are chosen such that we get the best fit to all experimental levels (ρ, ω, ρ', φ, φ', 1S to 4S states of the $c\bar{c}$ system and the 1S to 6S states of the $b\bar{b}$ system). Further, $q = P-k$, where P is the momentum of the meson and k is the momentum of the on-mass-shell quark (antiquark). [The antiquark (quark) was kept on mass shell as an approximation.] Using this model for confinement, and with the parameters given in Table A, we found good agreement of our theoretical spectrum with the experimental spectrum, as can be seen in Figures 1 and 2.

3.4 Self-Energy of a Quark in the Gluon Condensate :

This success prompted us to study models of this type in greater detail - that is, models in which the quark propagator has no singularities for real q^2. We recently obtained a self-energy of this form by considering a self-consistent approximation for the self-

energy of a quark in a gluon condensate [44, 45]. Here again, as in Chapter 2, we separate the gluon field into a condensate and a fluctuation part. We now work in a covariant gauge and, hence, define

$$\langle vac|g^2(\mu)\ A^a_\mu\ A^b_\nu|vac\rangle = g^2(\mu)\phi_0^2\ \frac{\delta_{ab}}{8}\ \frac{g_{\mu\nu}}{4}\ . \qquad (3.4.1)$$

This quantity can be related to the QCD sum-rule value for

$$\langle vac|\frac{g^2(\mu)}{4\pi^2}:G^a_{\mu\nu}(0)G^{\mu\nu}_a(0):|vac\rangle = 0.012\ GeV^4.$$

Using the last equation one may obtain

$$g^2(\mu)\phi_0^2 = 1.34\ (GeV)^2.$$

It is useful to define the parameter

$$\kappa^2 = \frac{1}{24}\ g^2(\mu)\phi_0^2\ .$$

Our approximation for the quark self-energy is shown in Fig.3, where the heavy line denotes the propagator

$$S_F(q) = \left[\not{q} - \Sigma(q^2) - m_q^{cur}\right]^{-1}$$

$$= \left[\not{q}[1-A(q^2)] - B(q^2) - m_q^{cur}\right]^{-1}. \qquad (3.4.2)$$

Here $\Sigma(q^2) = A(q^2)\not{q} + B(q^2)$ is the quark self-energy. We obtain (see Fig.3),

$$A(q^2)\not{q} + B(q^2) = -\frac{\kappa^2\gamma^\mu\left[\not{q}[1-A(q^2)] + B(q^2) + m_q^{cur}\right]\gamma_\mu}{q^2[1-A(q^2)]^2 - [B(q^2)+m_q^{cur}]^2}\ , \qquad (3.4.3)$$

where κ^2, defined earlier, includes a color factor (4/3). Using the properties of Dirac matrices, Eq.(3.4.3) reduces to

$$A(q^2)\not{q} + B(q^2) = -\frac{\kappa^2\left[-2\not{q}[1-A(q^2)] + 4[B(q^2)+m_q^{cur}]\right]}{q^2[1-A(q^2)]^2 - [B(q^2)+m_q^{cur}]^2}\ . \qquad (3.4.4)$$

Therefore,

$$A(q^2) = \frac{2\kappa^2[1-A(q^2)]}{[1-A(q^2)]^2q^2 - [B(q^2)+m_q^{cur}]^2}\ ,$$

and

$$B(q^2) = \frac{-4\kappa^2[B(q^2)+m_q^{cur}]}{[1-A(q^2)]^2q^2 - [B(q^2)+m_q^{cur}]^2}\ . \qquad (3.4.5)$$

Let us define a <u>dynamical mass</u>, $M(q^2)$, where

$$M^2(q^2) = \frac{[B(q^2)+m_q^{cur}]^2}{[1-A(q^2)]^2}\ .$$

Thus, the quark propagator is of the form

$$S_F(q) = \frac{\left[\not{q}[1-A(q^2)] + [B(q^2)+m_q^{cur}]\right]}{[1-A(q^2)]^2\ [q^2-M^2(q^2)]}\ . \qquad (3.4.6)$$

In terms of $M(q^2)$, $A(q^2)$ and $B(q^2)$ are given by

$$A(q^2) = \frac{m_q^{cur}}{M(q^2)} - 1 \ ,$$

$$B(q^2) = -2[m_q^{cur} - M(q^2)]. \qquad (3.4.7)$$

Inserting $A(q^2)$ and $B(q^2)$ from Eq.(3.4.7) in Eq.(3.4.5), we find

$$\left[1- \frac{m_q^{cur}}{M(q^2)}\right] \left[1- \frac{m_q^{cur}}{2M(q^2)}\right] \left[q^2-M^2(q^2)\right] = - \kappa^2. \qquad (3.4.8)$$

This equation for $M(q^2)$ is of fourth order and we solve it numerically. However, for $m_q^{cur}= 0$, Eq.(3.4.7) reduces to a simple form

$$q^2-M^2(q^2) = - \kappa^2, \text{ or}$$

$$M(q^2) = \sqrt{q^2 + \kappa^2} \quad ; \quad \left[q^2>-\kappa^2\right]. \qquad (3.4.9)$$

From Eq.(3.4.6), we find, if $m_q^{cur}= 0$,

$$A(q^2) = - 1 \ ,$$

$$B(q^2) = 2M(q^2) = 2 \sqrt{q^2 + \kappa^2} \ , \qquad (3.4.10)$$

for $q^2> -\kappa^2$. For $q^2< -\kappa^2$, $B(q^2)$ is zero. From Eq.(3.4.4), we find

$$A(q^2) = \frac{1}{2} \left[1 - \sqrt{1 - 8\kappa^2/q^2} \ \right] \text{ for } q^2< -\kappa^2. \qquad (3.4.11)$$

The quark propagator is, for $q^2 > -\kappa^2$,

$$S_F(q) = \frac{\left[\not{q}[1-A(q^2)] + B(q^2)\right]}{[1-A(q^2)]^2\ [-\kappa^2]} \qquad (3.4.12)$$

or

$$S_F(q) = [1-A(q^2)]^{-1}\left[\not{q} - M(q^2)\right]^{-1} .$$

Therefore, for $m_q^{cur} = 0$, the solution of Eq.(3.4.7) has the following properties:

(1) Chiral symmetry is broken for $q^2 > -\kappa^2$.

(2) The quark propagator behaves as $[\not{q}]^{-1}$ for large space-like q^2.

(3) There is no fermion pole, since the denominator of the propagator, has no zeroes for $q^2 > -\kappa^2$. Therefore, the fermion is a <u>nonpropagating mode</u>.

For $m_q^{cur} \neq 0$, the asymptotic solution is given below:

For $-q^2 \gg \kappa^2$ (i.e., for large space-like momenta)

$$\left[1- \frac{m_q^{cur}}{M(q^2)}\right]\left[1- \frac{m_q^{cur}}{2M(q^2)}\right] = \frac{\kappa^2}{[|q^2|+M^2(q^2)]}$$

$$\approx 0 .$$

This has a solution $M(q^2) = m_q^{cur}$.

For $q^2 >> \left[m_q^{cur}\right]^2$ (i.e., for large time-like momenta)

$$M^2(q^2) = q^2 + \frac{\kappa^2}{\left[1 - \frac{m_q^{cur}}{M(q^2)}\right]\left[1 - \frac{m_q^{cur}}{2M(q^2)}\right]},$$

$$M^2(q^2) = q^2 + \kappa^2 \left(\left[1 - \frac{m_q^{cur}}{M(q^2)}\right]\left[1 - \frac{m_q^{cur}}{2M(q^2)}\right] + \ldots\ldots \right),$$

$$\approx q^2 + \kappa^2 \left[1 + \frac{3}{2}\frac{m_q^{cur}}{|q|} + \ldots\ldots\right],$$

$$\approx q^2 + \kappa^2 .$$

Results of numerical calculations are presented in Fig.4. We see that, even in the case $m_q^{cur} \neq 0$, the quark propagator does not have pole. As can be seen from Fig.4, the phenomenological self-energy we chose earlier coincides remarkably well with the theoretical result.

3.5 Off-Mass-Shell Effects :

In our analysis we kept one quark (antiquark) on mass-shell as an approximation. (We will discuss the fully-off-shell problem in Chapter 5.) Let the four-momentum of the meson be P and that of on-mass-shell quark (antiquark) be k. The meson is also on-mass-shell. The antiquark (quark) is off-mass-shell and has momentum q = P-k. We work

in quark (antiquark) rest frame ($\vec{k}$=0). Since our analysis is fully covariant, we can work in any frame. For example, we can calculate the wave function in the meson rest frame ($\vec{P}$=0). The four momentum squared of the off-shell antiquark (quark), q^2, is

$$q^2 = (P-k)^2 = P^2 + k^2 - 2P.k$$

$$= M^2 + m_q^2 - 2M\sqrt{m_q^2 + \vec{k}^2} \quad , \qquad (3.5.1)$$

where M is the mass of the meson and m_q is the quark mass. The maximum value of q^2 is $(M-m_q)^2$ (obtained for $\vec{k} \to 0$) and the minimum is $-\infty$ (obtained for $\vec{k} \to \infty$). The probability, $P(q^2)$, of finding the off-mass-shell antiquark (quark) with squared four momentum between q^2 and q^2+dq^2 is given below: We have

$$|\Psi(|\vec{k}|)|^2 \, \vec{k}^2 \, d|\vec{k}| = |\Psi(q^2)|^2 \, J(q^2) \, dq^2$$

$$\equiv - P(q^2) \, dq^2 \quad , \qquad (3.5.2)$$

where $J(q^2)$ is the Jacobian and $\Psi(|\vec{k}|)$ is the normalized wave function. From Eq.(3.5.1) we have

$$\vec{k}^2 = \left(\frac{M^2+m_q^2-q^2}{2M}\right)^2 - m_q^2 \quad ,$$

$$d\vec{k}^2 = -\frac{1}{M}\left(\frac{M^2+m_q^2-q^2}{2M}\right) dq^2 \ .$$

Thus,

$$\vec{k}^2\ d\vec{k} = -\frac{|\vec{k}|}{2}\frac{1}{M}\left(\frac{M^2+m_q^2-q^2}{2M}\right) dq^2$$

$$= -\frac{1}{2}\left[\left(\frac{M^2+m_q^2-q^2}{2M}\right)^2 - m_q^2\right]^{\frac{1}{2}}\frac{1}{M}\left(\frac{M^2+m_q^2-q^2}{2M}\right) dq^2 \ .$$

Therefore,

$$J(q^2) = -\frac{1}{2}\left[\left(\frac{M^2+m_q^2-q^2}{2M}\right)^2 - m_q^2\right]^{\frac{1}{2}}\frac{1}{M}\left(\frac{M^2+m_q^2-q^2}{2M}\right) \ ,$$

or

$$P(q^2) = \frac{1}{2}\left[\left(\frac{M^2+m_q^2-q^2}{2M}\right)^2 - m_q^2\right]^{\frac{1}{2}}\frac{1}{M}\left(\frac{M^2+m_q^2-q^2}{2M}\right) |\Psi(q^2)|^2 \ . \qquad (3.5.3)$$

Values of $P(q^2)$ are plotted in Fig.5 for Υ and in the Fig.6 for J/ψ. The light arrow denotes the value of m_0^2 chosen and the heavy arrow denotes the value of m_q^2 in Eq.(3.3.1). Therefore, we see that the 1S and 2S states of Υ do not encounter the "confining part" of $\Sigma(q^2)$. The 3S state is only slightly modified by the confining part of

$\Sigma(q^2)$, while the position of the 4S, 5S and 6S states are totally dependent on the values of $\Sigma(q^2)$ for $q^2>m_0^2$. Similarly, in the case of J/ψ, the 1S state is not affected by confinement. The 2S state is only slightly modified by confinement, while the properties of the 3S and 4S states are totally dependent upon the confining aspect of $\Sigma(q^2)$.

CHAPTER 4

Method of Solution

4.1 General Form of the Integral Equation :

In this chapter we will show how we can make a covariant description of the structure of mesons. We obtain equations for the vertex function, which is described in a covariant manner, in terms of Lorentz-invariant amplitudes. Our equations represent an eigenvalue problem, with the mass of the meson as the eigenvalue. An extensive discussion of this analysis is given in [30, 50-52]. Here we quote those results which we have used in our work.

The field equations that we obtain from our Lagrangian, Eq(2.3.6), are

$$[i\gamma_\mu\partial^\mu - m_q]q(x) = g_\chi^{eff}\,\chi(x)q(x)\ , \tag{4.1.1}$$

$$[\partial_\mu\partial^\mu + m_\chi^2]\chi(x) = -\,g_\chi^{eff}\,\bar{q}(x)q(x)\ . \tag{4.1.2}$$

Let $|\vec{k},s,t,b\rangle$ and $|\overline{\vec{k},s,t,b}\rangle$ be quark and antiquark states of momentum $\vec{k}$, color b, and spin and isospin projections, s and t, respectively. Let $|\vec{P},M_T,\lambda\rangle$ be a state of a meson of momentum $\vec{P}$, isospin projection,

M_T, and helicity λ.

We form an equation for the matrix element $\overline{<\vec{k},s,t,b|q(x)|\vec{P},M_T,\lambda>}$. Using Eq(4.1.1), we find

$$[i\gamma_\mu\partial^\mu - m_q]\overline{<\vec{k},s,t,b|q^a(x)|\vec{P},M_T,\lambda>} = g_\chi^{eff}\overline{<\vec{k},s,t,b|\chi(x)q^a(x)|\vec{P},M_T,\lambda>} \ .$$

The translational invariance of the theory implies

$$\hat{f}(x) = e^{i\hat{P}.x}\ \hat{f}(0)\ e^{-i\hat{P}.x} \ ,$$

where $\hat{f}(x)$ denotes either the field $q(x)$ or $\chi(x)$. We find

$$[\not{P}-\not{K} - m_q]\overline{<\vec{k},s,t,b|q^a(0)|\vec{P},M_T,\lambda>} = g_\chi^{eff}\overline{<\vec{k},s,t,b|\chi(0)q^a(0)|\vec{P},M_T,\lambda>}$$

$$= g_\chi^{eff}\sum_{M_T'\lambda'}\int d^3P'\ \overline{<\vec{k},s,t,b|q^a(0)|\vec{P}',M_T',\lambda'>}<\vec{P}',M_T',\lambda'|\chi(0)|\vec{P},M_T,\lambda> . \tag{4.1.3}$$

In Eq.(4.1.3) we have inserted a set of soliton states between the operators $q^a(0)$ and $\chi(0)$.

Similarly, using Eq.(4.1.2), we obtain

$$[-(P-P')^2 + m_\chi^2]<\vec{P}',M_T',\lambda'|\chi(0)|\vec{P},M_T,\lambda>$$

$$= - g_\chi^{eff}\ <\vec{P}',M_T',\lambda'|:\bar{q}_\alpha^c(0)q_\alpha^c(0):|\vec{P},M_T,\lambda>$$

$$= -g_{\chi}^{eff} \sum_{s't'b'} \int d^3k' \left\{ \langle \vec{P}', M_T', \lambda' | \overline{q_\alpha^c(0)} | \overline{\vec{k}', s', t', b'} \rangle \right.$$

$$\times \overline{\langle \vec{k}', s', t', b' | q_\alpha^c(0) | \vec{P}, M_T, \lambda \rangle} - \langle \vec{P}', M_T', \lambda' | q_\alpha^c(0) | \vec{k}', s', t', b' \rangle$$

$$\left. \times \langle \vec{k}', s', t', b' | \overline{q_\alpha^c(0)} | \vec{P}, M_T, \lambda \rangle \right\} . \qquad (4.1.4)$$

Inspection of Eqs. (4.1.3) and (4.1.4) shows that these equations are coupled and nonlinear. A diagrammatic representation of those equations is given in Fig.7. Equations (4.1.3) and (4.1.4) are then our general covariant mean-field equations, which describe mesons of different quantum numbers.

Our notation, and various parameters, are specified below: The states $|\vec{k},s,t,b\rangle$, $|\overline{\vec{k},s,t,b}\rangle$, and $|\vec{P},M_T,\lambda\rangle$ are defined to have noncovariant normalization. That is

$$\langle \vec{k},s,t,b | \vec{k}',s',t',b' \rangle = \delta^3(\vec{k}-\vec{k}')\ \delta_{ss'}\ \delta_{tt'}\ \delta_{bb'} ,$$

$$\overline{\langle \vec{k},s,t,b |} \overline{| \vec{k}',s',t',b' \rangle} = \delta^3(\vec{k}-\vec{k}')\ \delta_{ss'}\ \delta_{tt'}\ \delta_{bb'} ,$$

and

$$\langle \vec{P},M_T,\lambda | \vec{P}',M_T',\lambda' \rangle = \delta^3(\vec{P}-\vec{P}')\ \delta_{M_T M_T'}\ \delta_{\lambda\lambda'} . \qquad (4.1.5)$$

We have also defined

$$\omega(\vec{P}) = \sqrt{\vec{P}^2 + M^2} \quad ,$$

$$E_{\bar{q}}(\vec{k}) = \sqrt{\vec{k}^2 + m_{\bar{q}}^2} \quad ,$$

and

$$\epsilon_q \equiv E_q(\vec{k}) + m_q \quad , \tag{4.1.6}$$

where m_q is the quark mass and M is the mass of the meson.

4.2 Invariant Amplitudes :

The next step is to express the matrix element $\overline{<\vec{k},s,t,b|q(0)|\vec{P},M_T,\lambda>}$, in terms of appropriate Lorentz-invariant amplitudes.

For pseudoscalar and scalar mesons (J=0) one can define

$$\overline{<\vec{k},s,t,b|q^a(0)|\vec{P},M_T>} = N\, \mathbb{m}(P,k) v(\vec{k},s)\, I_t \quad , \tag{4.2.1}$$

where

$$N = \frac{\delta_{ab}}{(2\pi)^3} \sqrt{\frac{m_q}{3\, E_q[2\omega(\vec{P})]}} \quad ,$$

and

$$I_t = (-1)^{\frac{1}{2}-t} (\vec{\tau}.\hat{e}_{M_T})\, \chi_{-t} \quad , \tag{4.2.2}$$

is an isospin factor. Here $\mathbb{M}(P,k)$ is a 4x4 matrix which depends upon P and k. It can be expanded in terms of 16 Dirac matrices as

$$\mathbb{M}(P,k) = a\,1 + a^{\mu}\gamma_{\mu} + a^{\mu\nu}\sigma_{\mu\nu} + \tilde{a}\,\gamma_5 + \tilde{a}^{\mu}\gamma_{\mu}\gamma_5$$

$$= a_1 1 + a_2 \not{k} + a_2' \not{P} + (a_3 k^{\mu}k^{\nu} + a_3' P^{\mu}P^{\nu} + a_4 P^{\mu}k^{\nu} + a_4' k^{\mu}P^{\nu})\,\sigma_{\mu\nu}$$

$$+ \tilde{a}_1\,\gamma_5 + \tilde{a}_2 \not{k}\,\gamma_5 + \tilde{a}_2' \not{P}\,\gamma_5 \ , \qquad (4.2.3)$$

where the coefficients (the a's and $\tilde{a}$'s) are functions of (P.k). Using the fact that

$$\not{k}\, v(\vec{k},s) = -\, m_q\, v(\vec{k},s) \ ,$$

$$k^{\mu}k^{\nu}\sigma_{\mu\nu} = P^{\mu}P^{\nu}\sigma_{\mu\nu} = 0 \ ,$$

and

$$P^{\mu}k^{\nu}\sigma_{\mu\nu} = (-i)[P.k - \not{P}\not{k}] \ , \qquad (4.2.4)$$

the above equation reduces to

$$\mathbb{M}(p,k) = \tilde{E}(P.k) + \tilde{F}(P.k)\,\frac{\not{P}}{M} + \gamma_5\left[E(P.k) + F(P.k)\frac{\not{P}}{M}\right] \ . \qquad (4.2.5)$$

where the E's and F's are Lorentz-invariant amplitudes and depend only on (P.k). Therefore,

$$\overline{\langle \vec{k},s,t,b|q^a(0)|\vec{P},M_T\rangle} = N\, I_t$$

$$\times \left\{\tilde{E}(P.k) + \tilde{F}(P.k)\,\frac{\not{P}}{M} + \gamma_5\left[E(P.k) + F(P.k)\frac{\not{P}}{M}\right]\right\} v(\vec{k},s). \tag{4.2.6}$$

Using the properties of states and fields under the parity transformation, $\mathcal{P}$,

$$\mathcal{P}\ |\vec{k},s,t,b\rangle = |-\vec{k},s,t,b\rangle\ ,$$

$$\mathcal{P}\ \overline{|\vec{k},s,t,b\rangle} = -\ \overline{|-\vec{k},s,t,b\rangle}\ ,$$

$$\mathcal{P}|\vec{P},M_T\rangle = \eta\ |-\vec{P},M_T\rangle\ ,$$

and

$$\mathcal{P}q^a(x)\mathcal{P} = \gamma_0 q^a(x)\ , \tag{4.2.7}$$

we have

$$\overline{\langle \vec{k},s,t,b|}\ \mathcal{P}q^a(0)\mathcal{P}\ |\vec{P},M_T\rangle = (-1)\gamma_0\overline{\langle -\vec{k},s,t,b|q^a(0)|-\vec{P},M_T\rangle}\ \eta$$

$$= -\,\eta\gamma_0 N \left\{\tilde{E}(P.k) + \tilde{F}(P.k)\,\frac{\not{\underset{\sim}{P}}}{M} + \gamma_5\left[E(P.k) + F(P.k)\frac{\not{\underset{\sim}{P}}}{M}\right]\right\} v(-\vec{k},s)\ I_t\ , \tag{4.2.8}$$

where η is the intrinsic parity of the meson and $\underset{\sim}{P}^{\mu} = (P^0,-\vec{P})$. Moving γ_0 to the right, and using the properties of Dirac matrices given in Appendix B, the right-hand side is found to be

$$\eta\, N \left\{\tilde{E}(P.k) + \tilde{F}(P.k)\,\frac{\not P}{M} - \gamma_5\left[E(P.k) + F(P.k)\frac{\not P}{M}\right]\right\} v(\vec{k},s)\; I_t \;.$$

The left-hand side is

$$N \left\{\tilde{E}(P.k) + \tilde{F}(P.k)\,\frac{\not P}{M} + \gamma_5\left[E(P.k) + F(P.k)\frac{\not P}{M}\right]\right\} v(\vec{k},s)\; I_t \;,$$

where we have used the relation $\gamma_0 v(-\vec{k},s) = -v(\vec{k},s)$. This implies that, for a <u>scalar meson</u> (η =+1), E and F are zero. Therefore,

$$\overline{<\vec{k},s,t,b|q^a(0)|\vec{P},M_T>} = N \left\{\tilde{E}(P.k) + \tilde{F}(P.k)\,\frac{\not P}{M}\right\} v(\vec{k},s)\; I_t \;. \qquad (4.2.9)$$

For a <u>pseudoscalar meson</u> (η =−1), we find that $\tilde{E}$ and $\tilde{F}$ are zero. Therefore,

$$\overline{<\vec{k},s,t,b|q^a(0)|\vec{P},M_T>} = N\, \gamma_5\left[E(P.k) + F(P.k)\frac{\not P}{M}\right] v(\vec{k},s)\; I_t. \qquad (4.2.10)$$

For vector and pseudovector mesons (J=1), we have

$$\overline{<\vec{k},s,t,b|q^a(0)|\vec{P},M_T,\lambda>} = N\, \xi^\mu_\lambda\, \mathfrak{M}_\mu\, v(\vec{k},s)\; I_t \;, \qquad (4.2.11)$$

where $\xi^\mu_\lambda = \xi^\mu_\lambda(\vec{P})$ is the polarization vector of the meson. Here $\mathfrak{M}_\mu$ is a 4x4 matrix which transforms as a vector and is a function of P and k. Using the same procedure as for the J=0 mesons, we can write

$$\not{m}_{\mu}\xi_{\lambda}^{\mu} = A\,\frac{k.\xi_{\lambda}}{m_q} - B\,\frac{\not{P}\,(k.\xi_{\lambda})}{M\,m_q} - \not{\xi}_{\lambda}\left[\tilde{A} + \tilde{B}\,\frac{\not{P}}{M}\right]$$

$$+ \gamma_5\left[A'\,\frac{k.\xi_{\lambda}}{m_q} + B'\,\frac{\not{P}\,(k.\xi_{\lambda})}{M\,m_q} + \not{\xi}_{\lambda}\,\tilde{A}'\right] , \qquad (4.2.12)$$

where the A's and B's are Lorentz-invariant amplitudes and depend only on (P.k). Using the properties of the parity transformation, we find, for <u>vector mesons</u> (η=-1),

$$\overline{<\vec{k},s,t,b|q^a(0)|\vec{P},M_T,\lambda>} = NI_t\left\{A\,\frac{k.\xi_{\lambda}}{m_q} - B\,\frac{\not{P}\,(k.\xi_{\lambda})}{M\,m_q} - \not{\xi}_{\lambda}\left[\tilde{A} + \tilde{B}\,\frac{\not{P}}{M}\right]\right\}v(\vec{k},s). \qquad (4.2.13)$$

The properties of the helicity vectors, which are used in deriving the above expressions, are given in Appendix C. A similar expression, with a γ_5 factor, in the case of pseudovector mesons (η=+1), was used in the study of P-wave solitons in [51].

Using charge conjugation, as discussed in Appendix D, one can obtain the matrix elements with a quark, rather than an antiquark, on-mass-shell.

These expressions for the matrix element, [Eq.(4.2.10) or Eq.(4.2.13)], are then introduced in Eq.(4.1.3) and Eq.(4.1.4). Both equations now can be expressed in terms of Lorentz-invariant amplitudes. Therefore, one can work in any convenient frame [the meson

rest frame ($\vec{P}$=0) or the quark rest frame ($\vec{k}$=0)].

4.3 Wave Functions and Normalization :

As we saw in the last section, scalar and pseudoscalar mesons have two invariant amplitudes to be determined, while vector and pseudovector mesons have four such amplitudes. Let us first consider the pseudoscalar mesons. In the meson rest frame we have

$$\overline{<\vec{k},s,t,b|q^a(0)|\vec{0},M_T>} = N\,\gamma_5\left[E + F\,\gamma_0\right]v(\vec{k},s)\;I_t\;,$$

$$= N\sqrt{\frac{\epsilon_q}{2\,m_q}}\begin{bmatrix} E - F \\ (E + F)\frac{k}{\epsilon_q}\,\vec{\sigma}.\hat{k} \end{bmatrix}\chi_{-s}\;I_t\;. \tag{4.3.1}$$

The structure of this expression is similar to that of a Dirac spinor arising in the study of the relativistic hydrogen atom. Thus, we define wave functions as follows,

$$\overline{R}_u(k) = \left\{\frac{4\pi\,\epsilon_q}{M(2\pi)^3\,E_q}\right\}^{\frac{1}{2}}(E - F)\;,$$

$$\overline{R}_l(k) = \left\{\frac{4\pi\,\epsilon_q}{M(2\pi)^3\,E_q}\right\}^{\frac{1}{2}}(E + F)\frac{k}{\epsilon_q}\;, \tag{4.3.2}$$

such that the normalization condition

$$\int_0^\infty dk\ k^2\left[\bar{R}_u^2(k) + \bar{R}_l^2(k)\right] = 1 \ , \tag{4.3.3}$$

is satisfied. The invariant amplitudes are function of x, where x is defined as

$$x = \sqrt{\left[\frac{P.k}{M}\right]^2 - m_q^2} \ . \tag{4.3.4}$$

In the meson rest frame, $x = |\vec{k}| \equiv k$.

The normalization condition, Eq.(4.3.3), is derived as follows: The charge operator is

$$\hat{Q} = \int d^3x\ :\ \bar{q}(x)\gamma^0\left[\frac{1}{6} + \frac{\tau_3}{2}\right]q(x)\ :\ \ , \tag{4.3.5}$$

where τ_3 is the third isospin matrix. It is seen that

$$\langle\vec{P},M_T,\lambda|\hat{Q}|\vec{P}',M_T',\lambda'\rangle = M_T\ \delta_{M_T M_T'}\ \delta(\vec{P}-\vec{P}')\ \delta_{\lambda\lambda'} \ , \tag{4.3.6}$$

for vector mesons and

$$\langle\vec{P},M_T|\hat{Q}|\vec{P}',M_T'\rangle = M_T\ \delta_{M_T M_T'}\ \delta(\vec{P}-\vec{P}') \ \ , \tag{4.3.7}$$

for pseudoscalar mesons. Substituting for $\hat{Q}$, we have

$$\langle \vec{P}, M_T, \lambda | \hat{Q} | \vec{P}', M_T', \lambda' \rangle =$$

$$= \sum_{s't'b'} \int d^3k' \int d^3x \left\{ \langle \vec{P}', M_T', \lambda' | \overline{q^c_{\alpha i}(0) | \vec{k}', s', t', b'} \rangle \right.$$

$$\times \overline{\langle \vec{k}', s', t', b' | q^c_{\beta j}(0) | \vec{P}, M_T, \lambda \rangle} - \langle \vec{P}', M_T', \lambda' | q^c_{\beta j}(0) | \vec{k}', s', t', b' \rangle$$

$$\left. \times \langle \vec{k}', s', t', b' | \overline{q^c_{\alpha i}(0) | \vec{P}, M_T, \lambda \rangle} \right\} \gamma^0_{\alpha\beta} \left[\frac{1}{6} + \frac{\tau_3}{2} \right]_{ij} e^{i(P-P').x} ,$$

$$= \delta^3(\vec{P}-\vec{P}')(2\pi)^3 \sum_{s't'b'} \int d^3k' \left\{ \langle \vec{P}', M_T', \lambda' | \overline{q^c_{\alpha i}(0) | \vec{k}', s', t', b'} \rangle \right.$$

$$\times \overline{\langle \vec{k}', s', t', b' | q^c_{\beta j}(0) | \vec{P}, M_T, \lambda \rangle} - \langle \vec{P}', M_T', \lambda' | q^c_{\beta j}(0) | \vec{k}', s', t', b' \rangle$$

$$\left. \times \langle \vec{k}', s', t', b' | \overline{q^c_{\alpha i}(0) | \vec{P}, M_T, \lambda \rangle} \right\} \gamma^0_{\alpha\beta} \left[\frac{1}{6} + \frac{\tau_3}{2} \right]_{ij} , \qquad (4.3.8)$$

where i, j denote isospin components. Now, using the expressions for the matrix elements, and for the corresponding charge conjugate elements, we obtain the normalization condition. In the case of pseudoscalar mesons, after defining the wave function as in Eq.(4.3.2), we obtain the normalization condition of Eq.(4.3.3).

In the case of a vector meson, in the meson rest frame, we have

$$\overline{\langle \vec{k}, s, t, b | q^a(0) | \vec{0}, M_T, \lambda \rangle} = NI_t \left\{ A \frac{k.\xi_\lambda}{m_q} - B \frac{\not{P}\,(k.\xi_\lambda)}{M\, m_q} - \not{\xi}_\lambda \left[\tilde{A} + \tilde{B} \frac{\not{P}}{M} \right] \right\}_{\vec{P}=0} v(\vec{k}, s),$$

$$= - N \sqrt{\frac{\epsilon_q}{2\, m_q}} \begin{bmatrix} (A-B)\frac{k^2}{\epsilon_q m_q} \vec{\xi}_\lambda . \hat{k}\ \vec{\sigma}.\hat{k} - (\tilde{A}-\tilde{B})\vec{\xi}_\lambda . \vec{\sigma} \\ (\tilde{A}+\tilde{B})\frac{k}{\epsilon_q} \vec{\xi}_\lambda . \vec{\sigma}\ \vec{\sigma}.\hat{k} + (A+B)\frac{k}{m_q} \vec{\xi}_\lambda . \hat{k} \end{bmatrix} \chi_{-s}\ I_t \ , \tag{4.3.9}$$

where we have used the properties of the helicity vector, $\xi^{\mu}_{\lambda}(\vec{P})$, given in Appendix C. Here A, $\tilde{A}$, B and $\tilde{B}$ are function of k.

In order to construct tensors built out of the spin operators, we define the second-rank tensor

$$Q_{ij} = \frac{3}{2} \hat{k}_i \hat{k}_j - \frac{1}{2} \delta_{ij} \ , \tag{4.3.10}$$

where $\hat{k}_i$ is the i^{th} component of the unit vector $\hat{k}$. Then

$$\begin{aligned} \vec{\xi}_\lambda . \hat{k}\ \hat{k} . \vec{\sigma} &= \xi^i_\lambda\ \sigma^j\ \hat{k}_i\ \hat{k}_j \\ &= \xi^i_\lambda\ \sigma^j \left[\frac{2}{3} Q_{ij} + \frac{1}{3} \delta_{ij} \right] , \\ &= \frac{2}{3}\, t - \frac{1}{3}\, c \quad , \end{aligned} \tag{4.3.11}$$

where $t = Q_{ij}\ \xi^i_\lambda\ \sigma^j$ and $c = \vec{\xi}_\lambda . \vec{\sigma}$. In terms of t and c the wave function of the vector meson is

$$\overline{\langle \vec{k},s,t,b|q^a(0)|\vec{0},M_T,\lambda\rangle} = N\sqrt{\frac{\epsilon_q}{2\,m_q}}$$

$$\times \begin{bmatrix} \left[(\tilde{A}-\tilde{B}) - (A-B)\frac{k^2}{3\epsilon_q m_q}\right] c - (A-B)\frac{2}{3}\frac{k^2}{3\epsilon_q m_q} t \\ \left[-(A+B)\frac{k}{3m_q} + (\tilde{A}+\tilde{B})\frac{k}{3\epsilon_q}\right] ec - \frac{2}{3}\left[(A+B)\frac{k}{m_q} + (\tilde{A}+\tilde{B})\frac{2k}{\epsilon_q}\right] et \end{bmatrix} \chi_{-s}\, I_t \ , \tag{4.3.12}$$

or

$$\overline{\langle \vec{k},s,t,b|q^a(0)|\vec{0},M_T,\lambda\rangle} = \frac{\delta_{ab}\, I_t}{2\left[3(2\pi)^3(4\pi)\right]^{\frac{1}{2}}} \begin{bmatrix} \bar{R}_u^{(0)}(k)c + \bar{R}_u^{(2)}(k)t\sqrt{2} \\ \bar{R}_l^{(0)}(k)ec + \bar{R}_u^{(2)}(k)et\sqrt{2} \end{bmatrix} \chi_{-s} \ . \tag{4.3.13}$$

The normalization condition is then seen to be

$$\int_0^\infty dk\ k^2 \left\{ \left[\bar{R}_u^{(0)}(k)\right]^2 + \left[\bar{R}_u^{(2)}(k)\right]^2 + \left[\bar{R}_l^{(0)}(k)\right]^2 + \left[\bar{R}_l^{(2)}(k)\right]^2 \right\} = 1 \ , \tag{4.3.14}$$

where $e \equiv \vec{\sigma}.\hat{k}$. Here superscripts 0 and 2 refer to the S-wave and D-wave components of the vector-meson wave function. These are

$$\bar{R}_u^{(0)}(k) = \Pi(k)\left[(\tilde{A}-\tilde{B}) - (A-B)\frac{k^2}{3\epsilon_q m_q}\right] ,$$

$$\bar{R}_u^{(2)}(k) = \Pi(k)\left[-\frac{\sqrt{2}}{3}\right](A-B)\frac{k^2}{3\epsilon_q m_q} ,$$

$$\bar{R}_l^{(0)}(k) = \Pi(k)\left[-(A+B)\frac{k}{3m_q} + (\tilde{A}+\tilde{B})\frac{k}{3\epsilon_q}\right] ,$$

$$\bar{R}_1^{(2)}(k) = \eta(k)\left[-\frac{\sqrt{2}}{3}\right]\left[(A+B)\frac{k}{m_q} + (\tilde{A}+\tilde{B})\frac{2k}{\epsilon_q}\right] , \qquad (4.3.15)$$

where

$$\eta(k) = \frac{1}{\pi}\sqrt{\frac{\epsilon_q}{2ME_q}} .$$

In the case of the vector mesons (see [53]), the kernel of the integral equation is a 4x4 matrix. In this work we have simplified our analysis by making an S-wave approximation, that is, the D-wave components of the above wave function are put equal to zero. This leads an equation with a kernel which is a 2x2 matrix. In other words, in this approximation, we have to solve for only <u>two</u> invariant amplitudes. Note that in the case of a meson with isospin 0, such as φ, charmonium and b-quarkonium, the isospin factor I_t has to be replaced by a factor $1/\sqrt{2}$, so that we can use the same integral equations and normalization conditions as those used for mesons of non-zero-isospin.

4.4 <u>Integral Equations for Pseudoscalar and Vector Mesons</u> :

Finally, we quote the integral equation, which is obtained using the above procedure, after the introduction of various form factors. We follow [52], where the analysis is carried out in the quark rest frame ($\vec{k}$=0).

For pseudoscalar mesons, the integral equation is

$$w(\vec{p})\begin{bmatrix} R_u(p) \\ R_l(p) \end{bmatrix} = -\left[g_\chi^{eff}\right]^2 \int \frac{d^3\vec{P}'}{(2\pi)^3} \frac{4M}{\sqrt{4w(\vec{P})w(\vec{P}')}} \frac{F_s(q^2)}{[m_\chi^2 - q^2]} \begin{bmatrix} 1 & 0 \\ 0 & -\hat{P}'.\hat{P} \end{bmatrix} \begin{bmatrix} R_u(p') \\ R_l(p') \end{bmatrix}$$

$$- \frac{4}{3}g^2 \int \frac{d^3\vec{P}'}{(2\pi)^3} \frac{f_G(q_k^2)}{\sqrt{w(\vec{P})w(\vec{P}')}} \frac{1}{[m_{gl}^2 - q^2]} \frac{m_q^3\,[w+w']^2}{[ww'+M^2+\vec{P}.\vec{P}']^2}$$

$$\times \begin{bmatrix} 2 - \frac{E_q'}{m_q} & -\frac{\hat{P}'.\vec{k}'}{m_q} \\ \frac{\vec{k}'.\hat{P}}{m_q} & \hat{P}'.\hat{P} + \frac{\hat{P}.\vec{k}'\ \hat{P}'.\vec{k}'}{m_q \epsilon_q} \end{bmatrix} \begin{bmatrix} R_u(p') \\ R_l(p') \end{bmatrix} , \qquad (4.4.1)$$

where $w \equiv w(\vec{P})$, $E_q \equiv E_q(\vec{k})$ and $\epsilon_q \equiv E_q + m_q$. In this equation we have also included a term representing "one-gluon-exchange" (the second integral on the right-hand side). [The Lagrangian of Eq.(2.4.8) has been used.] Here $f_G(q_k^2)$ is a high-momentum cutoff for the gluon-exchange kernel and

$$\begin{bmatrix} R_u(p) \\ R_l(p) \end{bmatrix} = \frac{1}{\sqrt{w(\vec{P})}} \begin{bmatrix} E(p) - F(p)\frac{w(\vec{P})}{M} \\ -F(p)\,\frac{p}{M} \end{bmatrix} . \qquad (4.4.2)$$

Further, $F_s(q^2)$ is a scalar form factor, which is given by

$$F_s(q^2) = \frac{4}{2M}\int\frac{d^3k}{(2\pi)^3}\,\frac{m_q}{E_q}\left\{EE' + FF'\,\frac{P'.P}{M^2} - E'F\,\frac{P.k}{M\,m_q} - EF'\frac{P'.k}{M\,m_q}\right\}, \qquad (4.4.3)$$

where

$$E = E\left[\left\{\left[\frac{P.k}{m_q}\right]^2 - M^2\right\}^{\frac{1}{2}}\right],$$

$$E' = E'\left[\left\{\left[\frac{P'.k}{m_q}\right]^2 - M^2\right\}^{\frac{1}{2}}\right], \qquad (4.4.4)$$

with similar expressions for F and F'. These definitions are different from those given in Eq.(4.3.4). [Those definitions are more useful, when we work in the meson rest frame.]

In the case of the vector mesons, the appropriate integral equation is found to be

$$w(\vec{p})\begin{bmatrix} R_u(p) \\ R_l(p) \end{bmatrix} = -\left[g_\chi^{eff}\right]^2 \frac{1}{3}\int \frac{d^3\vec{P}'}{(2\pi)^3} \frac{4M}{\sqrt{4w(\vec{P})w(\vec{P}')}} \frac{1}{[m_\chi^2 - q^2]}$$

$$\times \left\{ \begin{bmatrix} V_{11}^1 & V_{12}^1 \\ V_{21}^1 & V_{22}^1 \end{bmatrix} F_1(q^2) + \begin{bmatrix} V_{11}^2 & V_{12}^2 \\ V_{21}^2 & V_{22}^2 \end{bmatrix} F_2(q^2) \right\} \begin{bmatrix} R_u(p') \\ R_l(p') \end{bmatrix}$$

$$- \frac{4}{3}g^2 \frac{1}{3}\int \frac{d^3\vec{P}'}{(2\pi)^3} \frac{f_G(q_k^2)}{\sqrt{w(\vec{P})w(\vec{P}')}} \frac{1}{[m_{gl}^2 - q^2]} \frac{m_q^3 [w+w']^2}{[ww'+M^2+\vec{P}.\vec{P}']^2}$$

$$\times \begin{bmatrix} V_{11}^G & V_{12}^G \\ V_{21}^G & V_{22}^G \end{bmatrix} \begin{bmatrix} R_u(p') \\ R_l(p') \end{bmatrix}, \qquad (4.4.5)$$

where

$$V_{11}^1 = -\frac{w\vec{P}'^2}{M^3} - \frac{w'\vec{P}^2}{M^3} + \frac{\vec{P}.\vec{P}'}{M^2}\left[\frac{w}{M} + \frac{w'}{M} + \frac{ww'}{M^2} - 1\right]$$

$$- (\hat{P}.\hat{P}')^2 \frac{\vec{P}^2\,\vec{P}'^2}{M^4}\left[\frac{w}{w+M} + \frac{w'}{w'+M}\right] + (\hat{P}.\hat{P}')^3 \frac{p\,p'}{M^2}\left[1 - \frac{w'}{M} - \frac{w}{M} + \frac{ww'}{M^2}\right],$$

$$V_{22}^1 = \frac{p\,p'}{M^2}\left[1 - \frac{ww'}{M^2}\right] + (\hat{P}.\hat{P}')\left[\frac{w^2\vec{P}'^2 + w'^2\vec{P}^2}{M^4}\right]$$

$$- (\hat{P}.\hat{P}')^2 \frac{p\,p'}{M^2}\left[1 + \frac{ww'}{M^2}\right],$$

$$V_{11}^2 = \frac{\vec{P}.\vec{P}'}{M^2} - \frac{w}{M} - \frac{w'}{M} - 1 + (\hat{P}.\hat{P}')^2 \left[\frac{w'}{M} + \frac{w}{M} - \frac{ww'}{M^2} - 1 \right] ,$$

$$V_{22}^2 = - \frac{p\,p'}{M^2} + (\hat{P}.\hat{P}') \left[2 + \frac{ww'}{M^2} \right] ,$$

$$V_{12}^1 = V_{21}^1 = V_{21}^2 = V_{12}^2 = 0, \qquad (4.4.6)$$

and

$$V_{11}^G = \left[2 + \frac{w}{M} \right] - \frac{1}{\left[1 + \frac{w'}{M} \right]} \left\{ \left[\frac{-\vec{k}'^2}{m_q^2} + \frac{(k'.\hat{P})^2}{m_q^2} \right] + \left[\frac{p}{M} \frac{E_q}{m_q} - \frac{(k'.\hat{P})}{m_q} \frac{w}{M} \right] \left[\frac{p}{M} + \frac{(k'.\hat{P})}{m_q} \right] \right\} ,$$

$$V_{12}^G = \frac{1}{\left[1 + \frac{w}{M} \right]} \left[\frac{p'}{M} \frac{E_q}{m_q} + \frac{(k'.\hat{P}')}{m_q} \frac{w'}{M} \right] \left[\frac{w'}{M} + \frac{E_q}{m_q} \right] - \frac{p'}{M} ,$$

$$V_{21}^G = \frac{1}{\left[1 + \frac{w'}{M} \right]} \left[\frac{p}{M} \frac{E_q}{m_q} - \frac{(k'.\hat{P})}{m_q} \frac{w}{M} \right] \left[\frac{w}{M} + \frac{E_q}{m_q} \right] - \frac{p}{M} ,$$

$$V_{22}^G = - \frac{M}{p'} \left\{ \left[\frac{p}{M} \frac{E_q}{m_q} - \frac{(k'.\hat{P})}{m_q} \frac{w}{M} \right] \left[\frac{w}{M} + \frac{E_q}{m_q} - 4 \right] - \frac{w'p}{M^2} + \frac{\vec{k}'.\hat{P}}{m_q} \right\} , \qquad (4.4.7)$$

with $p \equiv |\vec{P}|$, $p' \equiv |\vec{P}'|$ and $w \equiv w(\vec{P})$, $w' \equiv w(\vec{P}')$. $F_1(q^2)$ and $F_2(q^2)$ are form factors given by the expressions

$$F_1(q^2) = \frac{2}{M}\int\frac{d^3k}{(2\pi)^3}\frac{m_q}{E_q}\left\{\frac{f_1}{4}\left[\frac{(\tilde{\pi}.k)^2}{m_q^2(\tilde{\pi}^2)^2} - \frac{(\tilde{q}.k)^2}{m_q^2(\tilde{q}^2)^2}\right]\right.$$

$$+\frac{f_1}{8}\left[1 - \frac{(\tilde{\pi}.k)^2}{m_q^2\,\tilde{\pi}^2} - \frac{(\tilde{q}.k)^2}{m_q^2\,\tilde{q}^2}\right]\left[\frac{1}{\tilde{q}^2} - \frac{1}{\tilde{\pi}^2}\right]$$

$$\left.+\frac{f_2}{2}\left[\frac{\tilde{\pi}.k}{m_q\,\tilde{\pi}^2} - \frac{\tilde{q}.k}{m_q\,\tilde{q}^2}\right] + \frac{f_3}{2}\left[\frac{\tilde{\pi}.k}{m_q\,\tilde{\pi}^2} + \frac{\tilde{q}.k}{m_q\,\tilde{q}^2}\right] + f_5\right\}, \quad (4.4.8)$$

and

$$F_2(q^2) = \frac{2}{M}\int\frac{d^3k}{(2\pi)^3}\frac{m_q}{E_q}\left\{f_4 + \frac{f_1}{2}\left[1 - \frac{(\tilde{\pi}.k)^2}{m_q^2\,\tilde{\pi}^2} - \frac{(\tilde{q}.k)^2}{m_q^2\,\tilde{q}^2}\right]\right\}, \quad (4.4.9)$$

Here we have defined

$$\tilde{q}^\mu = \frac{(P'-P)^\mu}{2M},$$

and

$$\tilde{\pi}^\mu = \frac{(P'+P)^\mu}{2M}.$$

Further, f_1, f_2, f_3, f_4 and f_5 are functions of P.k and P'.k and are given as

$$f_1 = -A_1A_1'\left\{1 + \frac{P.k}{m_qM} + \frac{P'.k}{m_q\,M} + \frac{P'.P}{M^2}\right\} - A_1'\tilde{A} - A_1\tilde{A}' - \frac{P'.P}{M^2}\left[A_1'\tilde{B} + A_1\tilde{B}'\right],$$

$$f_2 = A_1' \tilde{B} \frac{P.k}{m_q M} - A_1' \tilde{A} - \tilde{B}' \tilde{A} ,$$

$$f_3 = A_1 \tilde{B}' \frac{P'.k}{m_q M} - A_1 \tilde{A}' - \tilde{B} \tilde{A}' ,$$

$$f_4 = -\tilde{A} \tilde{A}' + \tilde{A}' \tilde{B} \frac{P.k}{m_q M} + \tilde{B}' \tilde{A} \frac{P'.k}{m_q M} - \tilde{B} \tilde{B}' \frac{P'.P}{M^2} ,$$

$$f_5 = \tilde{B} \tilde{B}' , \qquad (4.4.10)$$

where

$$A_1 \equiv - \frac{\tilde{A} + \tilde{B}}{\left[1 + \frac{P.k}{M m_q}\right]} . \qquad (4.4.11)$$

4.5 Leptonic Widths :

As we noted in Chapter 1, there are many models which may be used to fit the spectra of various mesons. However, a good model should also yield wave functions that allow one to calculate various decay properties in agreement with experimental values. As a test of our wave functions, we calculated the leptonic widths of various vector mesons. We found that we must include the "one-gluon-exchange" interaction in our model in order to obtain good values for the leptonic widths. It is interesting to see that the calculation of decay properties requires the knowledge of the vertex function, which is obtained as the solution of our integral equation. In other words,

decay widths depend upon the invariant amplitudes and, therefore, we can obtain fully relativistic results in our formalism.

The calculation of the Feynman diagram of Fig.9 yields an expression for the leptonic width of a meson,

$$\Gamma_{e^+e^-} = \frac{4\,\alpha^2 e_q^2}{M_V^2}\left[\frac{\kappa}{2}\right]^2 , \tag{4.5.1}$$

where

$$\frac{\kappa}{2} = [2\pi]^{-\frac{3}{2}} \int d^3k \,\frac{m_q}{E_q}\sqrt{\frac{2\nu}{(\nu+1)}}\left\{\frac{\nu+1}{2}\,\overline{R}_u^{(0)}(k) - \sqrt{\frac{\nu^2-1}{6}}\,\overline{R}_1^{(0)}(k)\right\} , \tag{4.5.2}$$

and

$$\nu = \frac{P.k}{M\,m_q} . \tag{4.5.3}$$

The details of this calculation are given in [51].

In the frame where $\vec{P}=0$, $\nu = \frac{E_q}{m_q}$. Now, in the nonrelativistic limit, $\nu \to 1$, so that,

$$\frac{\kappa}{2}^{NR} = [2\pi]^{-\frac{3}{2}} \int d^3k \;\overline{R}_u^{(0)}(k)$$

$$= \hat{R}_u(r=0) , \tag{4.5.4}$$

where $\hat{R}_u(r=0)$ is the coordinate-space wave function evaluated at the

origin. Thus, the nonrelativistic limit of Eq.(4.5.1) is

$$\Gamma^{NR}_{e^+e^-} = \frac{4\,\alpha^2 e_q^2}{M_V^2}\left|\hat{R}_u(0)\right|^2 . \tag{4.5.5}$$

This is the Van Royen-Weisskopf [54] result, except for the fact that

$$\int_0^\infty dr\; r^2\,\hat{R}_u^2(r) \neq 1.$$

In this work the coordinate-space wave functions are normalized such that

$$\int_0^\infty dr\; r^2\left[\hat{R}_u^2(r) + \hat{R}_l^2(r)\right] = 1. \tag{4.5.6}$$

We can now define a wave function, $\tilde{R}_u(r) = N\,\hat{R}_u(r)$, such that

$$\int_0^\infty dr\; r^2\,\tilde{R}_u^2(r) = 1\ , \tag{4.5.7}$$

and also define a leptonic width,

$$\Gamma^{NR}_{e^+e^-} = \frac{4\,\alpha^2 e_q^2}{M_V^2}\left|\tilde{R}_u(0)\right|^2 . \tag{4.5.8}$$

Note that the expressions given in Eq.(4.5.5) and Eq.(4.5.8) were used to generate the columns labelled by (a) and (b) in Table B. Equations (4.5.1) and (4.5.2) were used in the calculation of the leptonic

widths given in the first column (labelled covariant analysis) in Table B. We will discuss our numerical results in Chapter 6.

CHAPTER 5

Fully-Off-Shell Problem

5.1 Propagating and Nonpropagating Modes :

Yukawa introduced the idea that the nuclear force is the result of the exchange of mesons whose mass might be ≈100 Mev. After a period of confusion which followed the discovery of the μ meson, the π meson was discovered. It was believed that this was the strongly interacting meson predicted by Yukawa. Later researchers introduced σ(scalar), ρ (vector) and ω (vector) mesons to describe the nuclear force and to explain nuclear observables.

In recent years, the use of the Dirac equation for describing nucleon dynamics in nuclei has become quite popular [29, 30]. At the center of the success of the relativistic theories are phenomenological (Lorentz) scalar and vector fields which are coupled to the nucleons. These fields can be produced by the exchange of elementary fields with quantum number of the σ, π, ρ and ω mesons. As described in [30], one may first consider the coupling of these fields to quarks and then the coupling of these fields to nucleons can be inferred.

There is some confusion concerning the nature of these fields. Many authors do not distinguish between these fields and the physical mesons observed in the laboratory. We note that no "physical" σ field, that is, a scalar particle with mass equal to 600 MeV, has been found experimentally. Another point one should note is that the size of the ρ, ω and other mesons is of the order of 0.7 fm [55]. However, the average separation between the nucleons inside the nucleus is $\approx$ 1.2 fm. Therefore it is hard to see how the physical mesons can be accomodated inside the nucleus. Our successful calculation of leptonic widths suggests that the mesons we constructed using the covariant soliton model are of the correct size. It seems that the meson fields used in nuclear physics are just "meson-like" fields. One reason for confusion may be that the masses of these meson-like fields, which are used to fit nuclear data, are the same as the masses of physical mesons.

Similar meson-like fields are used in the chiral soliton model [56] and in the global color model of Cahill, Roberts and Praschifka [42]. The chiral soliton model might be used to describe mesons, as well as nucleons. The Lagrangian is

$$\mathcal{L}_{\text{chiral}}(x) = \bar{q}(x)\left[i\gamma_\mu\partial^\mu - g_\pi[S(x)+i\vec{\tau}.\vec{P}(x)\gamma_5]\right]q(x)$$

$$+ \frac{1}{2}\left([\partial_\mu S(x)]^2+[\partial_\mu\vec{P}(x)]^2\right) - \frac{\lambda}{4}\left(S^2(x)+\vec{P}^2(x) - f_\pi^2\right)^2, \tag{5.1.1}$$

where $S(x)$ and $\vec{P}(x)$ are meson-like fields. The above equation can be taken to represent an <u>effective</u> Lagrangian for the Nambu - Jona-Lasinio model, if the effective potential is calculated through two-loop order. One may also add a term which gives the pseudoscalar field a mass and which explicitly breaks chiral symmetry.

Now, by defining

$$\Sigma(x) = g_\pi[S(x)+i\vec{\tau}.\vec{P}(x)\gamma_5],$$

the above Lagrangian reduces to

$$\mathcal{L}_{\text{chiral}}(x) = \bar{q}(x)\left[i\gamma_\mu\partial^\mu - \Sigma(x)\right]q(x)$$

$$+ \frac{1}{2}\left([\partial_\mu S(x)]^2+[\partial_\mu\vec{P}(x)]^2\right) - \frac{\lambda}{4}\left(S^2(x)+\vec{P}^2(x) - f_\pi^2\right)^2. \tag{5.1.2}$$

That is, the $S(x)$ and $\vec{P}(x)$ fields can be interpreted as parameterizing the self-energy of the quark. If Eq.(5.1.2) is to represent a good model of QCD, the physical pion should appear as a nontopological soliton. This further requires that the $S(x)$ and $\vec{P}(x)$ fields are

nonpropagating modes. If the pion emerges as a soliton solution of the Lagrangian of Eq.(5.1.2), it is essential that $\vec{P}(x)$ be nonpropagating. Otherwise one would have two zero-mass 0^- excitations in the theory, which would not correspond to the particles observed in nature.

Thus, it seems that the meson-like fields used in relativistic nuclear physics, in the chiral soliton model, and in "skyrmion" physics [57] are nonpropagating modes. In the last chapter we have shown that, under certain assumptions, the quark is nonpropagating in the QCD vacuum. Similarly, gluons are also nonpropagating modes, as shown in [58]. Propagating modes of QCD are the physical hadrons. They can be described as nontopological solitons, which may be constructed using the nonpropagating modes of QCD as the degrees of freedom. [The field, $\chi(x)$, is also a nonpropagating field. However, we need not introduce a self-energy of the form we used for the quark in (time-like region) for the χ field, since the momentum components of $\chi(x)$ are always space-like in our model.

5.2 On-Mass-Shell Approximation :

As we noted earlier, it should be possible to describe all physical mesons as nontopological solitons of the effective Lagrangian we derived from QCD. We have been able to describe all mesons except the pion and the open-flavor mesons. In the case of the pion, the

meson (pion) mass is less than the dynamical mass of the constituents (u and d quark). In the case of open-flavor mesons, the meson mass is close to the heavier quark mass. As a result, the approximation of keeping one quark on mass-shell causes the off-shell quark to be driven too far from the on-mass-shell condition. In other words, there is a large asymmetry in the treatment of the quarks, if we apply our on-mass-shell approximation in the case of the pion or in the case of open-flavor mesons. These problems may be seen in the case of the ρ meson where the dynamical mass of the u or d quark used to fit the experimental mass is different from the theoretical value quoted in Chapter 2. It is also troubling that the leptonic widths of the states close to and above the open-flavor threshold are not in good agreement with the experimental values. We believe that by allowing both quarks to go off-mass-shell, the above-mentioned problems may be resolved.

Placing one quark on mass shell simplifies the problem greatly. Since the meson is also on mass shell, the construction of the wave function (or the vertex functions) only involves the specification of amplitudes which are functions of a single variable. This approximation is best if the system is weakly coupled. In that case the particles stay quite close to their mass shells and placing the

spectator particle on mass shell does not introduce a significant asymmetry into the dynamics of the fermions.

Let us assume that a meson with momentum P decays (virtually) into its constituents. For simplicity, we consider the constituents to be two scalar particles with momentum k and P-k. We have, $P^2=M^2$, since the meson is on mass shell. Therefore, the wave function of the system is a function of two variables, which can taken to be $(P-k)^2$ and k^2. We write, therefore, $\Phi = \Phi[(P-k)^2,k^2]$. If the system is weakly coupled, we may look for an approximate solution of the form

$$\Phi[(P-k)^2,k^2] \approx f_1[(P-k)^2]\ \delta(k^2-m^2)\ \theta(k^0) \quad , \tag{5.2.1}$$

where the function $f_1[(P-k)^2]$ is to be determined from the dynamical equations. A more symmetrical treatment would involve the approximation,

$$\Phi[(P-k)^2,k^2] \approx \frac{1}{\sqrt{2}} \Big[f_1[(P-k)^2]\ \delta(k^2-m^2)\ \theta(k^0) + f_2(k^2)\ \delta[(P-k)^2-m^2]\ \theta(P^0-k^0) \Big]. \tag{5.2.2}$$

The corresponding equations in the case of (virtual) mesonic decay into a quark and an antiquark are more complicated since, several amplitudes are needed to describe the wave function, if the particles have spin. However, the off-mass-shell kinematics are similar to the

scalar case. Therefore, we choose this model to study the fully off-mass-shell problem in this chapter as a first step.

When we work with a quark (antiquark) on-mass-shell, the off-mass-shell antiquark (quark) has a squared four momentum $(P-k)^2$ in the meson rest frame ($\vec{P}=0$) which is given by given by Eq.(3.5.1),

$$(P-k)^2 = M^2 + m_q^2 - 2P.k \ ,$$

$$= M^2 + m_q^2 - 2M\sqrt{\vec{k}^2 + m_q^2} \quad . \qquad (5.2.3)$$

Now if $\vec{k}=0$, we have $(P-k)^2=(M-m_q)^2$. Thus, we see that $(P-k)^2 \leq (M-m_q)^2$. In the weak-coupling case, where $M \approx 2m_q$, we have $(P-k)^2 \approx m_q^2$, so that in this case the spectator and the off-shell fermion have similar dynamics. Now this discussion raises the question as to whether hadrons are weakly coupled in the sense that $M \approx 2m_q$. In the previous analysis of this model [52] it was found that the binding effects were of the order of 25% in low-lying hadronic states. [We are here discussing the situation where $\Sigma[(P-k)^2]$ is taken to be a constant equal to m_q.] Therefore, the approximation of placing the spectator quark (or antiquark) on mass shell introduces a non-negligible asymmetry in the dynamics of the fermions. This inherent asymmetry of treatment becomes more apparent in the extension of our model to

include confinement. However, in Fig.1 we see that for the 3S, 4S and 5S states there is a degree of consistency achieved for the description of the off-mass-shell quark and spectator antiquark.

5.3 Covariant Soliton Dynamics: Fully-Off-Mass-Shell Dynamics

For simplicity, we consider a toy model, a meson made up of two scalar constituents, interacting with a scalar field, $\chi(x)$. The Lagrangian is

$$\mathcal{L}(x) = \frac{1}{2}[\partial_\mu\varphi(x)\partial^\mu\varphi(x) - m^2\,\varphi^2(x)]$$

$$+\frac{1}{2}[\partial_\mu\chi(x)\partial^\mu\chi(x) - m_\chi^2\,\chi^2(x)] + \frac{g_\chi}{2}\,\varphi^2(x)\chi(x). \qquad (5.3.1)$$

The equations of motion are

$$[\partial^2 + m^2]\varphi(x) = g_\chi\,\varphi(x)\chi(x),$$

$$[\partial^2 + m_\chi^2]\chi(x) = \frac{g_\chi}{2}\,\varphi^2(x) \quad . \qquad (5.3.2)$$

This model was first studied by Wick and Cutkosky [59, 60] in the ladder approximation. Further studies of this model, with different approximations, were carried out by various groups [61, 25]. In [25], one constituent was kept on mass shell and a linear (ladder approximation) and a nonlinear (covariant soliton) version of this model were studied. In this section we discuss the nonlinear version of this model with both constituents off-mass-shell. Let

$$\Psi_P(x_1,x_2) \equiv \langle 0|T[\varphi(x_1)\varphi(x_2)]|\vec{P}\rangle ,$$

where $|\vec{P}\rangle$ is a meson with momentum $\vec{P}$. We have

$$[\partial_1^2 + m_1^2]\varphi(x_1) = g_\chi \varphi(x_1)\chi(x_1),$$

and

$$[\partial_2^2 + m_2^2]\varphi(x_2) = g_\chi \varphi(x_2)\chi(x_2) .$$

Therefore,

$$[\partial_1^2 + m_1^2]T[\varphi(x_1)\varphi(x_2)] = g_\chi T[\varphi(x_1)\chi(x_1)\varphi(x_2)],$$

and

$$[\partial_2^2 + m_2^2]T[\varphi(x_1)\varphi(x_2)] = g_\chi T[\varphi(x_1)\chi(x_2)\varphi(x_2)]. \qquad (5.3.3)$$

Note that, when we operate with ∂_1^2 or ∂_2^2 in forming these expressions, we will find some delta functions whose contributions may be seen to be zero. We also note that we will shortly replace m^2 by $\Sigma^2(q^2)$, a self-energy of the form described earlier.

From the above equations it follows that

$$[\partial_2^2 + m_2^2][\partial_1^2 + m_1^2]\langle 0|T[\varphi(x_1)\varphi(x_2)]|\vec{P}\rangle$$

$$= g_\chi [\partial_2^2 + m_2^2]\langle 0|T[\varphi(x_1)\chi(x_1)\varphi(x_2)]|\vec{P}\rangle, \qquad (5.3.4)$$

and

$$[\partial_1^2 + m_1^2][\partial_2^2 + m_2^2] \langle 0|T[\varphi(x_1)\varphi(x_2)]|\vec{P}\rangle$$

$$= g_\chi[\partial_1^2 + m_1^2]\langle 0|T[\varphi(x_1)\chi(x_2)\varphi(x_2)]|\vec{P}\rangle. \quad (5.3.5)$$

We may add these two equations to get

$$[\partial_1^2 + m_1^2][\partial_2^2 + m_2^2]\langle 0|T[\varphi(x_1)\varphi(x_2)]|\vec{P}\rangle$$

$$= \frac{g_\chi}{2}[\partial_1^2 + m_1^2]\langle 0|T[\varphi(x_1)\chi(x_2)\varphi(x_2)]|\vec{P}\rangle$$

$$+ \frac{g_\chi}{2}[\partial_2^2 + m_2^2]\langle 0|T[\varphi(x_1)\chi(x_1)\varphi(x_2)]|\vec{P}\rangle. \quad (5.3.6)$$

Note that $\varphi(x)$ and $\chi(x)$ are different fields and therefore commute. Rearranging the fields and inserting a complete set of soliton states leads to

$$[\partial_1^2 + m_1^2][\partial_2^2 + m_2^2]\langle 0|T[\varphi(x_1)\varphi(x_2)]|\vec{P}\rangle$$

$$= \frac{g_\chi}{2}\int d^3P' \Big\{[\partial_1^2 + m_1^2]\langle 0|T[\varphi(x_1)\varphi(x_2)]|\vec{P}'\rangle\langle\vec{P}'|\chi(x_2)|\vec{P}\rangle$$

$$+[\partial_2^2 + m_2^2]\langle 0|T[\varphi(x_1)\varphi(x_2)]|\vec{P}'\rangle\langle\vec{P}'|\chi(x_1)|\vec{P}\rangle\Big\}. \quad (5.3.7)$$

Using

$$\langle 0|T[\varphi(x_1)\varphi(x_2)]|\vec{P}\rangle = \langle 0|T[\varphi(0)\varphi(x_2-x_1)]|\vec{P}\rangle\, e^{-iP.x_1},$$

and defining

$$\langle 0|T[\varphi(0)\varphi(x_2-x_1)]|\vec{P}\rangle = \int \frac{d^4k}{(2\pi)^4}\, e^{-ik.(x_2-x_1)}\, \Psi_P(k) \ ,$$

the above equation becomes

$$[-(P-k)^2 + m_1^2][-k^2 + m_2^2]\ \Psi_P(k)$$

$$= \frac{g_\chi}{2}\int d^3\vec{P}'\langle\vec{P}'|\chi(0)|\vec{P}\rangle[-k^2 + m_2^2]\ \Psi_{P'}(k)$$

$$+ \frac{g_\chi}{2}\int d^3\vec{P}'\langle\vec{P}'|\chi(0)|\vec{P}\rangle[-(P-k)^2 + m_1^2]\ \Psi_{P'}(P-k) \ ,$$

or

$$[-(P-k)^2 + m_1^2][-k^2 + m_2^2]\ \Psi_P(k)$$

$$= \frac{g_\chi}{2}\int d^3\vec{P}'\langle\vec{P}'|\chi(0)|\vec{P}\rangle\Big[[-k^2 + m_2^2]\Psi_{P'}(k) + [-(P-k)^2 + m_1^2]\Psi_{P'}(P-k)\Big]. \tag{5.3.8}$$

The diagrammatic representation of this integral equation is given in Figures 10 and 11. Note that Eq.(5.3.8) is symmetric with respect to $P-k \to k$ and $k \to P-k$. The equation determining the wave function is

$$\Psi_P(k) = \frac{g_\chi}{2}\int d^3\vec{P}'\langle\vec{P}'|\chi(0)|\vec{P}\rangle\Big[[-(P-k)^2+m_1^2]^{-1}\Psi_{P'}(k) + [-k^2+m_2^2]^{-1}\Psi_{P'}(P-k)\Big].$$

We now introduce the self-energy:

$$\Psi_P(k)= \frac{g_\chi}{2}\int d^3\vec{P}' \langle\vec{P}'|\chi(0)|\vec{P}\rangle\Big[\Big\{-(P-k)^2+ \Sigma^2[(P-k)^2]\Big\}^{-1}\Psi_{P'}(k)$$

$$+ \Big\{-k^2+ \Sigma^2(k^2)\Big\}^{-1}\Psi_{P'}(P-k)\Big] \ . \qquad (5.3.9)$$

In writing the above equation we assumed that both the constituents have the same mass or self-energy.

From the equation of motion for $\chi(x)$ we obtain

$$\langle\vec{P}'|\chi(0)|\vec{P}\rangle = \frac{g_\chi}{2}\frac{\langle\vec{P}'|\varphi^2(0)|\vec{P}\rangle}{[-(P'-P)^2+m_\chi^2]} \ ,$$

$$\equiv -\Big[\frac{g_\chi}{2}\Big]\frac{1}{[q^2 - m_\chi^2]}\frac{1}{(2\pi)^3\sqrt{4w(\vec{P})w(\vec{P}')}}F(q^2), \qquad (5.3.10)$$

where $q^2 \equiv (P-P')^2$. We define the <u>form factor</u> by means of the following expression,

$$F(q^2) = (2\pi)^3\sqrt{4w(\vec{P})w(\vec{p}')}\int\frac{d^4k'}{(2\pi)^4}\Psi_P(k')\Big\{-k'^2 + \Sigma^2(k'^2)\Big\}\Psi_{P'}(k'). \qquad (5.3.11)$$

This form represents an assumption of the model, since we are dealing with confined particles and do not have Feynman rules available to us. We also do not know how to obtain our previous on-mass-shell approximation from the fully-off-shell version of the model at this point. (In the current model, the quark can never go on-mass-shell.)

Substituting for $\langle\vec{P}'|\chi(0)|\vec{P}\rangle$ in Eq.(5.3.9), we get

$$\Psi_P(k) = + \frac{g_\chi^2}{4}\int \frac{d^3\vec{P}'}{[q^2-m_\chi^2]}\int \frac{d^4k'}{(2\pi)^4}\Psi_P(k')\left\{-k'^2 + \Sigma^2(k'^2)\right\}\Psi_{P'}(k')$$

$$\times \left[\left\{-(P-k)^2+ \Sigma^2[(P-k)^2]\right\}^{-1}\Psi_{P'}(k) + \left\{-k^2+ \Sigma^2(k^2)\right\}^{-1}\Psi_{P'}(P-k)\right], \tag{5.3.12}$$

Interchanging the integrals, we have

$$\Psi_P(k) = + \frac{g_\chi^2}{4}\int \frac{d^4k'}{(2\pi)^4}\,\Psi_P(k')\int \frac{d^3\vec{P}'}{[q^2- m_\chi^2]}\left\{-k'^2+ \Sigma^2(k'^2)\right\}\Psi_{P'}(k')$$

$$\times \left[\left\{-(P-k)^2+ \Sigma^2[(P-k)^2]\right\}^{-1}\Psi_{P'}(k) + \left\{-k^2+ \Sigma^2(k^2)\right\}^{-1}\Psi_{P'}(P-k)\right]. \tag{5.3.13}$$

In the second term we can make a change of variables, $k' \to P-k'$, and obtain

$$\Psi_P(k) = + \frac{g_\chi^2}{4}\int \frac{d^4k'}{(2\pi)^4}\,\Psi_P(k')\int \frac{d^3\vec{P}'}{[q^2- m_\chi^2]}\left(\left\{-k'^2 + \Sigma^2(k'^2)\right\}\right.$$

$$\times \Psi_{P'}(k')\left\{-(P-k)^2+ \Sigma^2[(P-k)^2]\right\}^{-1}\Psi_{P'}(k)$$

$$\left. + \left\{-(P-k')^2+ \Sigma^2[(P-k')^2]\right\}\Psi_{P'}(P-k')\left\{-k^2+ \Sigma^2(k^2)\right\}^{-1}\Psi_{P'}(P-k)\right), \tag{5.3.14}$$

or

$$\left\{-k^2+\Sigma^2(k^2)\right\}\left\{-(P-k)^2+\Sigma^2[(P-k)^2]\right\}\Psi_P(k)$$

$$= +\frac{g_\chi^2}{4}\int\frac{d^4k'}{(2\pi)^4}\Psi_P(k')\int\frac{d^3\vec{P}'}{[q^2-m_\chi^2]}\Bigg(\left\{-k'^2+\Sigma^2(k'^2)\right\}\left\{-k^2+\Sigma^2(k^2)\right\}$$

$$\times\Psi_{P'}(k')\Psi_{P'}(k)+\left\{-(P-k)^2+\Sigma^2[(P-k)^2]\right\}$$

$$\times\left\{-(P-k')^2+\Sigma^2[(P-k')^2]\right\}\Psi_{P'}(P-k')\,\Psi_{P'}(P-k)\Bigg). \tag{5.3.15}$$

The kernel of the above equation is symmetric in k and k'. Defining the vertex function, $\Gamma[k^2,(P-k)^2]$, by the relation

$$\Psi_P(k)=\frac{1}{\sqrt{2w(\vec{P})(2\pi)^3}}\left\{-k^2+\Sigma^2(k^2)\right\}^{-1}\left\{-(P-k)^2+\Sigma^2[(P-k)^2]\right\}^{-1}\Gamma[k^2,(p-k)^2], \tag{5.3.16}$$

we can rewrite Eq.(5.3.15) in terms of the vertex function:

$$\Gamma[k^2,(P-k)^2] = + \frac{g_\chi^2}{4}\int \frac{d^4k'}{(2\pi)^4}\,\Gamma[k'^2,(P-k')^2]$$

$$\times \left\{-k'^2+\Sigma^2(k'^2)\right\}^{-1} \left\{-(P-k')^2+\Sigma^2[(P-k')^2]\right\}^{-1}$$

$$\times \int \frac{d^3\vec{P}'}{[q^2-m_\chi^2]}\,\frac{1}{2w(\vec{P}')(2\pi)^3}\Bigg(\left\{-(P'-k')^2+\Sigma^2[(P'-k')^2]\right\}^{-1}$$

$$\times \left\{-(P'-k)^2+\Sigma^2[(P'-k)^2]\right\}^{-1} \Gamma[k'^2,(P'-k')^2]\;\Gamma[k^2,(P'-k)^2]$$

$$+ \left\{-(P'-P+k')^2+\Sigma^2[(P'-P+k')^2]\right\}^{-1} \left\{-(P'-P+k)^2+\Sigma^2[(P'-P+k)^2]\right\}^{-1}$$

$$\times \Gamma[(P-k')^2,(P'-P+k')^2]\;\Gamma[(P-k)^2,(P'-P+k)^2]\Bigg). \tag{5.3.17}$$

The wave function is a function of two variables, $(P-k)^2$ and k^2, and is symmetric with respect to these variables. Equivalently, one can choose x and y as two variables, defined as

$$x = \sqrt{\left\{\frac{P.k}{M}\right\}^2 - k^2} \quad \text{and} \quad y = \left\{\frac{P.k}{M}\right\}. \tag{5.3.18}$$

In the meson rest frame ($\vec{P} = 0$), $x = |\vec{k}| = k$ and $y = k_0$. Thus, Eq.(5.3.15) reduces to

$$\left\{-k^2+\Sigma^2(k^2)\right\}\left\{-v^2+\Sigma^2(v^2)\right\}\Psi(k,k^0)=$$

$$+\frac{g_\chi^2}{4}\int\frac{dk'\,k'^2}{(2\pi)^4}\,dk'_0\;\chi(k,k')\;\Psi(k',k'^0), \qquad (5.3.19)$$

where

$$\chi(k,k') \equiv \int d\cos\theta_k,\; d\phi_k,\; \int\frac{d^3\vec{P}'}{[q^2-m_\chi^2]}\left(\left\{-k'^2+\Sigma^2[k'^2]\right\}\left\{-k^2+\Sigma^2(k^2)\right\}\right.$$

$$\left.\times\,\Psi_{P'}(k')\Psi_P(k)+\left\{-v^2+\Sigma^2(v^2)\right\}\left\{-v'^2+\Sigma^2(k'^2)\right\}\Psi_{P'}(v')\;\Psi_P(v)\right). \qquad (5.3.20)$$

We have defined

$$v \equiv (P-k)\Big|_{\vec{P}=0} \quad \text{and} \quad v' \equiv (P-k')\Big|_{\vec{P}=0}\ .$$

We see that we have to solve a nonlinear equation in <u>two variables</u>, Eq.(5.3.18), with the approximate normalization condition:

$$\frac{(2\pi)^3 2M}{2}\int\frac{d^4k}{(2\pi)^4}\,\Psi(k,k^0)\left\{-k^2+\Sigma^2(k^2)\right\}^{-1}\frac{\left\{M-k_0\right\}}{M}\,\Psi(k,k^0)=1\ . \qquad (5.3.21)$$

Again, as in our expression for the form factor [Eq.(5.3.11)], the equations given above are generalizations of equations where one quark was kept on mass shell. Numerical work is yet to be done.

CHAPTER 6

Numerical Results and Conclusions

We have solved the nonlinear, homogeneous equation, Eq.(4.4.1) [or Eq.(4.4.5)] numerically (in a self-consistent manner) as an eigenvalue problem. The procedure used is as follows. We guess the form factor for the first iteration and obtain the eigenvalue and eigenfunction. From the normalized eigenfunction we calculate the invariant amplitudes, which we then use to construct a new form factor for the next iteration. The iteration procedure is continued until the form factor of the n^{th} iteration is same as that of $(n-1)^{th}$ iteration. The wave function obtained at the final iteration is used to calculate the radius and decay properties of the meson.

The parameters of the model include the coupling constant, g_χ, and the current quark masses. We took $g_\chi = 7$, which is the value used in the previous studies of nucleon and meson structure in this model. Current quark masses are fixed by fitting the ground state of each quarkonium species. The strong coupling constant, α_s, and the gluon mass, M_{gl}, are two more parameters needed when we include a

description of one-gluon-exchange. (We used α_s=0.28.)

From the arguments in Chapter 2, we have $M_{gl}(\phi_0) \rightarrow M_{gl}(\phi(x))$ inside the hadron. This replacement involves the specification of the coupling of the gluon to the χ field. This is a complicated problem, which we do not attempt to solve here. Therefore, we used a constant value for M_{gl} and varied M_{gl} and α_s so that we obtained a reasonable η_c-J/ψ mass splitting and a satisfactory leptonic width for the J/ψ meson.

In addition to the parameters mentioned above, we also included a cutoff

$$f_c(q^2) = \left\{\frac{\Lambda^2}{\Lambda^2 - q^2}\right\}^3 , \qquad (6.1)$$

in the χ-field kernel in order to regulate the high-momentum components in the theory. In most of our work, we chose Λ = 10 fm^{-1} =2 GeV. This is a "physically" reasonable value, since we do not expect the χ field, which represents long-range (low-momentum) aspects of the dynamics, to describe short-distance (high-momentum) aspects. We also have a high-momentum cutoff

$$f_G(q_k^2) = \left\{\frac{\Lambda_k^2}{\Lambda_k^2 - q_k^2}\right\}^n , \qquad (6.2)$$

in Eq.(4.4.1) and Eq.(4.4.5). However, the results reported here are obtained without using the above form of cutoff. Instead we chose a different P_{max} (the upper limit of the "radial" P integration) for different mesons, so that we obtained good values for the leptonic widths. We also found that the P_{max} chosen to fit the leptonic widths had the following property: Once P_{max} was fixed the energy eigenvalue was stable with respect to further increase of P_{max}. (We saw, however, that the leptonic widths would change with further increase of P_{max} from the value originally chosen.) The values of P_{max} chosen for the different systems are given in Table B.

In the case of pseudoscalar mesons, it seems that the cutoff, $f_G(q_k^2)$, is necessary for the convergence of the integral. (Further numerical studies are in progress.

6.1 Mass of the Soliton :

First, we rewrote the left hand side of Eq.(4.4.1), or Eq.(4.4.5), putting $w(\vec{P})= \sqrt{\vec{P}^2+\lambda^2}$, where λ is the eigenvalue of interest. In all other places in our integral equations, we assumed a trial mass, M, for the soliton and then compared the calculated value of λ with M. Next, we chose M close to the calculated value for λ, and obtained

a new eigenvalue. This procedure was continued until the eigenvalue, λ, was almost equal to M, the meson mass. In other words, there are two iterations: one to obtain consistent solutions for the soliton mass M, and another to obtain consistent solutions for the form factors.

The spectra of various mesons are given in Tables C and D - F and in Figures 1 and 2. Table C and Figures 1 and 2 exhibit the results without the one-gluon-exchange contribution. We fit the center-of-gravity of pseudoscalar and vector meson states (in the case of charmonium) and the center-of-gravity of the triplets in the study of the P states. The masses which are underlined were used to fit the parameters of the model. In Fig.1, the long dashed line represents the open-flavor threshold energy. The continuum of our model (without confinement) is found to be close to the open-flavor threshold. Therefore, to obtain the states above the open-flavor threshold, we have to introduce a model for confinement, as mentioned in Chapter 3. Thus, we have two extra parameters: C=0.05, which is taken to be same for all mesons, and m_0, which is <u>flavor dependent</u>. C and m_0 are fixed so that we obtain a satisfactory fit to the spectrum of charmonium and of b-quarkonium. Values of m_0, m_q^{cur}, β and g_χ^{eff}, used in obtaining the results shown in Figures 1 and 2, are given in Table A. In

Figures 12 and 13 we compare the energy levels of J/ψ and Υ, obtained in various models and in our model, with experimental data. In Fig.2 we also show the ρ' and φ' states, which we obtained after introducing the confinement model.

Various results of our calculations, including the one-gluon-exchange contribution, are presented in Tables D - F. We performed some parameter searches to obtain satisfactory fits to the spectra and to the leptonic widths. The parameters determined in these searches are given in those tables.

6.2 Coordinate-Space Wave Functions and Meson Radii :

The wave functions we obtained are plotted in Figures 14 and 15. Without the one-gluon-exchange contribution, the wave functions are are too extended in coordinate space. The mesons are of rather large size, as shown in Fig.14. In Fig.15, the wave functions, which include the effects of one-gluon-exchange, are shown and we see that now the radii are smaller. [The coordinate-space wave functions are obtained by Fourier transformation of the momentum-space wave functions, Eq.(4.3.2) or Eq.(4.3.15). That is,

$$\hat{R}_u(r) = \sqrt{\frac{2}{\pi}} \int_0^\infty dk\ k^2\ \bar{R}_u(k)\ j_0(kr)\ , \qquad (6.2.1)$$

and

$$\hat{R}_l(r) = \sqrt{\frac{2}{\pi}} \int_0^\infty dk\ k^2\ \bar{R}_l(k)\ j_l(kr)\ , \qquad (6.2.2)$$

where $j_0(kr)$ and $j_1(kr)$ are Bessel functions of order 0 and 1, respectively.]

Once we have the coordinate-space wave functions, we can calculate the size of the meson: The root-mean-square radii of the baryon and scalar density of a meson are given by

$$\langle r^2 \rangle_B = \int_0^\infty dr\ r^2\ r^2\ \left[\hat{R}_u^2(r) + \hat{R}_l^2(r)\right]\ , \qquad (6.2.3)$$

and

$$\langle r^2 \rangle_S = \int_0^\infty dr\ r^2\ r^2\ \left[\hat{R}_u^2(r) - \hat{R}_l^2(r)\right]\ . \qquad (6.2.4)$$

The radii of various mesons, calculated using these formulae, are presented in Table D-F. In Fig. 16, we compare our wave functions with the wave functions given in [2]. Those wave functions were obtained in a lattice simulation, neglecting the spin of the quark (scalar-quark approximation), for the ρ, φ and J/ψ mesons. Our wave function agrees with that found in the lattice study for the J/ψ meson. For the ρ and φ mesons our results are different. This difference may reflect the fact that our analysis did not treat the quarks as scalar

particles and that the proper treatment of spin dynamics is important for light quark systems.

6.3 Leptonic Widths :

We have calculated the leptonic widths of various vector mesons using our covariant formulation - see Eq.(4.5.1). The results are presented in Table B. We have also calculated the leptonic widths using the nonrelativitic Van Royen-Weisskopf formula, Eq.(4.5.5) and Eq.(4.5.8), and have tabulated the results in Table B.

Generally, in potential models of meson structure, only the ratios of leptonic widths are calculated. The absolute values of leptonic widths are usually found to be too large. Therefore, workers in this field include "radiative" and relativistic corrections in their results [17]. [Since our calculation is covariant, and since our wave functions are expressed in terms of Lorentz-invariant amplitudes, we do not have significant uncertainties arising from the neglect of relativistic effects.] Researchers using potential models add "radiative corrections" to the Van Royen-Weisskopf formula. These corrections are patterned after the analysis used for radiative corrections in the case of positronium. Such corrections appear to be spurious, however. They are derived for a case in which the zero-order problem is governed by a Coulomb potential. The coordinate-space

potentials used in potential models of charmonium and b-quarkonium structure are certainly not of this character. From Table B, we see that, if we use our wave functions in the Van Royen-Weisskopf formula, we obtain satisfactory values for the leptonic widths. The results are particularly good for the states of the upsilon system. It is possible that this satisfactory outcome is due to the fact that we did not use a potential model to fit the spectra.

6.4 Conclusions :

We have studied a simple, field-theoretic model of nontopological solitons in a covariant formulation. We studied the relationship of our model, which is a unified model for all hadrons (both baryons and mesons), to QCD and studied various effective Lagrangians. Dynamical quark masses and the mass m_χ are related to the gluon condensate order-parameter ϕ_0. Our analysis leads to a flavor dependence of the coupling constant of the quark field to the scalar field. In fact, this modification considerably improved the fit to the spectra of mesons over the fit previously obtained in our model. (We saw that we needed to include "one-gluon-exchange" effects to obtain reasonable values for leptonic widths.)

We also introduced a covariant model of confinement which enabled us to describe the ρ', φ' mesons, the 3S and 4S states of charmonium,

and the 4S, 5S and 6S states of the upsilon system. Recently, we actually derived a model of confinement of this type by considering a self-consistent approximation for the self-energy of a quark in the presence of a gluon condensate. We found chiral symmetry breaking for the quarks and the absence of a fermion pole in the quark propagater. This study led us to believe that the presence of a gluon condensate in the QCD vacuum can explain the nonpropagation of colored objects. (Recently, it has also been shown that gluons do not propagate in the gluon condensate [58].)

From our results, it is clear that we have succeeded in reproducing the experimental spectra and the leptonic widths (of low-lying states) of various mesons rather accurately. However, the values of the leptonic widths and the radii of various mesonic states, close to and above the open-flavor threshold, do not agree with experiment. It appears that the one-gluon-exchange approximation we have used is not satisfactory. Of course, the approximation of keeping one quark (or antiquark) on mass-shell will affect our results. A study in which both constituents are allowed to propagate off mass-shell is in progress. It is also possible that what we have called "one-gluon-exchange" may not actually be one-gluon-exchange. One may require the description of the exchange of some (colored) composite fields. Such fields arise when one uses the auxiliary-field formalism to eliminate

the gluon degrees of freedom from the action.

Another feature we have not included in our model is the effect of channel-coupling. As in the case of linear confinement potentials, we have the unpleasant situation of obtaining an infinite number of bound states, if we neglect channel-coupling effects.

We have not as yet made a detailed study of radiative transition rates and hadronic decay rates. These properties should be calculated in our model so that we may compare the results of our model to the results obtained using potential models or other field-theoretic models. We remind the reader that our model of covariant soliton dynamics is of field-theoretic character and has some relation to QCD. It is seen to provide, in principle, a unified model of all hadrons. In our studies we have also included a covariant description of confinement and have developed some understanding of chiral symmetry breaking.

Appendix A

An Effective First-Order Equation and the Second-Order Equation :

In this appendix we make use of the procedure adopted by Sakurai [39] to "derive" the Dirac equation from a second-order equation. We have from Eq.(2.2.17),

$$[\ \partial^2 + m_q^2]q(x) = -[2\beta m_q g_\chi\ \chi(x) + g_\chi^2\ \chi^2(x)]q(x)\ .$$

From this equation it is clear that q(x) satisfies an equation of the Klein-Gordon form. Let us take the field satisfying the above equation to be a scalar field, φ_1. To obtain a spinor equation, we may proceed as follows. Write

$$-\partial^2\varphi_1(x) = [m_q^2 + 2\beta m_q g_\chi\ \chi(x) + g_\chi^2\ \chi^2(x)]\varphi_1(x)$$

and note that the left-hand side may be written as

$$\left[-\frac{\partial}{\partial t^2} + \nabla^2\right]\varphi_1(x) = \left[i\ \frac{\partial}{\partial t} + \vec{\sigma}.i\vec{\nabla}\right]\ \left[i\ \frac{\partial}{\partial t} - \vec{\sigma}.i\vec{\nabla}\ \right]\varphi_1(x),$$

and right-hand side as

$$[m_q + \beta g_\chi\ \chi(x)]^2\ \varphi_1(x) + (1-\beta^2)g_\chi^2\ \chi^2(x)\ \varphi_1(x).$$

Therefore,

$$\left[i \frac{\partial}{\partial t} + \vec{\sigma}.i\vec{\nabla} \right] \left[i \frac{\partial}{\partial t} - \vec{\sigma}.i\vec{\nabla} \right] \varphi_1(x)$$

$$= [m_q + \beta g_\chi \chi(x)]^2 \varphi_1(x) + (1-\beta^2) g_\chi^2 \chi^2(x) \varphi_1(x). \tag{A.1}$$

Let us put

$$\left[i \frac{\partial}{\partial t} - \vec{\sigma}.i\vec{\nabla} \right] \varphi_1(x) = \left[m_q + \beta g_\chi \chi(x) \right] \varphi_2(x) \tag{A.2}$$

in Eq.(A.1), to obtain

$$\left[i \frac{\partial}{\partial t} + \vec{\sigma}.i\vec{\nabla} \right] \left[m_q + \beta g_\chi \chi(x) \right] \varphi_2(x)$$

$$= [m_q + \beta g_\chi \chi(x)]^2 \varphi_1(x) + (1-\beta^2) g_\chi^2 \chi^2(x) \varphi_1(x).$$

Dividing both sides by $[m_q + \beta g_\chi \chi(x)]$, we have

$$\left[i \frac{\partial}{\partial t} + \vec{\sigma}.i\vec{\nabla} \right] \varphi_2(x) = [m_q + \beta g_\chi \chi(x)] \varphi_1(x) + \frac{(1-\beta^2) g_\chi^2 \chi^2(x)}{[m_q + \beta g_\chi \chi(x)]} \varphi_1(x)$$

$$- \frac{\beta g_\chi \left[i \frac{\partial}{\partial t} + i\vec{\sigma}.\vec{\nabla} \right] \chi(x)}{[m_q + \beta g_\chi \chi(x)]} \varphi_2(x) . \tag{A.3}$$

Adding Eq.(A.2) and (A.3), we find

$$i\frac{\partial}{\partial t}[\varphi_2(x)+\varphi_1(x)] + \vec{\sigma}.i\vec{\nabla}[\varphi_2(x)-\varphi_1(x)]$$

$$= [m_q + \beta g_\chi \chi(x)][\varphi_2(x)+\varphi_1(x)] + \frac{(1-\beta^2)g_\chi^2 \chi^2(x)}{[m_q + \beta g_\chi \chi(x)]}\varphi_1(x)$$

$$- \frac{\beta g_\chi \left[i\frac{\partial}{\partial t} + i\vec{\sigma}.\vec{\nabla} \right]\chi(x)}{[m_q + \beta g_\chi \chi(x)]} \varphi_2(x) \ . \qquad (A.4)$$

Now, subtracting Eq.(A.3) from Eq.(A.2), we have

$$-i\frac{\partial}{\partial t}[\varphi_2(x)-\varphi_1(x)] - \vec{\sigma}.i\vec{\nabla}[\varphi_2(x)+\varphi_1(x)]$$

$$= [m_q + \beta g_\chi \chi(x)][\varphi_2(x)-\varphi_1(x)] - \frac{(1-\beta^2)g_\chi^2 \chi^2(x)}{[m_q + \beta g_\chi \chi(x)]}\varphi_1(x)$$

$$+ \frac{\beta g_\chi \left[i\frac{\partial}{\partial t} + i\vec{\sigma}.\vec{\nabla} \right]\chi(x)}{[m_q + \beta g_\chi \chi(x)]} \varphi_2(x) \ . \qquad (A.5)$$

The two equations above can be combined to form,

$$\begin{bmatrix} i\frac{\partial}{\partial t} & \vec{\sigma}.i\vec{\nabla} \\ -\vec{\sigma}.i\vec{\nabla} & -i\frac{\partial}{\partial t} \end{bmatrix} \begin{pmatrix} \varphi_2(x)+\varphi_1(x) \\ \varphi_2(x)-\varphi_1(x) \end{pmatrix}$$

$$= [m_q + \beta g_\chi \chi(x)] \begin{pmatrix} \varphi_2(x)+\varphi_1(x) \\ \varphi_2(x)-\varphi_1(x) \end{pmatrix} - \frac{f_1(x)}{2} \begin{pmatrix} 1 & 1 \\ -1 & -1 \end{pmatrix} \begin{pmatrix} \varphi_2(x)+\varphi_1(x) \\ \varphi_2(x)-\varphi_1(x) \end{pmatrix}$$

$$+ \frac{f_2(x)}{2} \begin{pmatrix} 1 & -1 \\ -1 & 1 \end{pmatrix} \begin{pmatrix} \varphi_2(x)+\varphi_1(x) \\ \varphi_2(x)-\varphi_1(x) \end{pmatrix} , \qquad (A.6)$$

where

$$f_2(x) \equiv \frac{(1-\beta^2)g_\chi^2\,\chi^2(x)}{[m_q + \beta g_\chi\,\chi(x)]} \quad ,$$

and

$$f_1(x) \equiv \frac{\beta g_\chi\left[i\frac{\partial}{\partial t} + i\vec{\sigma}.\vec{\nabla}\right]\chi(x)}{[m_q + \beta g_\chi\,\chi(x)]} \quad . \tag{A.7}$$

Using Dirac matrices and defining the spinor field

$$q(x) = \begin{pmatrix} \varphi_2(x)+\varphi_1(x) \\ \varphi_2(x)-\varphi_1(x) \end{pmatrix} \quad , \tag{A.8}$$

Eq.(A.5) can be written as,

$$\left[\gamma_0 i\frac{\partial}{\partial t} - \vec{\gamma}.i\vec{\nabla}\right]q(x) = [m_q + \beta g_\chi\,\chi(x)]q(x) - \frac{f_1(x)}{2}\gamma_0(1+\gamma_5)q(x)$$

$$+ \frac{f_2(x)}{2}(1-\gamma_5)q(x) \quad . \tag{A.9}$$

For u, d and s quarks $\beta \approx 1$ and hence $f_2(x)$ vanishes. For c and b quarks, β is approximately 0.85 and 0.75, respectively. However by comparing $f_2(x)$ with the $[m_q + \beta g_\chi \chi(x)]$ term, we see that

$$\left|\frac{(1-\beta^2)[g_\chi\,\chi(x)]^2}{[m_q + \beta g_\chi \chi(x)]^2}\right| \approx \frac{(1-.85^2)[(7)(100)]^2}{[1900 - (.85)(700)]^2}$$

$$= 0.08$$

for the c quark and

$$\left|\frac{(1-\beta^2)[g_\chi\,\chi(x)]^2}{[m_q+\beta g_\chi\chi(x)]^2}\right| \approx \frac{(1-.75^2)[(7)(100)]^2}{[5000-(.75)(700)]^2}$$

$$= 0.01$$

for the b quark. Therefore, the second term on the right in Eq.(A.9) is negligible for both light and heavy quarks. Note that $f_1(x)$ involves the variation of $\chi(x)$ in space and time. However, $\chi(x)$ is the order-parameter field and so it may be assumed to vary slowly in space-time. Thus, we may neglect the first term as well. Our equation then reduces to Eq.(2.3.4).

Appendix B

B.1 Notation and Conventions :

We use the notation presented in the texts of Bjorken and Drell [62]:

$$x^{\mu} \equiv (x^0, \vec{x})$$

$$x_{\mu} \equiv (x^0, -\vec{x}) = g_{\mu\nu} x^{\nu} \ , \tag{B.1.1}$$

where

$$g_{\mu\nu} = g^{\mu\nu} = \begin{bmatrix} 1 & 0 & 0 & 0 \\ 0 & -1 & 0 & 0 \\ 0 & 0 & -1 & 0 \\ 0 & 0 & 0 & -1 \end{bmatrix} , \tag{B.1.2}$$

$$x_1 . x_2 = x_1^0 x_2^0 - \vec{x}_1 . \vec{x}_2 \ ,$$

$$p^{\mu} = i\frac{\partial}{\partial x_{\mu}} \equiv (i\,\frac{\partial}{\partial t},\ -i\vec{\nabla}\ ) = i\partial^{\mu} \ ,$$

$$p_{\mu} = i\frac{\partial}{\partial x^{\mu}} \equiv (i\,\frac{\partial}{\partial t},\ i\vec{\nabla}\ ) = i\partial_{\mu} \ . \tag{B.1.3}$$

Dirac matrices and spinors :

$$\gamma^{\mu} = (\gamma^0, \vec{\gamma}) \ , \tag{B.1.4}$$

where

$$\gamma^0 = \begin{bmatrix} 1 & 0 \\ 0 & -1 \end{bmatrix} ; \qquad \vec{\gamma} = \begin{bmatrix} 0 & \vec{\sigma} \\ -\vec{\sigma} & 0 \end{bmatrix} . \tag{B.1.5}$$

Here $\vec{\sigma}$ has there components, which are the Pauli matrices:

$$\sigma^1 = \begin{bmatrix} 0 & 1 \\ 1 & 0 \end{bmatrix} , \qquad \sigma^2 = \begin{bmatrix} 0 & -i \\ i & 0 \end{bmatrix} , \qquad \sigma^3 = \begin{bmatrix} 1 & 0 \\ 0 & -1 \end{bmatrix} . \tag{B.1.6}$$

The Dirac matrices satisfy the relations

$$\gamma^\mu\gamma^\nu + \gamma^\nu\gamma^\mu = 2\, g^{\mu\nu} ,$$

$$\sigma^{\mu\nu} \equiv \frac{i}{2} \left[\gamma^\mu\gamma^\nu - \gamma^\nu\gamma^\mu\right] .$$

Note the definition,

$$\gamma^5 = i\, \gamma^0\gamma^1\gamma^2\gamma^3 = \gamma_5 = \begin{bmatrix} 0 & 1 \\ 1 & 0 \end{bmatrix} . \tag{B.1.7}$$

The spinors $u(\vec{k},s)$ and $v(\vec{k},s)$ satisfy the Dirac equations,

$$[\not{k} - m]\, u(\vec{k},s) = 0 ,$$

$$[\not{k} + m]\, v(\vec{k},s) = 0 . \tag{B.1.8}$$

Further,

$$\overline{u}(\vec{k},s) \equiv u^{+}\gamma^{0} \ ,$$

and

$$\overline{v}(\vec{k},s) \equiv v^{+}\gamma^{0} \ , \tag{B.1.9}$$

satisfy the equation

$$\overline{u}(\vec{k},s)[\not{k} - m] = 0 \ ,$$

and

$$\overline{v}(\vec{k},s)[\not{k} + m] = 0 \quad . \tag{B.1.10}$$

The projection operators are

$$u_{\alpha}(\vec{k},s)\ \overline{u}_{\beta}(\vec{k},s) = \left[\frac{\not{k} + m}{2m} \cdot \frac{1+\gamma_5\gamma_\mu s^{\mu}}{2} \right]_{\alpha\beta} \ ,$$

and

$$v_{\alpha}(\vec{k},s)\ \overline{v}_{\beta}(\vec{k},s) = \left[\frac{\not{k} - m}{2m} \cdot \frac{1+\gamma_5\gamma_\mu s^{\mu}}{2} \right]_{\alpha\beta} \ , \tag{B.1.11}$$

where s^{μ} describes the direction of the spin of the physical particle.

The spinors $u(\vec{k},s)$ and $v(\vec{k},s)$ satisfy the normalization conditions:

$$\bar{u}(\vec{k},s)\ u(\vec{k},s) = 1 \ ,$$

$$\bar{v}(\vec{k},s)\ v(\vec{k},s) = -1 \ . \qquad \text{(B.1.12)}$$

The completeness relation is

$$\sum_s \left[u_\alpha(\vec{k},s)\ \bar{u}_\beta(\vec{k},s) - v_\alpha(\vec{k},s)\ \bar{v}_\beta(\vec{k},s)\right] = \delta_{\alpha\beta} \ . \qquad \text{(B.1.13)}$$

We also use the relation

$$\left[\bar{u}(\vec{k}',s')\ \Gamma\ u(\vec{k},s)\right]^+ = u(\vec{k},s)\ \bar{\Gamma}\ u(\vec{k}',s') \ , \qquad \text{(B.1.14)}$$

with $\bar{\Gamma} \equiv \gamma^0\ \Gamma^+\ \gamma^0$.

For example,

$$\bar{\gamma^\mu} = \gamma^0\ \gamma^{\mu^+}\ \gamma^0 = \gamma^\mu \ ,$$

$$\overline{\sigma^{\mu\nu}} = \gamma^0\ \sigma^{\mu\nu^+}\ \gamma^0 = \sigma^{\mu\nu} \ ,$$

$$\overline{i\gamma^5} = \gamma^0\ (i\gamma^5)^+\ \gamma^0 = i\gamma^5 \ , \qquad \text{(B.1.15)}$$

and

$$\Lambda^+(k) \equiv \left[\frac{\not{k} + m}{2m}\right] = \sum_{\pm s} u(\vec{k},s)\ \bar{u}(\vec{k},s) \ ,$$

$$\Lambda^{-}(k) \equiv \left[\frac{-\not{k} + m}{2m} \right] = - \sum_{\pm s} v(\vec{k},s)\ \bar{v}(\vec{k},s) \ . \tag{B.1.16}$$

Trace theorems and various identities are

$$\not{a}\not{b} = a.b - i\ \sigma_{\mu\nu} a^{\mu} b^{\nu} \ ,$$

$$\mathrm{Tr}\ \gamma_5 = 0 \ ,$$

$$\mathrm{Tr}(\text{odd number of } \gamma^{\mu}) = 0 \ ,$$

$$\mathrm{Tr}\ 1 = 4 \ ,$$

$$\mathrm{Tr}\ \not{a}\not{b} = 4\ a.b \ ,$$

$$\mathrm{Tr}\ \not{a}_1\not{a}_2\not{a}_3\not{a}_4 = 4 \left[a_1.a_2\ a_3.a_4 - a_1.a_3\ a_2.a_4 + a_1.a_4\ a_2.a_3 \right] \ ,$$

$$\mathrm{Tr}\ \gamma_5 \not{a}\not{b} = 0 \ ,$$

$$\mathrm{Tr}\ \gamma_5 \not{a}\not{b}\not{c}\not{d} = 4i\epsilon_{\alpha\beta\gamma\delta}\ a^{\alpha} b^{\beta} c^{\gamma} d^{\delta} \ ,$$

$$\gamma_{\mu}\not{a}\gamma^{\mu} = -2\not{a} \ ,$$

$$\gamma_{\mu}\not{a}\not{b}\gamma^{\mu} = 4\ a.b \ ,$$

$$\gamma_{\mu}\not{a}\not{b}\not{c}\gamma^{\mu} = -2\not{c}\not{b}\not{a} \ . \tag{B.1.17}$$

B.2 Gell-Mann matrices and identities :

$$\lambda_i = \begin{bmatrix} \sigma_i & 0 \\ 0 & 0 \end{bmatrix} \quad (\ i=1,2 \text{ and } 3)\ ;$$

$$\lambda_4 = \begin{bmatrix} 0 & 0 & 1 \\ 0 & 0 & 0 \\ 1 & 0 & 0 \end{bmatrix}\ ; \qquad \lambda_5 = \begin{bmatrix} 0 & 0 & -i \\ 0 & 0 & 0 \\ i & 0 & 0 \end{bmatrix}\ ;$$

$$\lambda_6 = \begin{bmatrix} 0 & 0 & 0 \\ 0 & 0 & 1 \\ 0 & 1 & 0 \end{bmatrix}\ ; \qquad \lambda_7 = \begin{bmatrix} 0 & 0 & 0 \\ 0 & 0 & -i \\ 0 & i & 0 \end{bmatrix}\ ;$$

$$\lambda_8 = \frac{1}{\sqrt{3}} \begin{bmatrix} 1 & 0 & 0 \\ 0 & 1 & 0 \\ 0 & 0 & -2 \end{bmatrix}\ . \qquad \text{(B.2.1)}$$

These matrices satisfy the commutation relations,

$$\left[\tfrac{1}{2}\lambda_i,\ \tfrac{1}{2}\lambda_j \right] = i\ f_{ijk}\left(\tfrac{1}{2}\lambda_k \right)\ , \qquad \text{(B.2.2)}$$

and the anticommutation relations

$$\left\{ \tfrac{1}{2}\lambda_i,\ \tfrac{1}{2}\lambda_j \right\} = \tfrac{1}{3}\delta_{ij} + d_{ijk}\left(\tfrac{1}{2}\lambda_k \right)\ , \qquad \text{(B.2.3)}$$

where the f_{ijk} are fully antisymmetric and the d_{ijk} are symmetric. Their values are

$$f_{123} = 1 \ ,$$

$$f_{147} = f_{246} = f_{257} = f_{345} = f_{516} = f_{637} = \frac{1}{2} \ ,$$

$$f_{458} = f_{678} = \frac{\sqrt{3}}{2} \ , \tag{B.2.4}$$

and

$$d_{118} = d_{228} = d_{338} = -d_{888} = \frac{1}{\sqrt{3}} \ ,$$

$$d_{146} = d_{157} = d_{256} = d_{344} = d_{355} = \frac{1}{2} \ ,$$

$$d_{247} = d_{366} = d_{377} = -\frac{1}{2} \ ,$$

$$d_{448} = d_{558} = d_{668} = d_{778} = -\frac{1}{2\sqrt{3}} \ . \tag{B.2.5}$$

Appendix C

C.1 Properties of the Helicity Vector :

The helicity vector satisfies the relations [63]

$$(1)\quad \xi_\lambda(\vec{P}).P = 0 \ . \tag{C.1.1}$$

$$(2)\quad \xi^*_{\lambda'}(\vec{P}).\xi_\lambda(\vec{P}) = -\,\delta_{\lambda',\lambda} \ . \tag{C.1.2}$$

$$(3)\quad \sum_\lambda \xi^{\mu*}_\lambda(\vec{P})\ \xi^\nu_\lambda(\vec{P}) = -\,g^{\mu\nu} + \frac{P^\mu P^\nu}{M^2} \ . \tag{C.1.3}$$

$$(4)\ \text{In the meson rest frame } (\vec{P}=0),\quad \xi^\mu_\lambda(\vec{0}) = (0\ ,\ \vec{\xi}_\lambda). \tag{C.1.4}$$

C.2 Parity transformations [63, 50, 51]:

Under the parity transformation, $\mathcal{P}$, the quark field transforms as

$$\mathcal{P}\ q(0)\ \mathcal{P}^{-1} = \gamma^0 q(0) \ . \tag{C.2.1}$$

Quark and antiquark states transform as

$$\begin{aligned} \mathcal{P}\ |\vec{k},s,t,b> &= e^{-i\varphi(\vec{k},s)}\ |-\vec{k},s,t,b> \ , \\ \mathcal{P}\ |\overline{\vec{k},s,t,b}> &= -\ e^{-i\varphi(\vec{k},s)}\ |\overline{-\vec{k},s,t,b}> \ , \end{aligned} \tag{C.2.2}$$

where $\varphi(\vec{k},s)$ is a phase factor.

A canonical state describing a single particle with spin j and momentum $\vec{P}$ transforms as

$$\mathcal{P}\ |\vec{P},j,m\rangle = \eta\ |-\vec{P},j,m\rangle = \eta\ |\pi+\varphi,\pi-\theta,|\vec{P}|,j,m\rangle\ , \qquad (C.2.3)$$

where η is the intrinsic parity of the particle.

The transformation of a helicity state under parity is given by

$$\mathcal{P}\ |\vec{P},j,\lambda\rangle = \eta\ e^{-i\pi j}\ |\pi+\varphi,\pi-\theta,|\vec{P}|,j,-\lambda\rangle\ . \qquad (C.2.4)$$

The helicity vector, $\xi^{\mu}_{\lambda}(\vec{P})$, transforms under the parity transformation as

$$\mathcal{P}\ \xi^{\mu}_{\lambda}(\vec{P}) = -\eta\ \xi^{\mu}_{-\lambda}(\pi+\varphi,\pi-\theta,|\vec{P}|) = -\eta\ \xi^{\mu}_{-\lambda}(-\vec{P})\ , \qquad (C.2.5)$$

where $\xi^{\mu}_{-\lambda}(-\vec{P}) = (\xi^{0}_{\lambda},-\vec{\xi}_{\lambda})$.

Appendix D

Charge Conjugation :

The following identities are used in obtaining the expression for the amplitude for a meson to decay into an on-mass-shell quark and an off-mass-shell antiquark from the expression with the antiquark on-mass-shell [50, 51] :

$$(1)\quad C\,|\vec{k},s,t,b\rangle = \eta_{-t}\,|\vec{k},s,-t,b\rangle\ , \tag{D.1}$$

$$(2)\quad C\,q^{b}(0)\,C^{-1} = C\left[\bar{q}^{b}(0)\right]^{T}\ , \tag{D.2}$$

$$(3)\quad C\,|\vec{P},M_{T},\lambda\rangle = (-1)^{M_{T}}\,|\vec{P},-M_{T},\lambda\rangle\ , \tag{D.3}$$

$$(4)\quad C\,\gamma_{\mu}\,C^{-1} = -\,\gamma_{\mu}^{T}\ . \tag{D.4}$$

Here T denotes matrix transposition,

$$C \equiv -\,i\,\gamma^{2}\,\gamma^{0}\ , \tag{D.5}$$

and

$$\eta_{t} \equiv (-1)^{\frac{1}{2}+t}\ . \tag{D.6}$$

Table A

The current quark masses, β, g_χ^{eff}, and the mass parameters which determine the quark self energy, $\Sigma(q^2)$.

Quark	m_q(Mev)	m_q^{cur}(Mev)	β	g_χ^{eff}	m_0(MeV)
u , d	484	0	1.0	7.0	350
s	656	95	.995	6.963	327
c	1884	1433	.829	5.803	1697
b	5245	4827	.736	5.155	5100

Table B

Leptonic widths of vector mesons and various parameters used in the calculation.

Meson	Covariant analysis	Van Royan - Weisskof formula		Expt.	Masses (MeV)		m_q	P_{max}
	KeV	(a) KeV	(b) KeV	KeV	Thoery	Expt.	MeV	fm^{-1}
ρ	4.62	3.55	4.28	6.90±0.30	775	775	495	8
ω	0.51	0.39	0.48	0.76±0.17	775	783		
φ	1.06	0.82	0.99	1.31±0.06	1020	1020	665	10
$\psi(1S)$	4.73	4.55	4.94	4.70±0.30	3050	3100	1922	15
$\psi(2S)$	1.08	1.07	1.10	2.10±0.20	3671	3685		
$\Upsilon(1S)$	1.13	1.13	1.16	1.22±0.05	9460	9460	5393	30
$\Upsilon(2S)$	0.548	0.553	0.588	0.54±0.03	10140	10023		
$\Upsilon(3S)$	0.266	0.27	0.268	0.40±0.03	10545	10355		

(a) See Eq.(4.5.5)

(b) See Eq.(4.5.8)

Table C

Results of calculations made using the Lagrangian without the gluon degrees of freedom and the covariant model of confinement :

Meson	Theoratical MeV	Expt. MeV
ρ	770	770
ρ'	1600	1600
ω	770	783
φ	1020	1020
φ'	1680	1680
η_c-ψ [C.O.G]	3070	3070
χ_c(1S) [C.O.G]	3480	3530
η_c'-ψ' [C.O.G]	3661	3661
ψ(3S) [C.O.G]	3980	4030
ψ(4S) [C.O.G]	4418	4415
Υ(1S)	9460	9460
χ_b(1S) [C.O.G]	9880	9904
Υ(2S)	10047	10023
χ_c(1S) [C.O.G]	10270	10263
Υ(3S)	10385	10355
Υ(4S)	10598	10575
Υ(5S)	10841	10860
Υ(6S)	11043	11020

Table D

Masses, leptonic widths and radii of the upsilon system for the parameter set given below :

m_q = 5263 MeV , m_0 = 5100 MeV , C = 0.05 ,

Λ = 7.8 fm^{-1} , P_{max} = 30 fm^{-1} , g_χ = 7.0 .

g^2 = 4.2 , m_{gl}^2 = 8 fm^{-2} ,

Υ states	Masses in Mev		Leptonic widths in KeV		rms radii in fm	
	Theory	Expt.	Theory	Expt.	Baryon density	Scalar density
1S	9460	9460	1.27	1.22±0.05	0.319	0.28
2S	10025	10023	0.45	0.54±0.03	0.631	0.62
3S	10345	10355	0.19	0.40±0.03	1.195	1.189
4S	10560	10575	0.11	0.24±0.05	1.539	1.529
5S	10830	10860	0.07	0.31±0.07	1.438	1.424
6S	11215	11020	0.02	0.13±0.03	1.447	1.426

Table E

Masses, leptonic widths and radii of the upsilon system for the parameter set given below :

$m_q = 5225$ MeV , $m_0 = 5100$ MeV , $C = 0.05$,

$A = 10.0$ fm^{-1} , $P_{max} = 30$ fm^{-1} , $g_\chi = 7.0$.

$g^2 = 2.8$, $m_{gl}^2 = 8$ fm^{-2} ,

Υ states	Masses in Mev		Leptonic widths in KeV		rms radii in fm	
	Theory	Expt.	Theory	Expt.	Baryon density	Scalar density
1S	9460	9460	0.76	1.22±0.05	0.291	0.275
2S	10042	10023	0.32	0.54±0.03	0.664	0.658
3S	10357	10355	0.10	0.40±0.03	1.411	1.407
4S	10566	10575	0.06	0.24±0.05	1.51	1.501
5S	10817	10860	0.02	0.31±0.07	1.539	1.525
6S	11146	11020	0.01	0.13±0.03	1.495	1.474

Table F

Masses, leptonic widths and radii of the J/ψ system for the parameter set given below :

$m_q = 1922$ MeV , $m_0 = 1697$ MeV , $C = 0.05$,

$\Lambda = 10.0$ fm^{-1} , $P_{max} = 15$ fm^{-1} , $g_\chi = 7.0$.

$g^2 = 3.5$, $m_{gl}^2 = 12$ fm^{-2} ,

J/ψ states	Masses in Mev		Leptonic widths in KeV		rms radii in fm	
	Theory	Expt.	Theory	Expt.	Baryon density	Scalar density
1S	3050	3100	4.73	4.70±0.3	0.531	0.385
2S	3671	3685	1.17	2.10±0.2	1.223	1.195
3S	4057	4030	0.26	0.75±0.15	1.479	1.443
4S	4430	4415	0.08	0.47±0.10	1.602	1.545

Fig. 1 Charmonium (a) and bottomonium (b) spectra obtained without the "one-gluon-exchange" effect. Light lines denote various states whose energies have been determined experimentally. The dashed lines are the spin-weighted averages, while the heavy lines are the theoretical predictions. [If we do not include our model of confinement, the continuum of our model starts at $2m_q$ (dot-dashed line), which is quite close to the open-flavor threshold (long dashed line).]

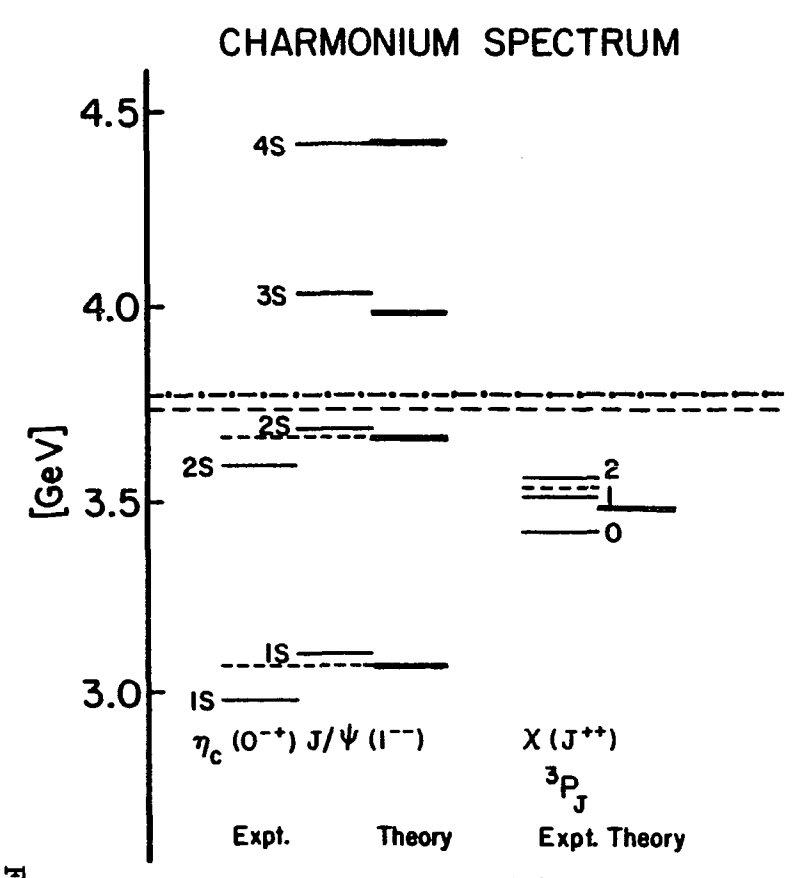

Fig. 1 - (a)

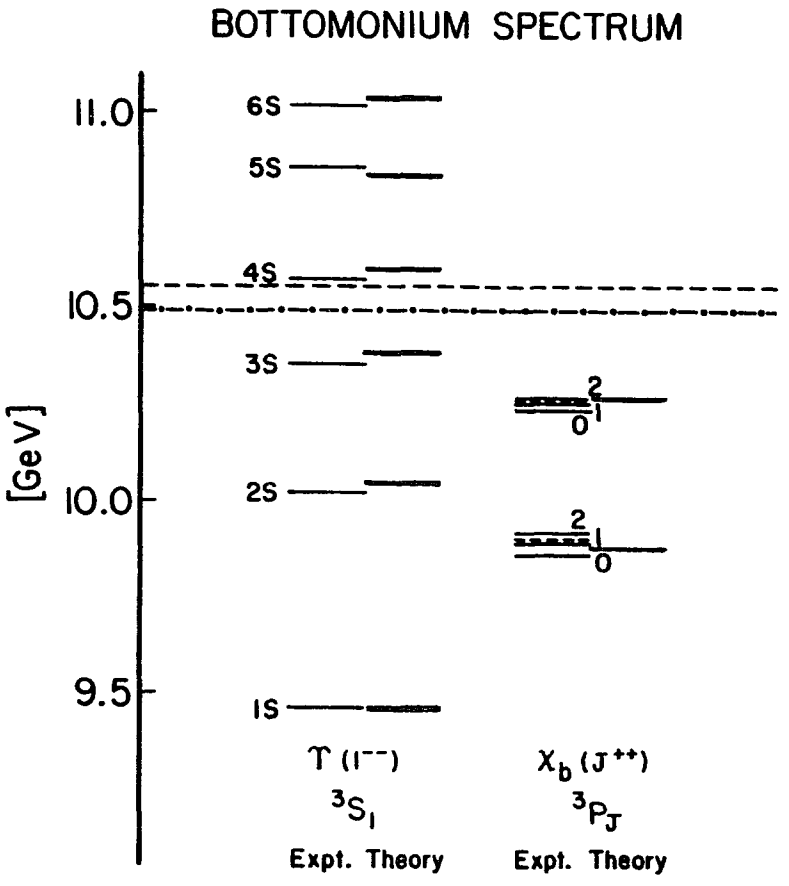

Fig. 1 - (b)

Fig. 1

Fig. 2 Theoretical and experimental spectra for the rho and phi mesons, states of charmonium and the upsilon system. In the case of charmonium, the dashed line represents the centers-of-gravity of η_c and J/ψ and of η_c' and ψ'.

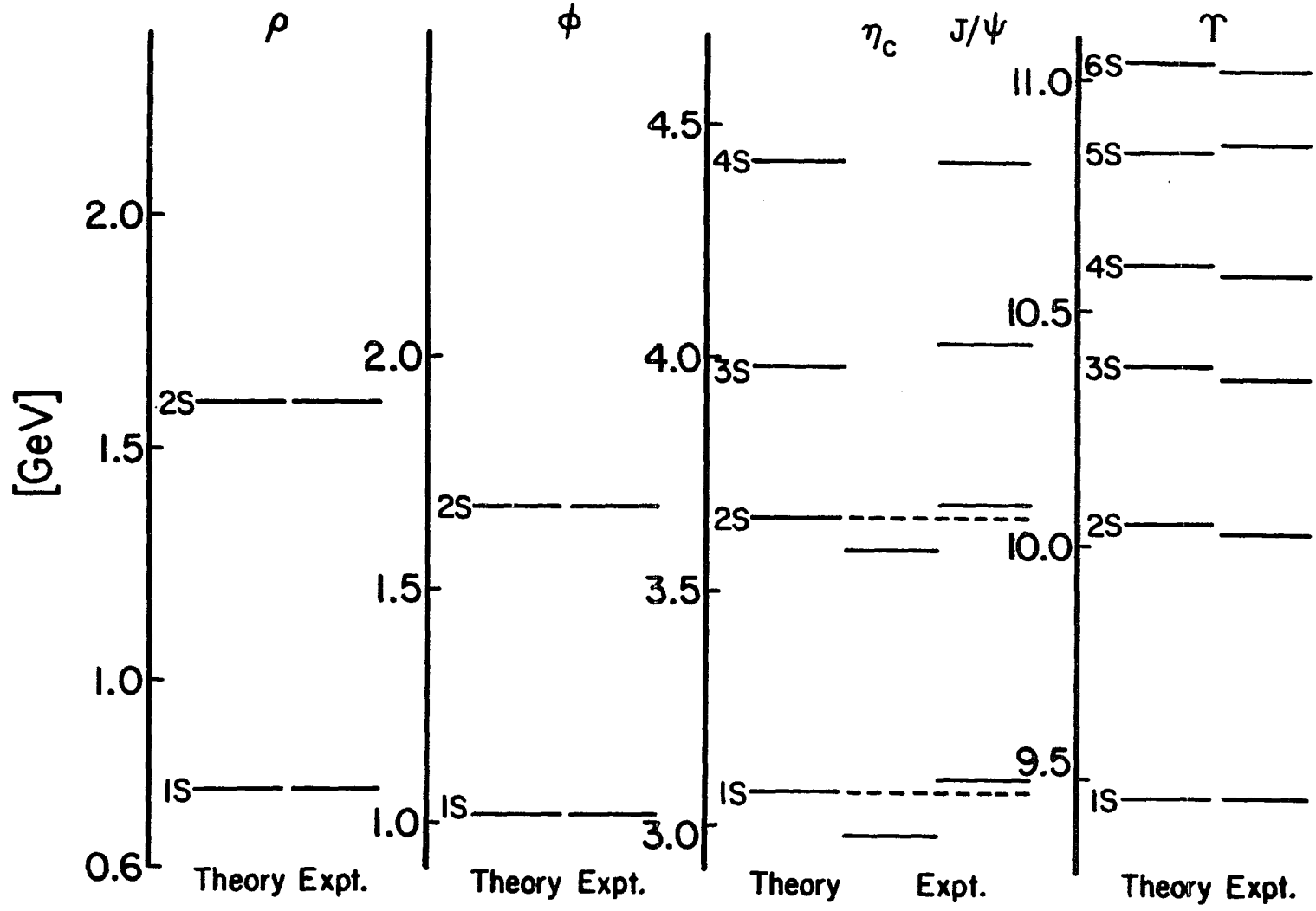
ρ
φ
η_c
J/ψ
Υ
[GeV]
2.0
1.5
1.0
0.6
2S
1S
Theory Expt.
2.0
1.5
1.0
2S
1S
Theory Expt.
4.5
4.0
3.5
3.0
4S
3S
2S
1S
Theory
Expt.
11.0
10.5
10.0
9.5
6S
5S
4S
3S
2S
1S
Theory Expt.

Fig. 2

Fig. 3 Equation for the quark propagator.

a) The solid line is the full propagator [Eq.(3.4.2)] and the light line is the propagator $[\not{p} - m_q^{cur}]^{-1}$.

b) A self-consistent model for the (irreducible) self-energy, $\Sigma(q^2)$. The cross-hatched circle denotes the condensate and the wavy lines are condensate gluons of zero momentum.

c) Here we show the type of nested diagrams which are summed in this model for the self-energy, $\Sigma(q^2)$.

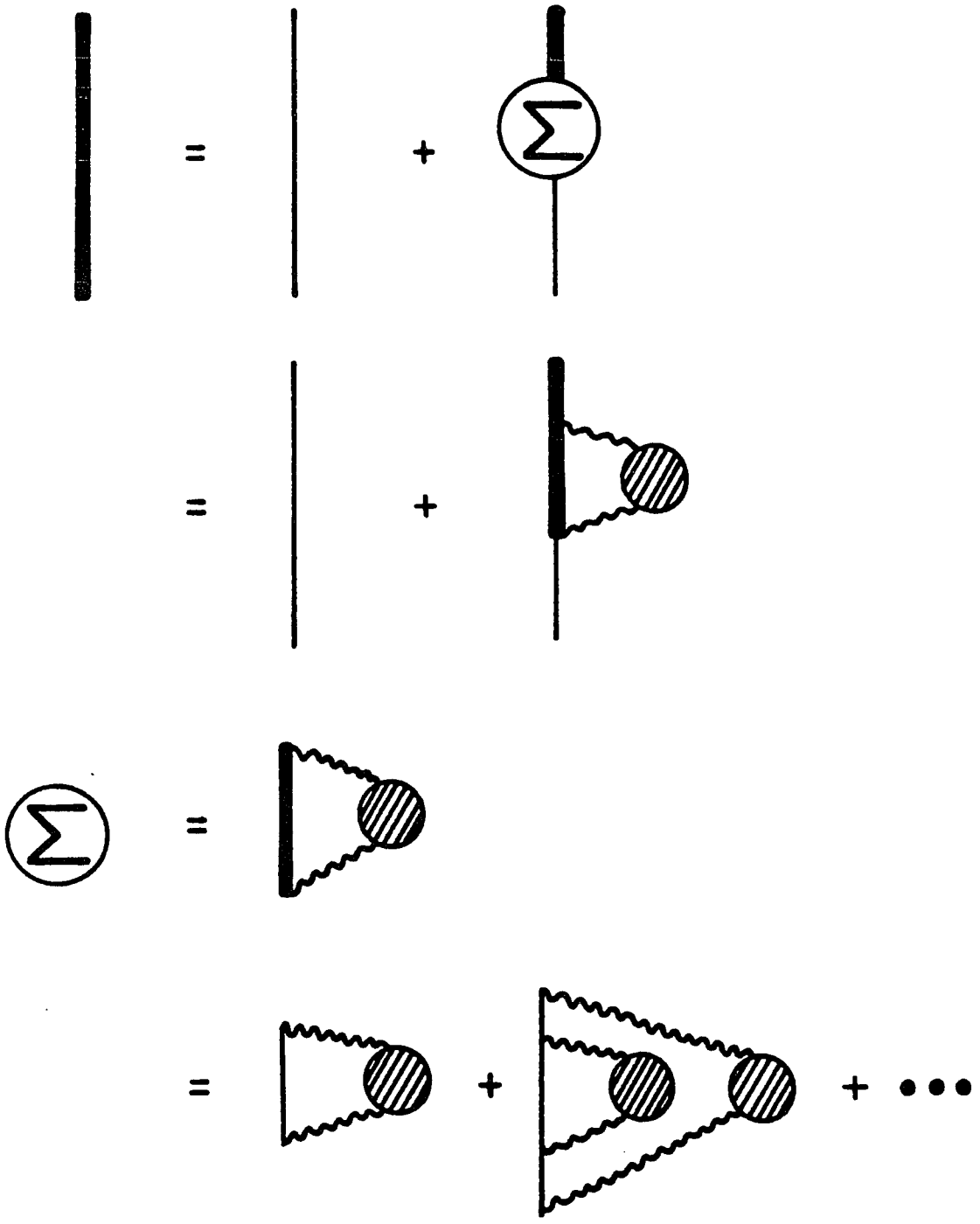

Fig.3

Fig. 4 (a) The square of dynamical mass, $M^2(q^2)$, for the charm quark. The dotted line represents a phenomenological model for this quantity adopted in ref. 49 [see Eq.(3.3.1)] in order to fit the spectrum of charmonium through the 4S level [see Fig.1a].

(b) Similar figure for bottom quark.

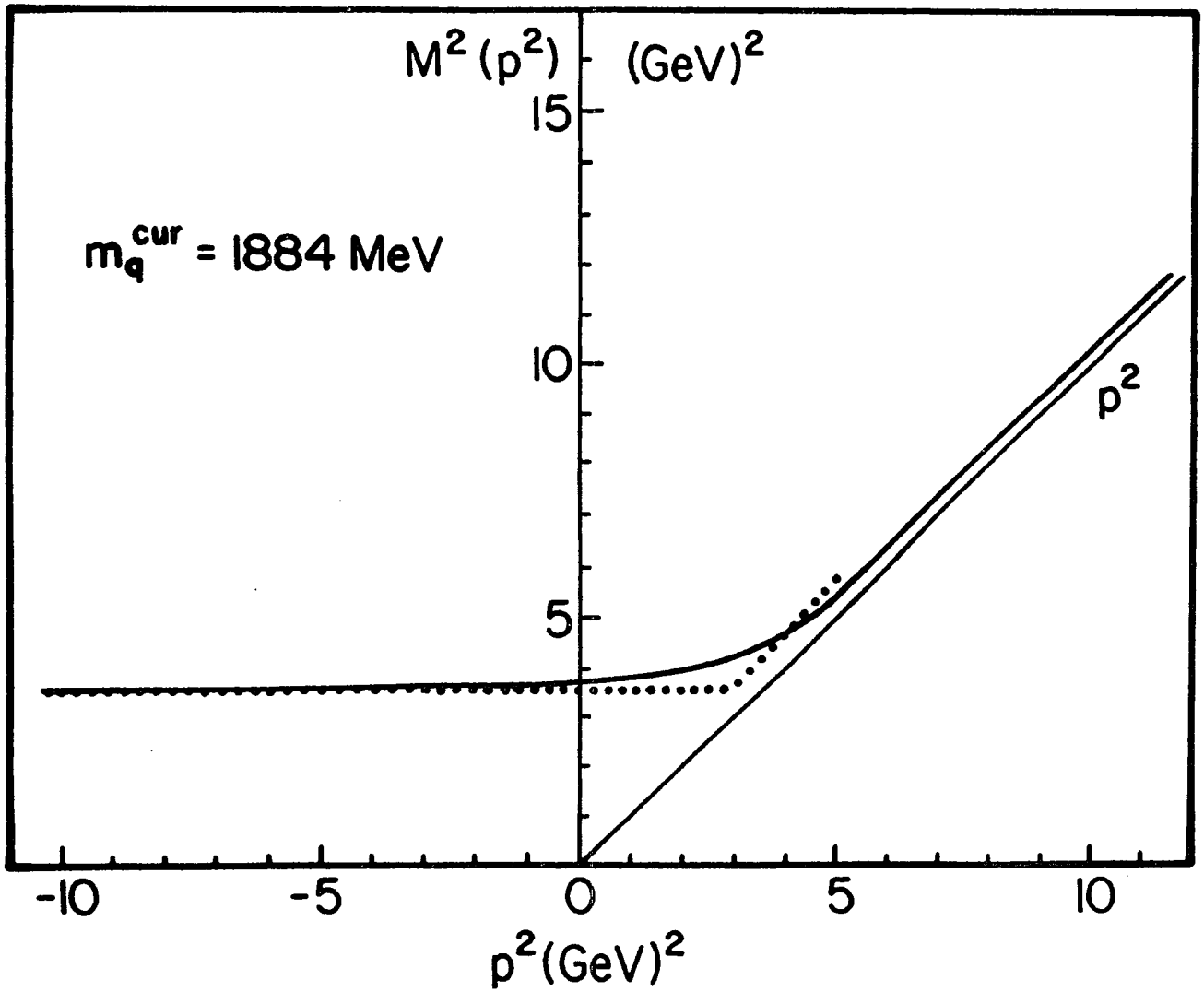

Fig.4-(a)

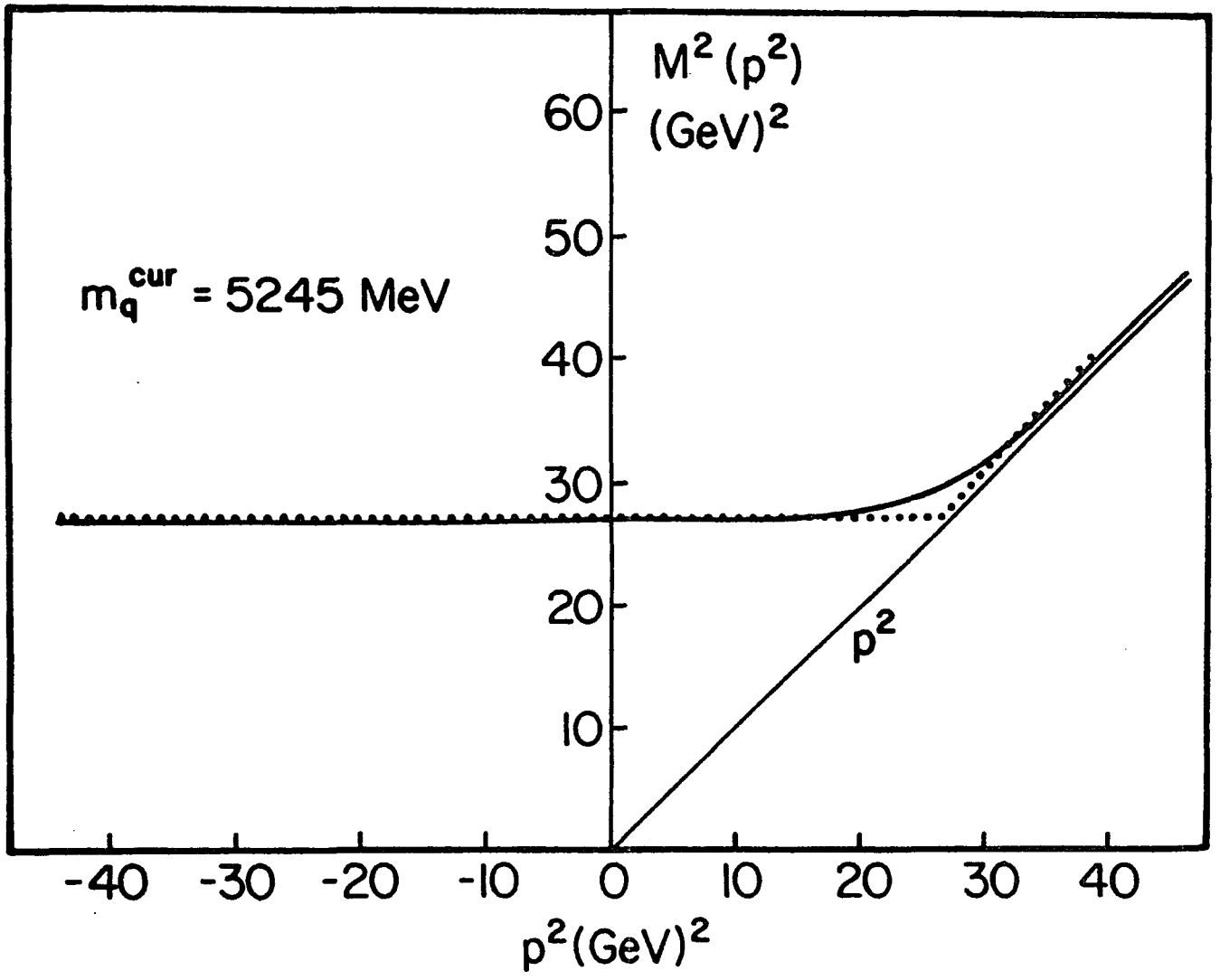
$M^2(p^2)$
$(GeV)^2$
60
50
40
30
20
10
m_q^{cur} = 5245 MeV
p^2
-40
-30
-20
-10
0
10
20
30
40
$p^2(GeV)^2$

Fig. 4-(b)

Fig. 5 The probability, $P(q^2)$, for the off-mass-shell quark to have a squared four vector $(P-k)^2=q^2$ in our model of the 1S-6S states of the upsilon system. The light arrow shows the value of m_0^2; $m_0^2 = 668\ fm^{-2}$ in this case. The heavy arrow shows the value of m_q^2 [$m_q^2=706\ fm^{-2}$] for the b-quark in this model.

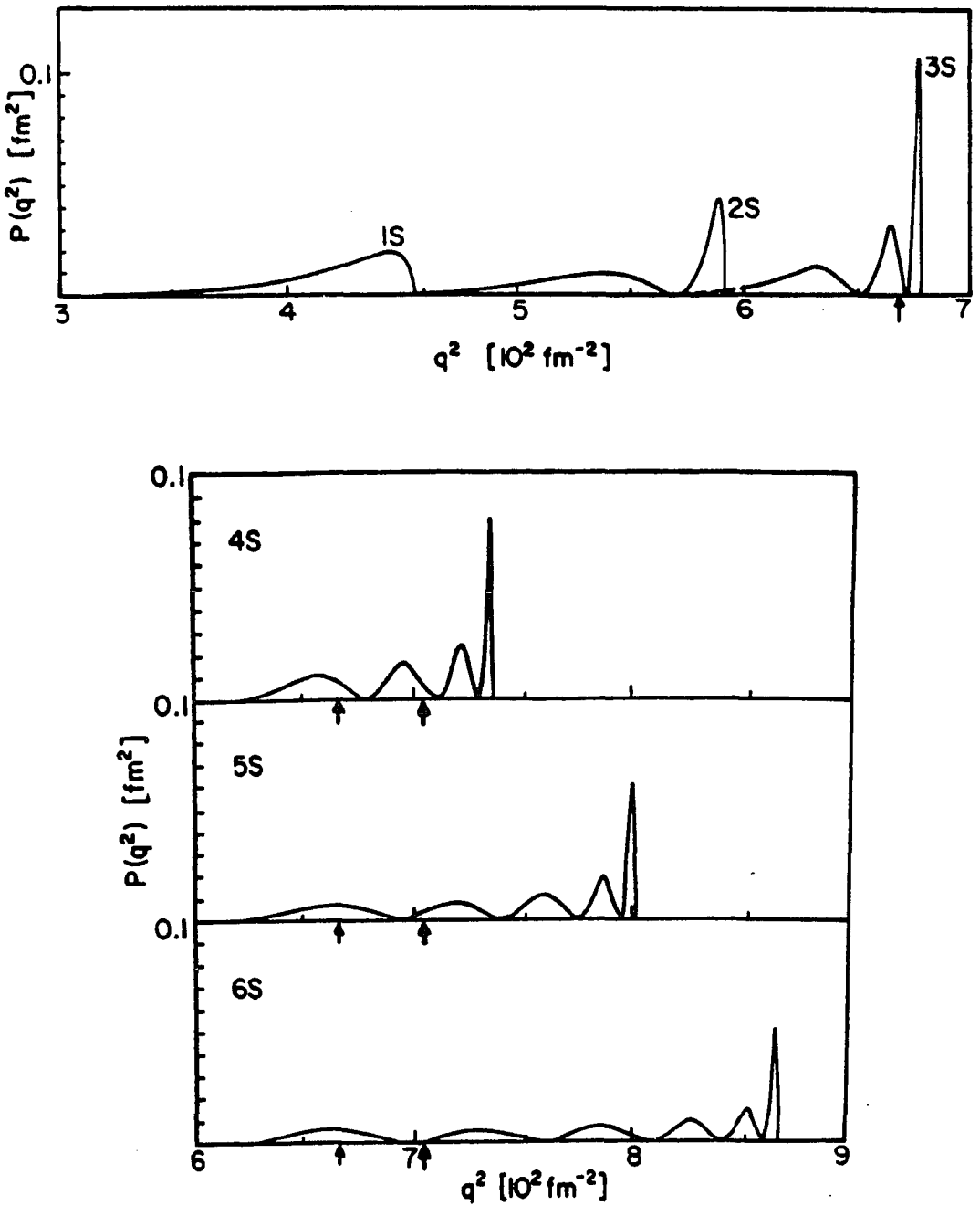
0.1
P(q²) [fm²]
1S
2S
3S
3
4
5
6
7
q² [10² fm⁻²]
0.1
4S
0.1
5S
0.1
6S
P(q²) [fm²]
6
7
8
9
q² [10² fm⁻²]

Fig.5

Fig. 6 The probability, $P(q^2)$, for the off-mass-shell quark to have a squared four vector $(P-k)^2=q^2$ in our model of the 1S-4S states of the charmonium system. The light arrow shows the value of m_0^2; $m_0^2 = 74\ fm^{-2}$ in this case. The heavy arrow shows the value of m_q^2 [$m_q^2 = 91\ fm^{-2}$] for the c-quark in this model.

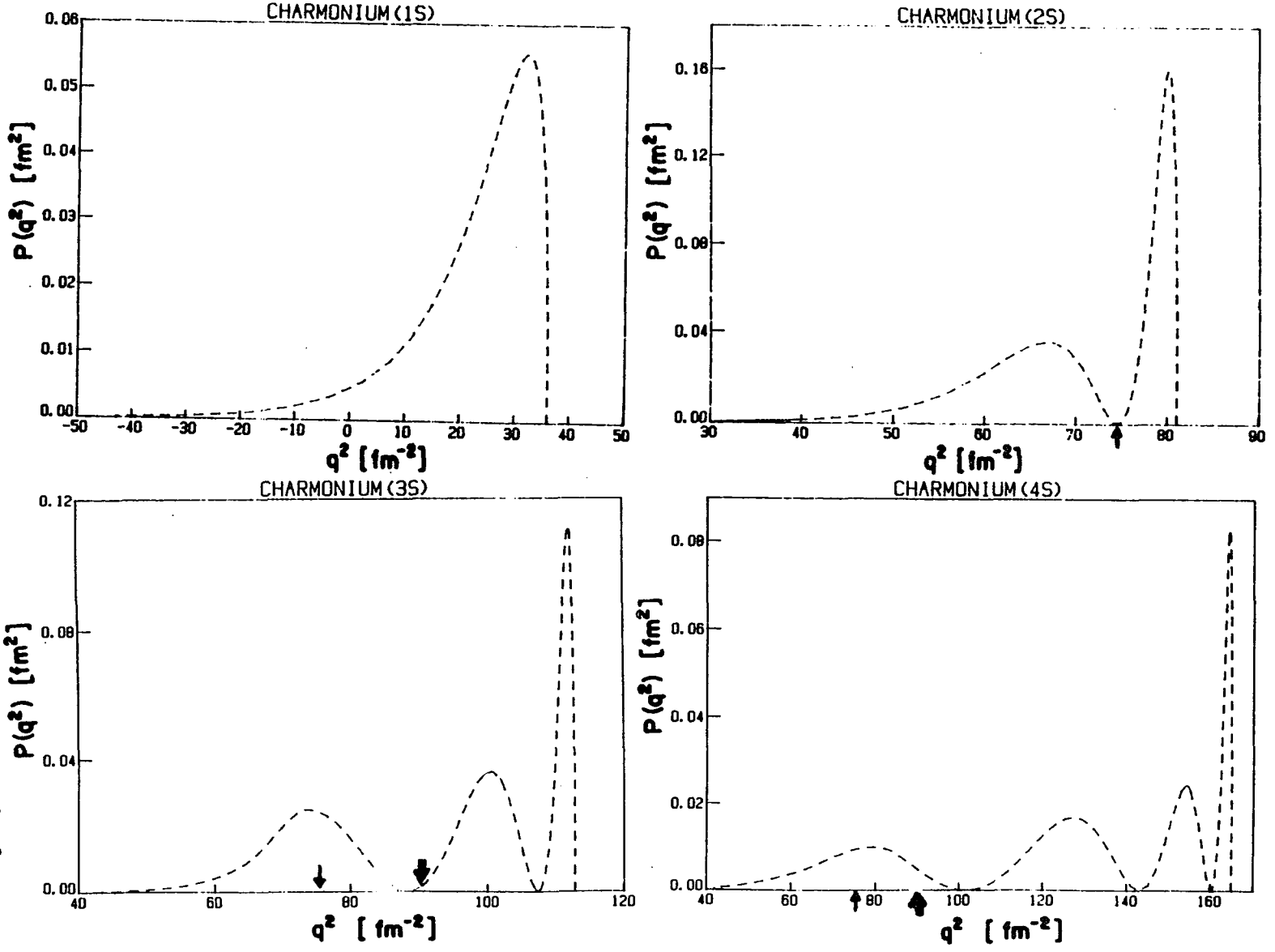
CHARMONIUM (1S)
CHARMONIUM (2S)
CHARMONIUM (3S)
CHARMONIUM (4S)
P(q²) [fm²]
q² [fm⁻²]

Fig. 6

Fig. 7 Schematic representation of the equations of our model. The filled circle denotes the amplitude for the on-mass-shell soliton to decay (vitually) to a quark and an antiquark. The open circle is a form factor and the wavy line denotes the propagator of the χ field. The second part of the figure denotes the scheme for calculating the form factor. (That calculation depends upon the knowledge of the vertex functions.)

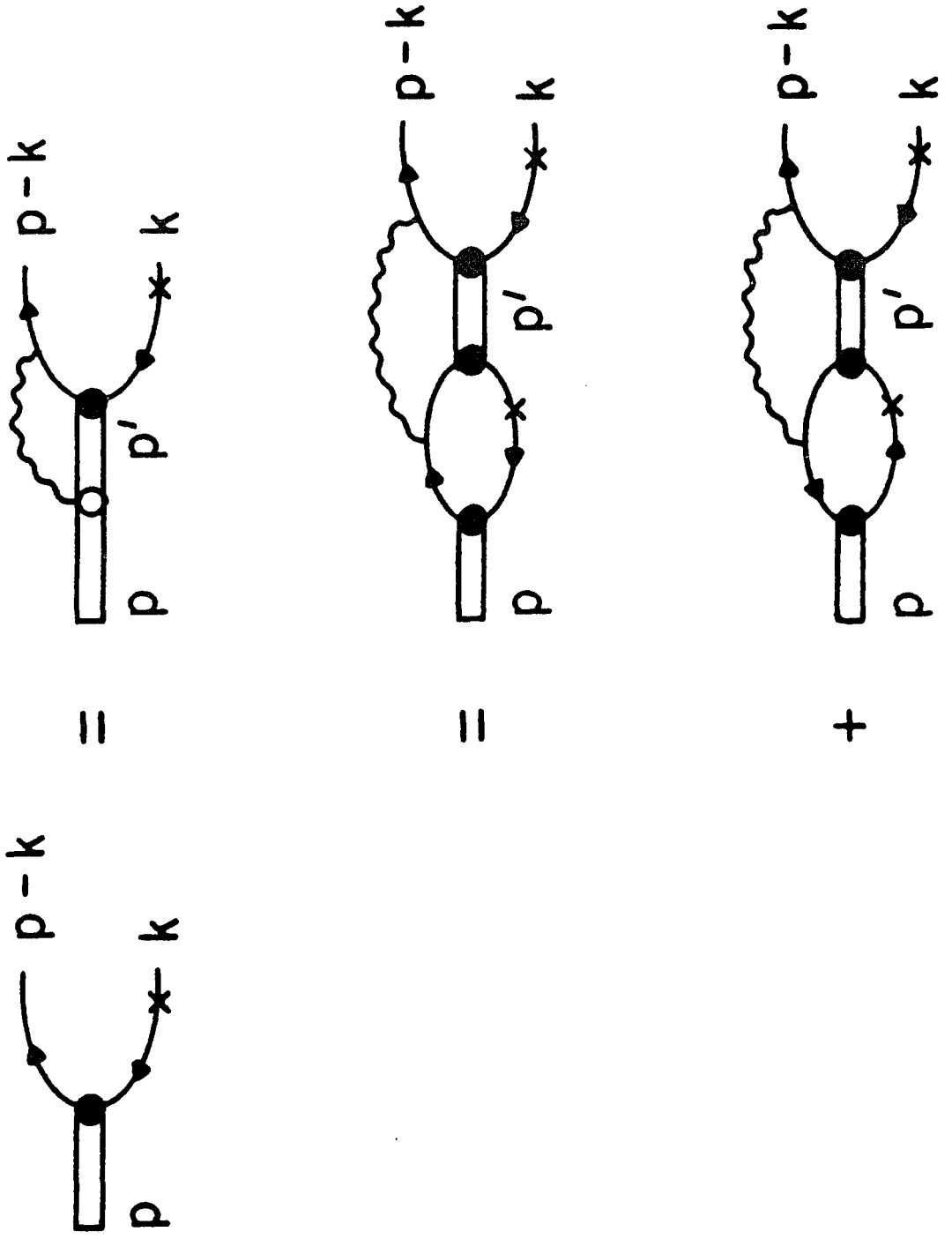

Fig.7

Fig. 8 Same as Fig.7, except that there is one more term - the last term depicted in (a) and (b), representing the "one-gluon-exchange" effect.

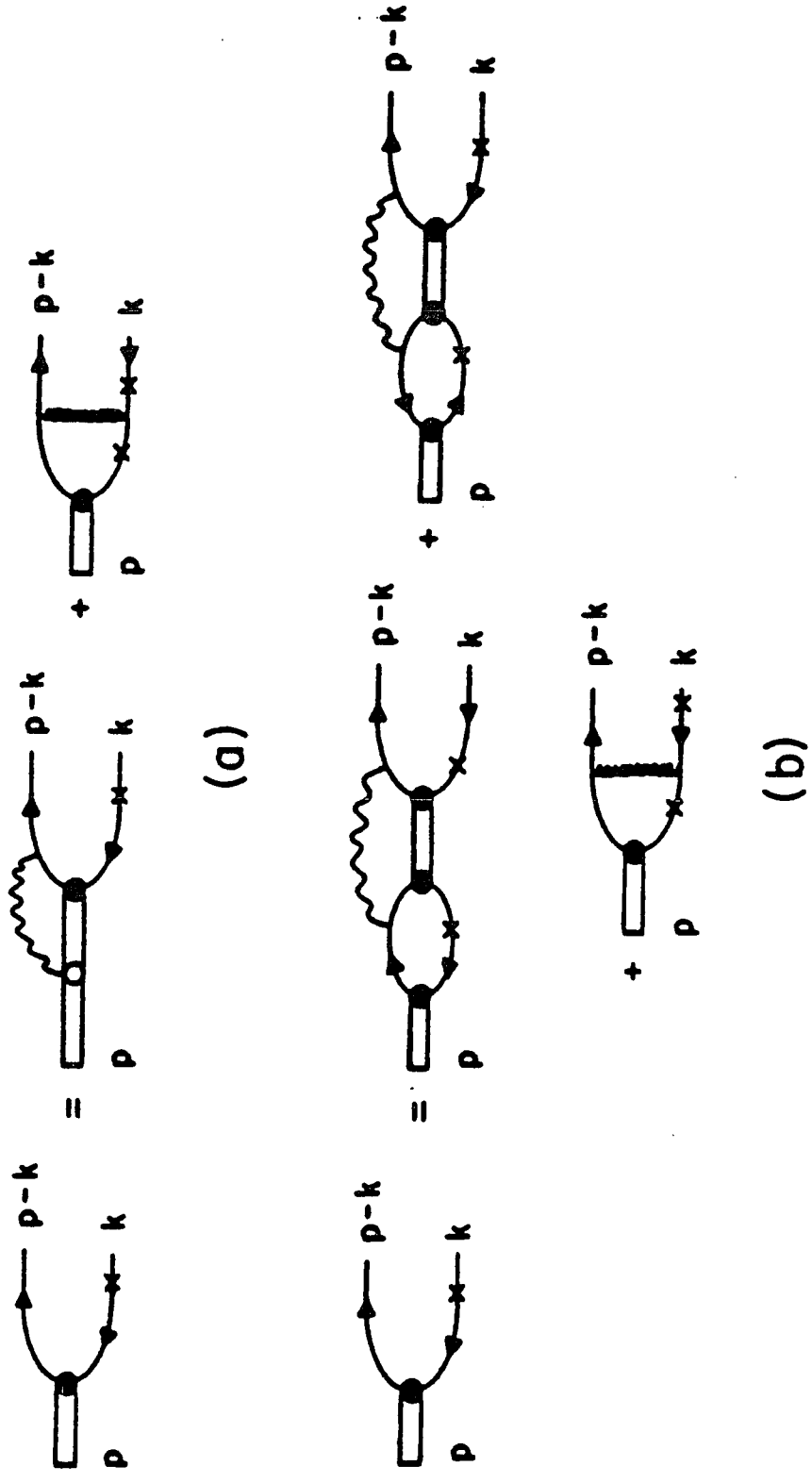

Fig.8

Fig. 9 Diagrammatic representation of the calculation of the leptonic width of a vector meson. The heavy lines denote the leptons and the dashed line denotes a photon. The vertex (black dot) is the same as that described in Fig.7. [The product of the vertex and the propagator of the off-mass-shell quark may be specified in terms of the various amplitudes (or wave functions) defined in Chapter 4.]

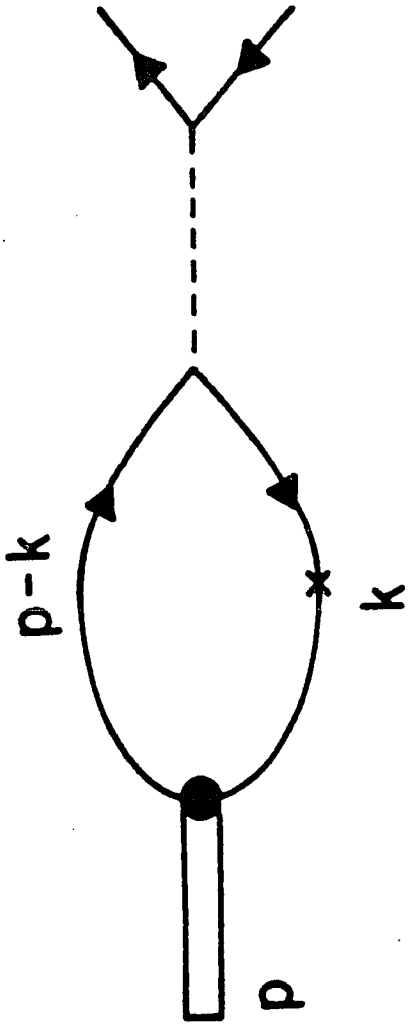

Fig.9

Fig.10 Schematic representation of Eq.(5.3.8).

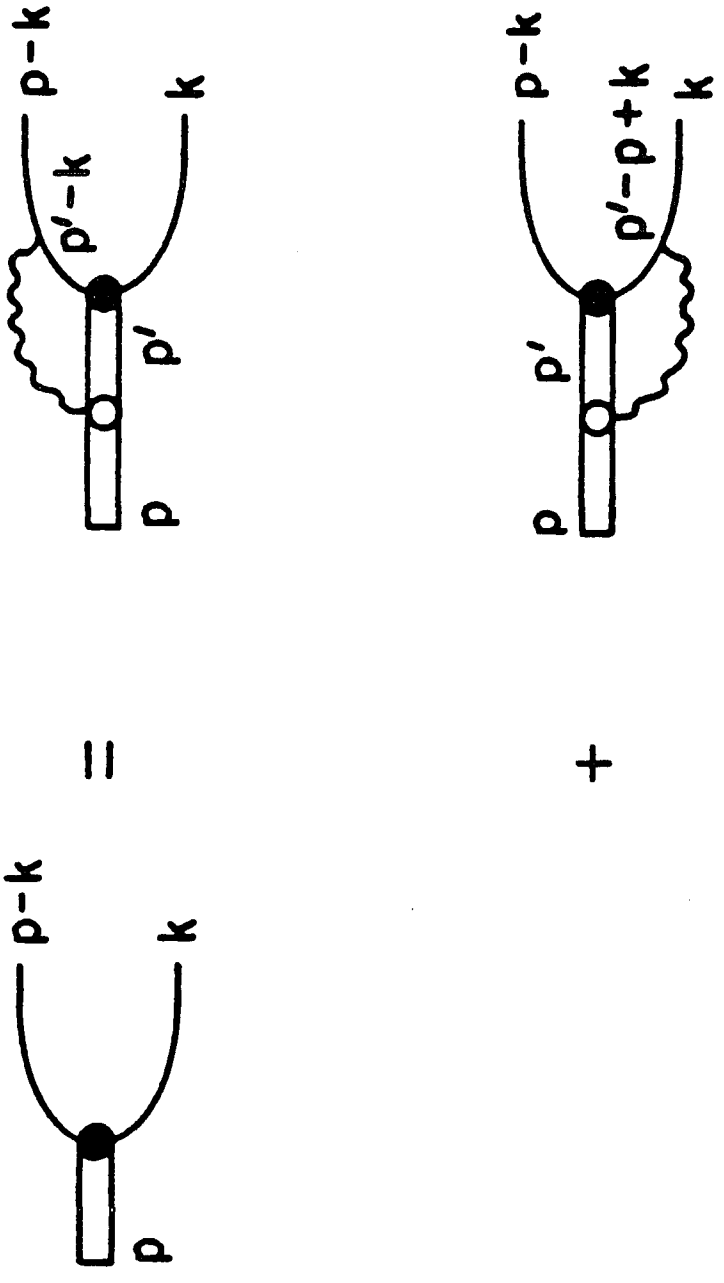

Fig.10

Fig.11 Schematic representation of Eq.(5.3.19). The second part of the figure shows how the kernel, X, may be identified.

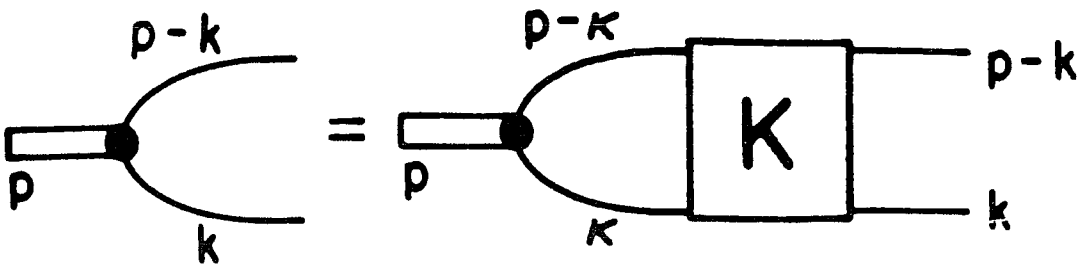

(a)

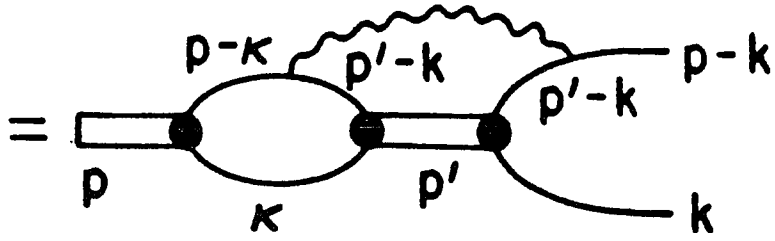

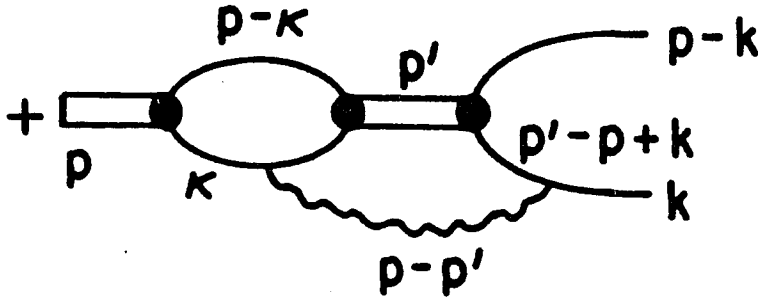

(b)

Fig.11

Fig.12 Comparison of S-wave spectrum of charmonium, obtained in various theoretical models, with the experimental data. The numbers in brackets refer to theoretical calculations listed in the references. The dashed line represents the centers-of-gravity of η_c and J/ψ and of η_c' and ψ'.

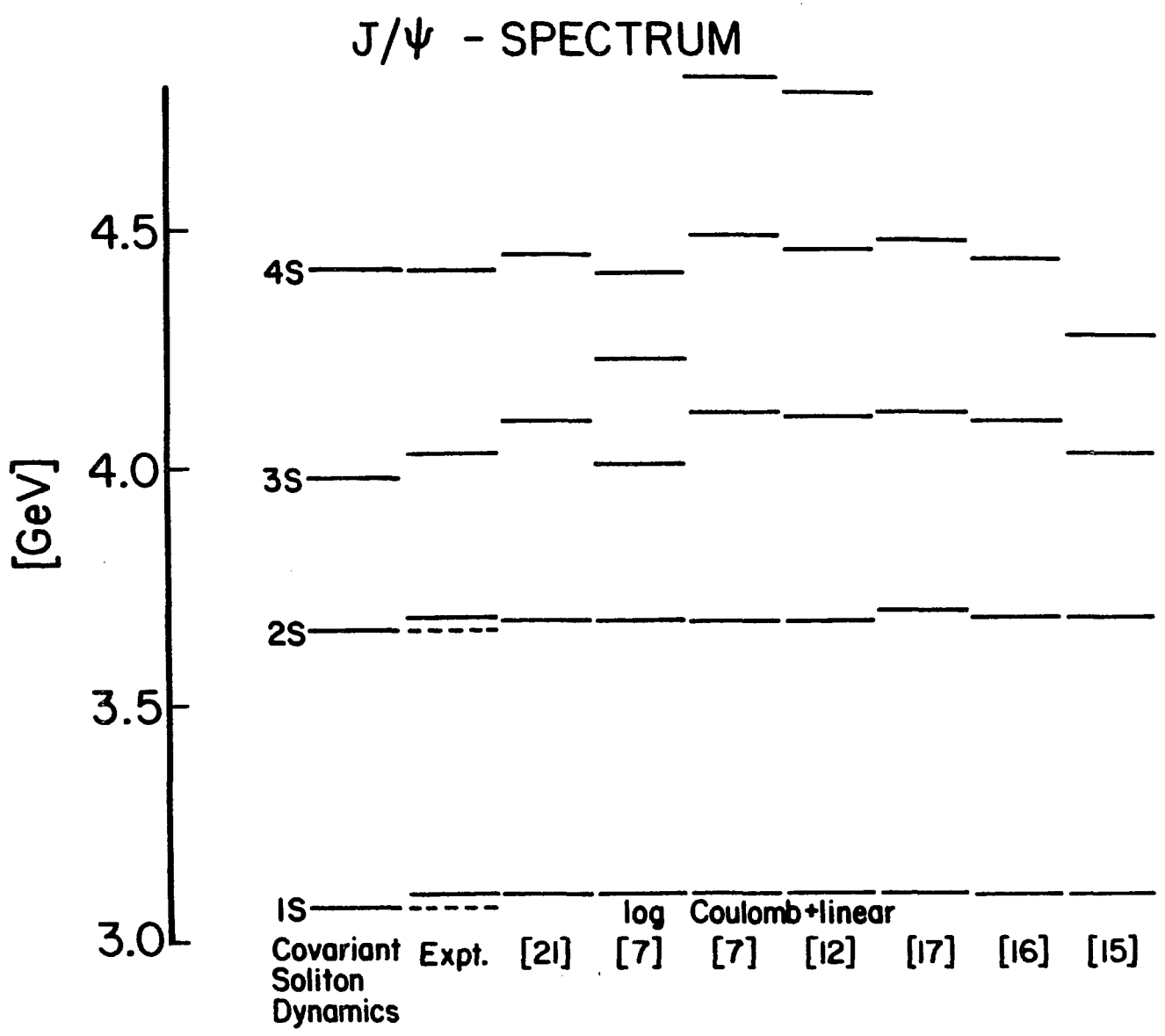
J/ψ - SPECTRUM
4.5
4.0
3.5
3.0
[GeV]
4S
3S
2S
1S
log Coulomb+linear
Covariant Soliton Dynamics
Expt.
[21]
[7]
[7]
[12]
[17]
[16]
[15]

Fig. 12

Fig.13 Similar comparison for the upsilon system. [See Fig.12.]

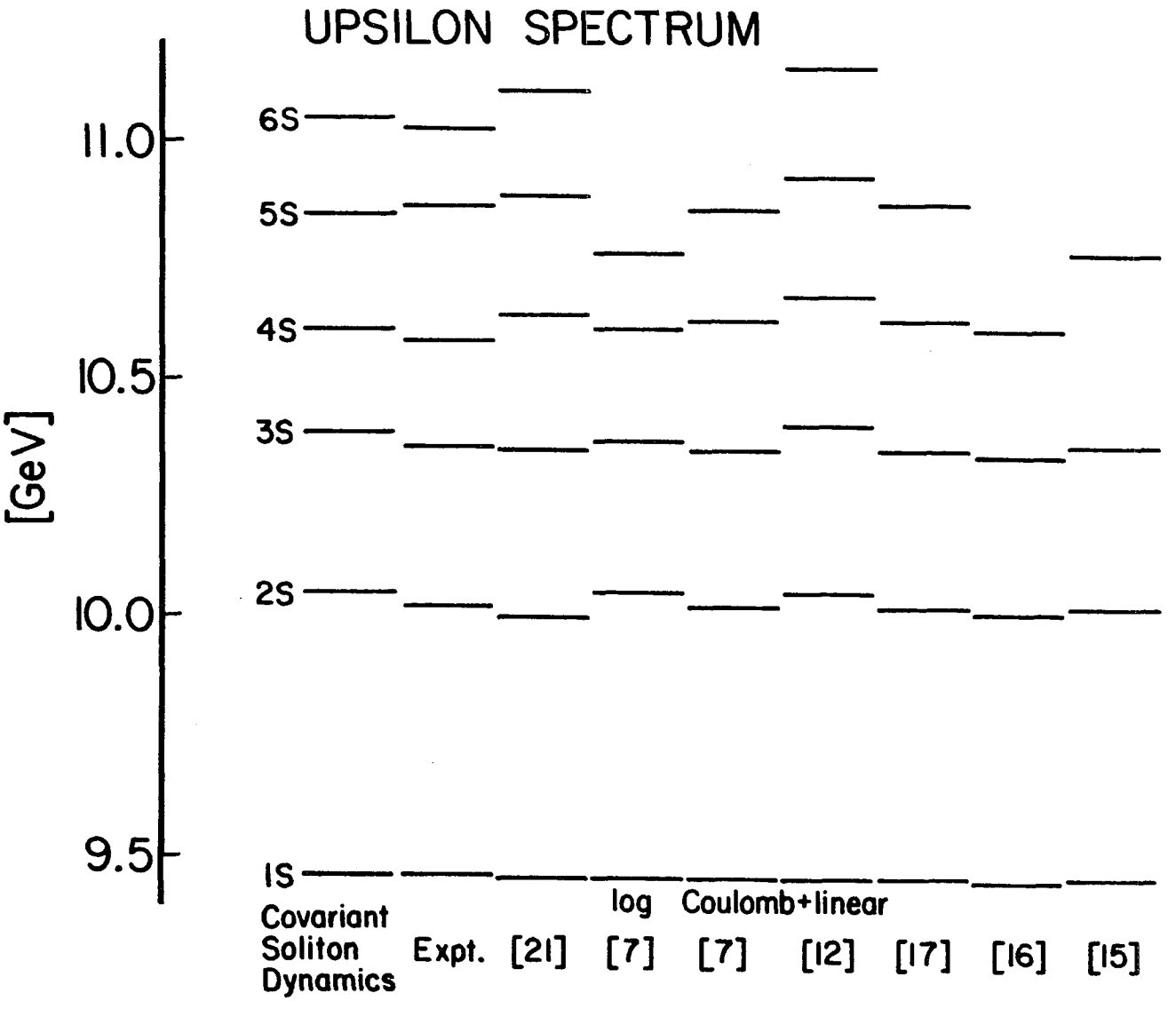
UPSILON SPECTRUM
[GeV]
11.0
10.5
10.0
9.5
6S
5S
4S
3S
2S
1S
log
Coulomb+linear
Covariant
Soliton
Dynamics
Expt.
[21]
[7]
[7]
[12]
[17]
[16]
[15]

Fig.13

Fig.14 (a) The large and small components of the 1S–4S states of charmonium, calculated without the "one-gluon-exchange" effect.

(b) The large and small components of the 1S–4S states of charmonium, calculated with the "one-gluon-exchange" effect included.

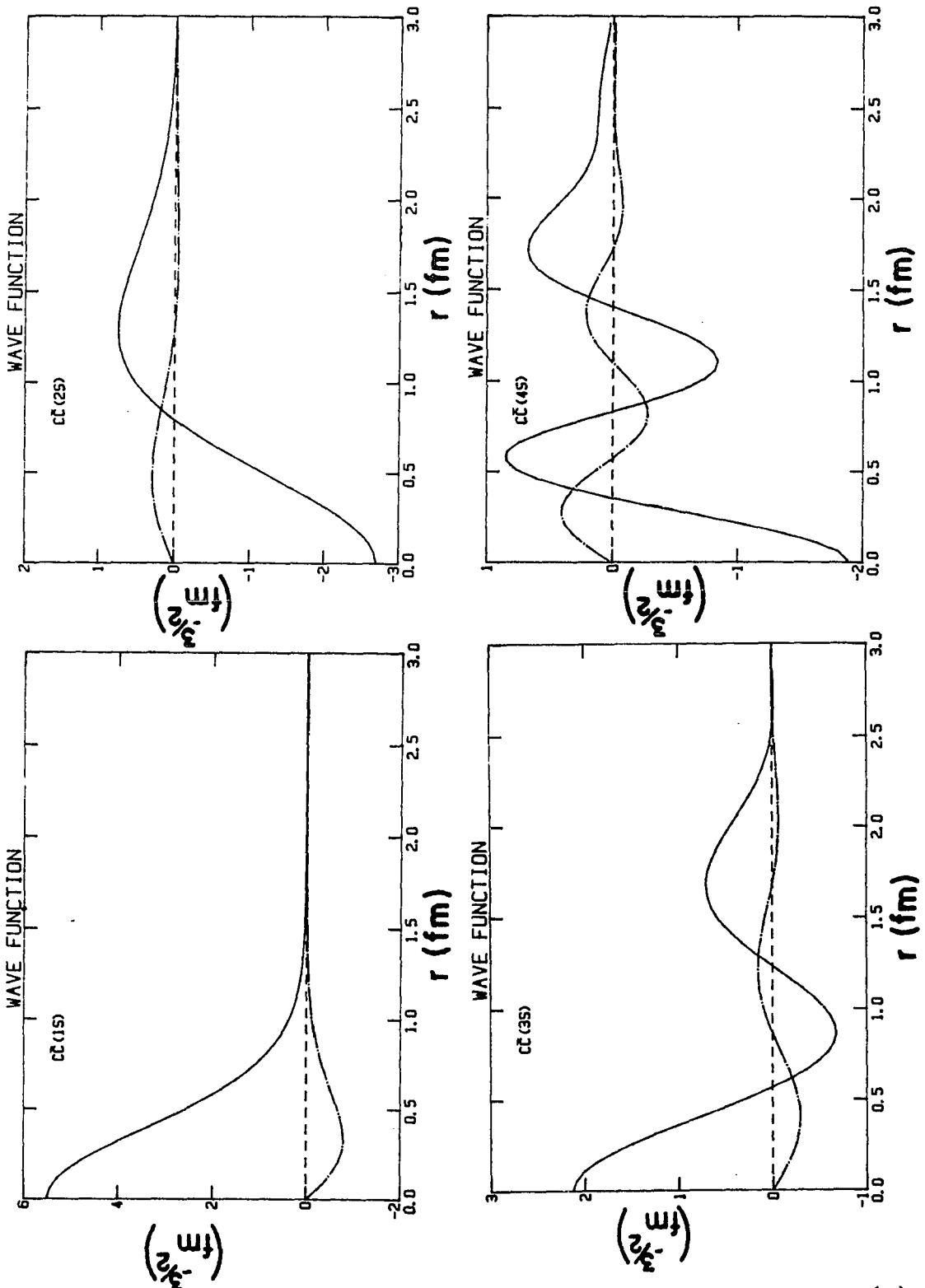

Fig.14-(a)

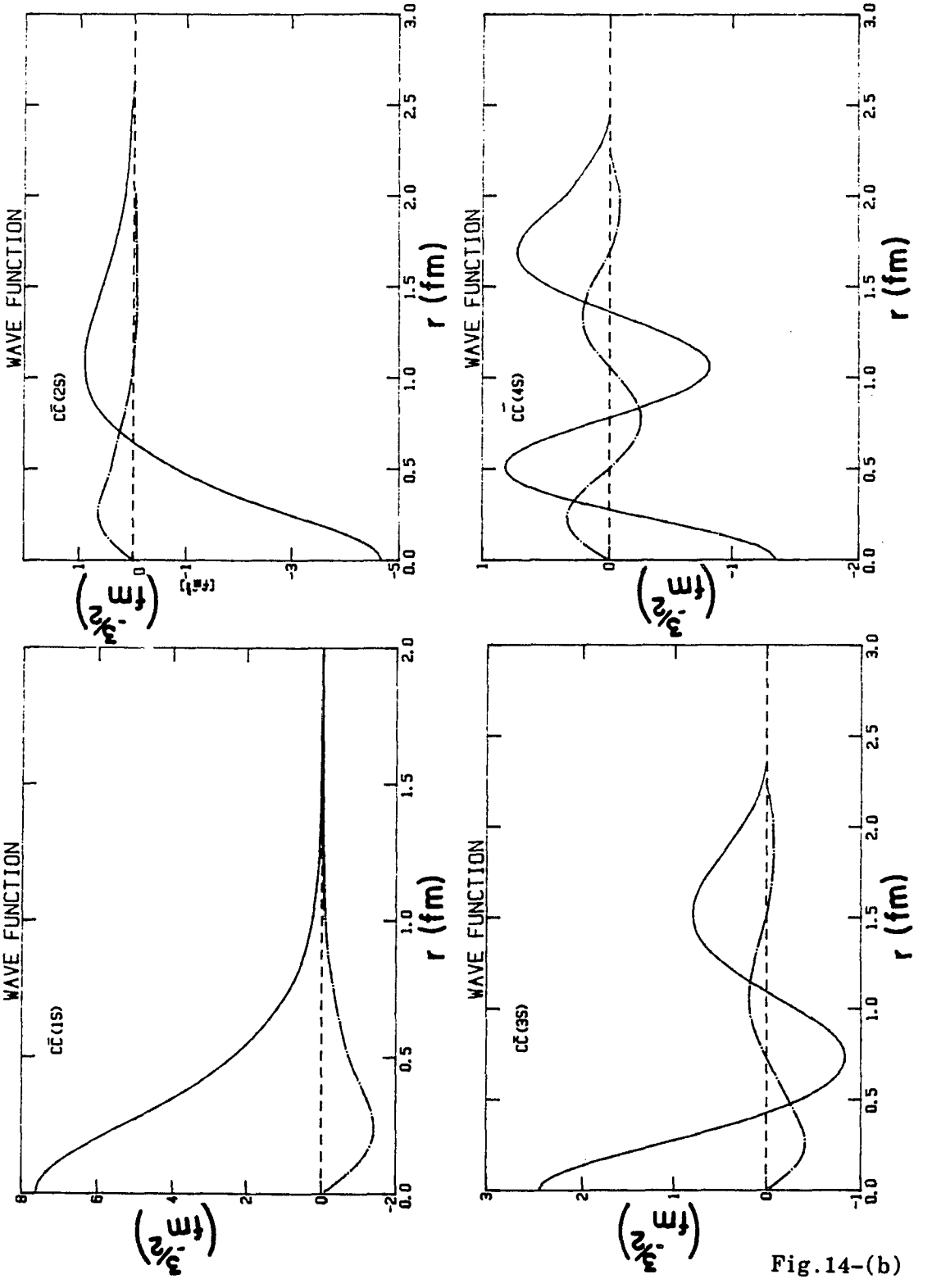

Fig.14-(b)

Fig.15 (a) The large and small components of the 1S–6S states of the upsilon system, calculated without the "one-gluon-exchange" effect.

(b) The large and small components of the 1S–6S states of the upsilon system, calculated with the "one-gluon-exchange" effect included.

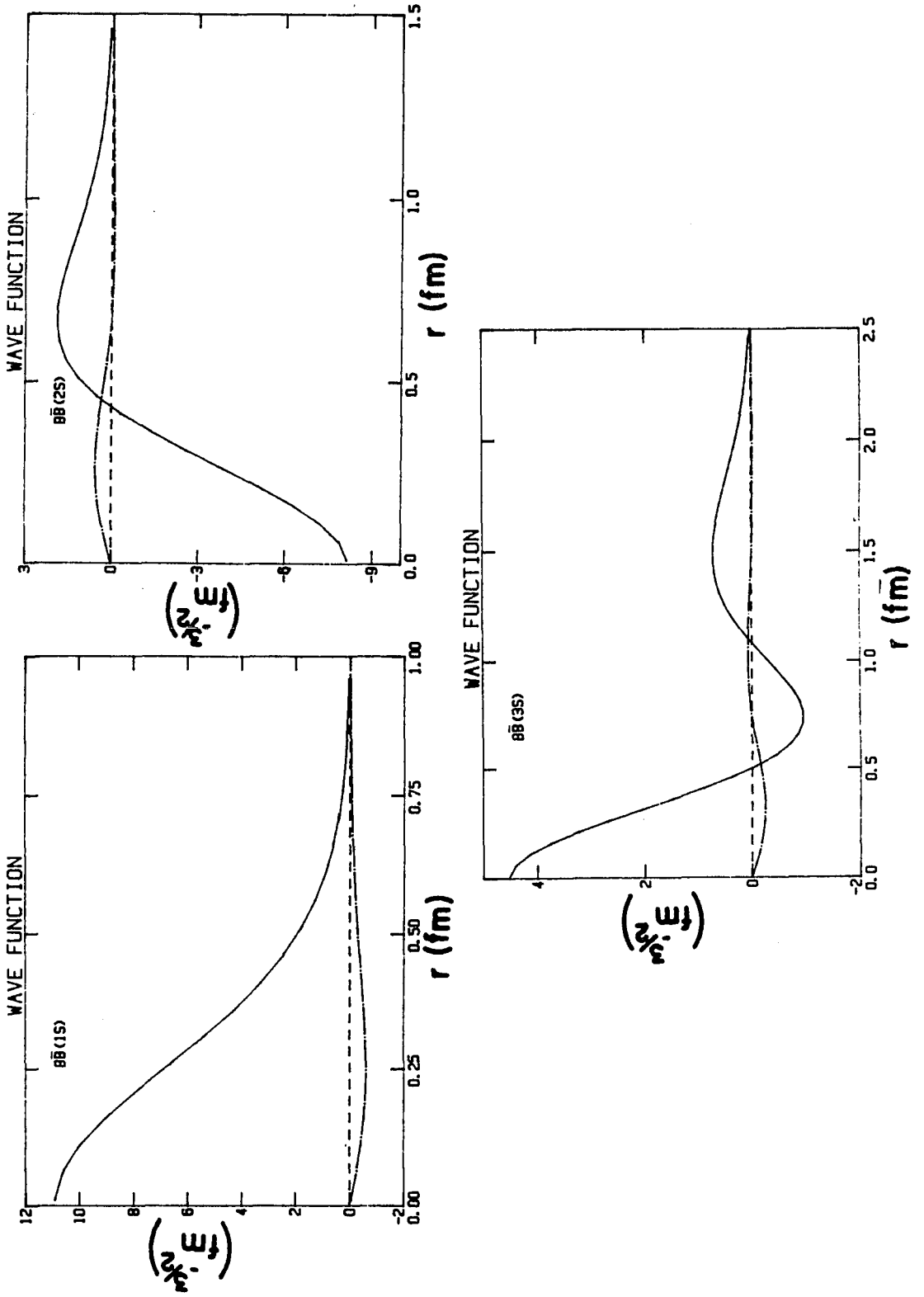
WAVE FUNCTION
$b\bar{b}$(1S)
r (fm)
WAVE FUNCTION
$b\bar{b}$(2S)
r (fm)
WAVE FUNCTION
$b\bar{b}$(3S)
r (fm)

Fig.15-(a)

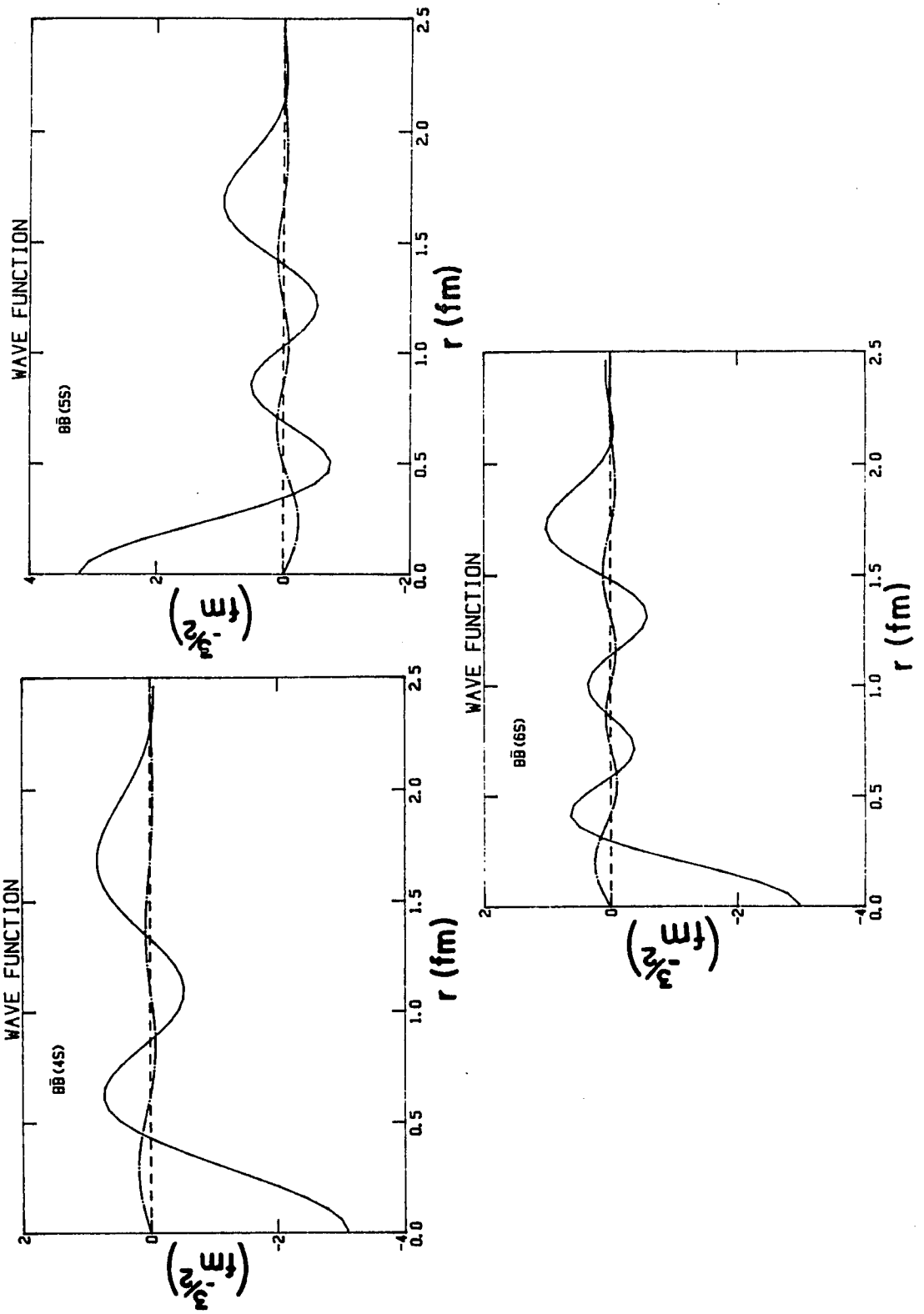

Fig.15-(a)
(continued)

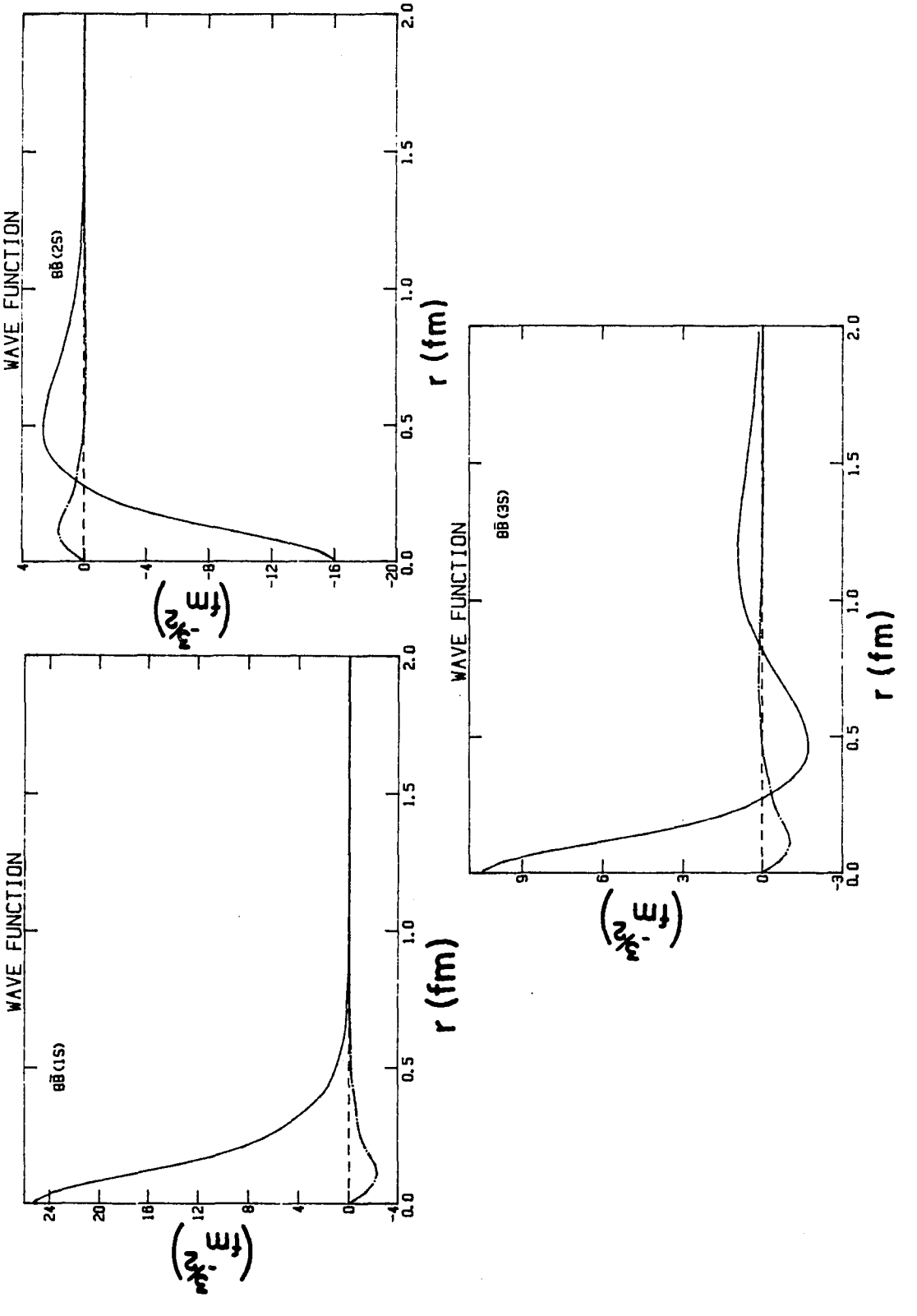
WAVE FUNCTION
bb̄(1S)
WAVE FUNCTION
bb̄(2S)
WAVE FUNCTION
bb̄(3S)
r (fm)
r (fm)
r (fm)

Fig.15-(b)

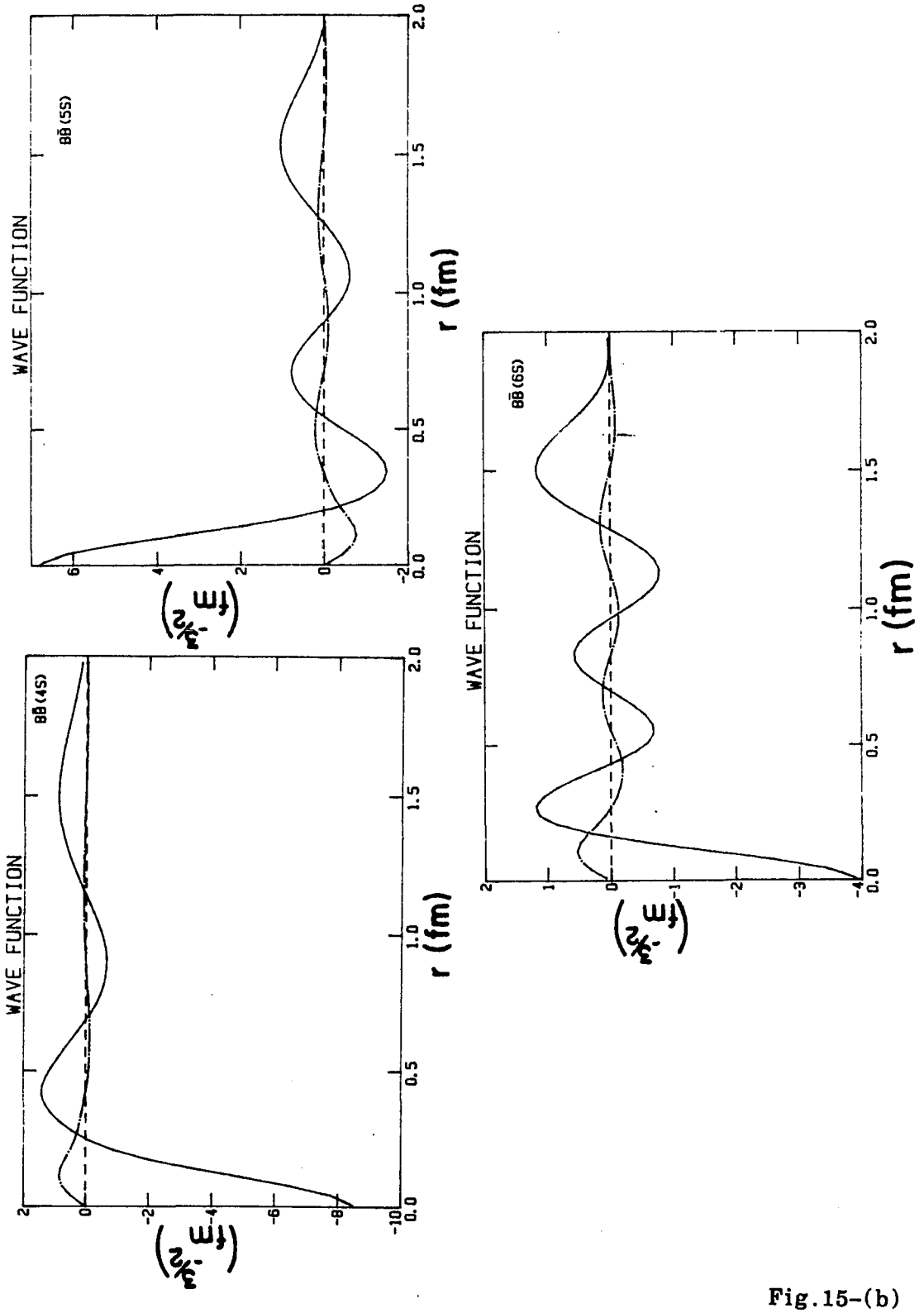

Fig.15-(b)
(continued)

Fig.16 Comparison of our wave function (solid line) with that of a lattice calculation (dashed line)[Sa] for ρ, φ, and J/ψ mesons.

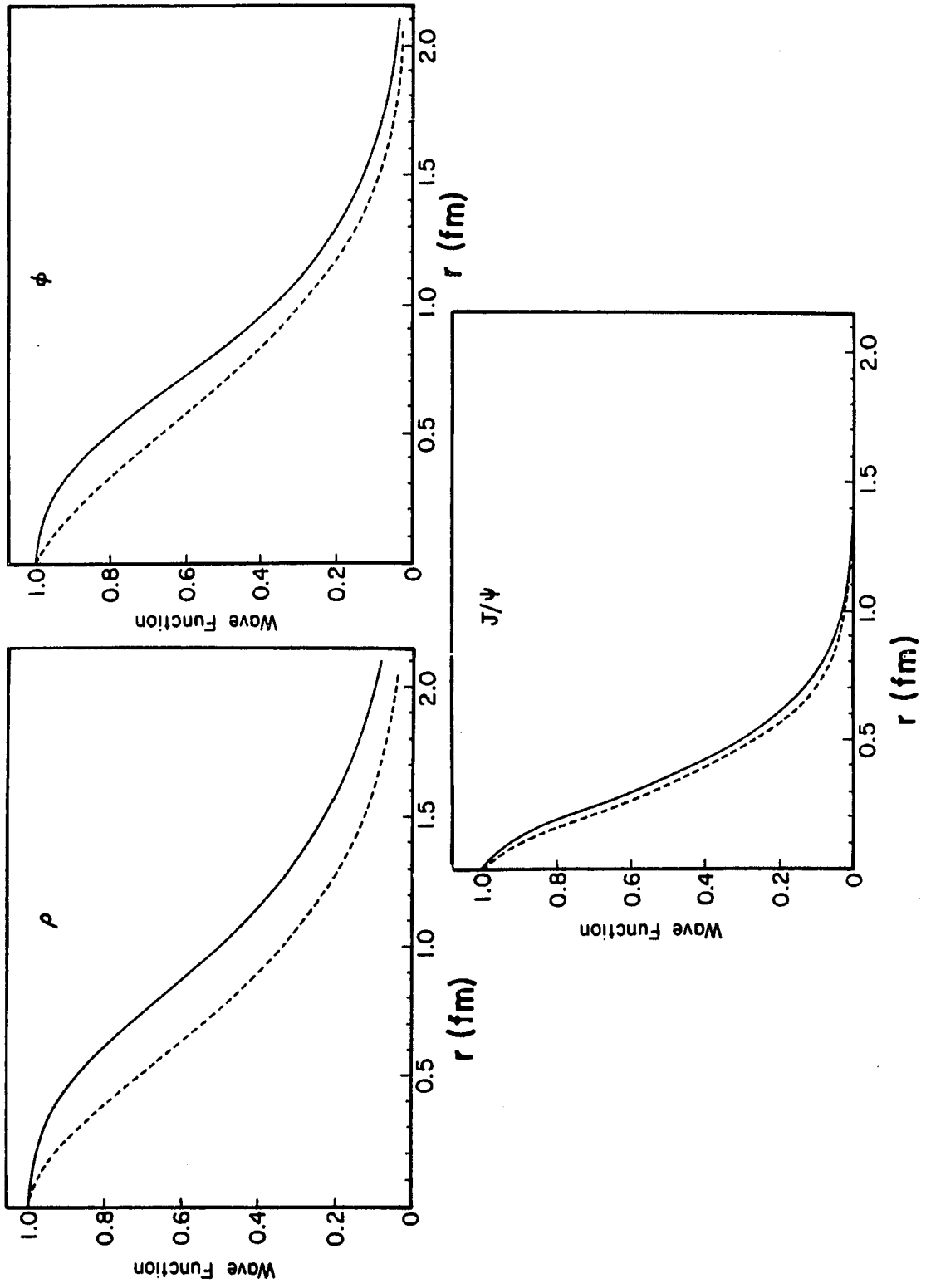

Fig.16

REFERENCES

1. L.S. Celenza, V.K. Mishra, C.M. Shakin and K.F. Liu, Phys. Rev. Lett. 57, 55(1986).

2. S. Samuel and K.J.M. Moriarty, preprint(1986).

3. L.J. Reinders, H. Rubinstein and S. Yazaki, Phys. Rep. 127, 1(1985).

4. M.A. Shifman, Ann. Rev. Nucl. Part. Sci. 33, 199(1983).

5. F.J. Gilman, preprint -SLAC -PUB- 4253(1987).

6. D.B. Lichtenberg, Indiana Univ. preprint- 40048-17-N7(1987).

7. C. Quigg and J.L. Rosner, Phys. Rep. 56, 167(1979); Fermilab-Conf-85/126-T.

8. R.H. Schindler, preprint -SLAC-PUB-4248(1987).

9. Solitons in Nuclear and Elementary Particle Physics edited by A. Chodos et al., Proceedings of Lewes Workshop(1984) - (World Scientific, Singapore, 1985).

10. Solitons and Particles edited by C. Rebbi and G. Soliani (World Scientific, Singapore, 1984).

11. Chiral Solitons edited by K.F. Liu (World Scientific, Singapore, 1987).

12. E. Eichten et al., Phys. Rev. D17, 3090(1978); ibid. Phys. Rev. D21, 203(1980).

13. K.G. Wilson, Phys. Rev. D10, 2445(1974).

14. J. Kogut and L. Susskind, Phys. Rev. D11, 395(1975).

15. A. Martin, Phys. Lett. 93B, 338(1980); Phys.Lett. 100B, 511(1981).

16. J.L. Richardson, Phys. Lett. 81B, 272(1979).

17. W. Buchmüller and S.H.H. Tye, Phys. Rev. D24, 132(1981).

18. E. Eichten, Fermi National Accelerator Lab. preprint (1983).

19. S.N. Gupta et al., Phys. Rev. D26, 3305(1982).

20. R. McClary and N. Byers, Phys. Rev. D28, 1692(1983).

21. S. Godfrey and N. Isgur, Phys. Rev. D32, 189(1985).

22. K. Konigsman, preprint (1986).

23. M. Rho and G.E. Brown, Phys. Lett. 82B, 177(1979).

24. D. Lurie, Particles and Fields, (Interscience Publishers, New York, 1968).

25. L.S. Celenza, Chueng-Ryong Ji and C.M. Shakin, Phys. Rev. D36, 2506(1987).

26. T.D. Lee, Particle Physics and Introduction to Field Theory, (Harwood Academic Publishers, 1981).

27. R. Rajaraman, Solitons and Instantons, (North Holland, Amsterdam, 1984).

28. L. Wilets, page 362 in reference [11].

29. L.S. Celenza and C.M. Shakin, Relativistic Nuclear Physics: Theories of Structure and Scattering, (World Scientific, Singapore, 1986).

30. L.S. Celenza and C.M. Shakin, Phys. Rev. C28, 2042(1983); L.S. Celenza, A. Rosenthal and C.M. Shakin, Phys. Rev. C31, 212(1985); Phys. Rev. C31, 232(1985); Phys. Rev. Lett. 53, 892(1984).

31. C.M. Shakin, Brooklyn College Report: BCCNT 87/031/164 and the references therein. (Invited talk presented at the Workshop on Electronuclear Physics with Internal Targets, SLAC-1987.)

32. "Effective Lagrangian Methods in QCD" by L.S. Celenza and C.M. Shakin in [11]; L.S. Celenza and C.M. Shakin, Phys. Rev. D34, 1591(1986).

33. A.L. Fetter and J.D. Walecka, Quantum Theory of Many-Particle Systems, (McGraw-Hill, New York, 1971).

34. L.S. Celenza, Chueng-Ryong Ji and C.M. Shakin, Phys. Rev. D36, 895(1987).

35. R. Gupta et al., Phys. Rev. D36, 2813(1987).

36. R. Manka, preprint, TPJU-15/86; Ann. of Phys. 171, 1(1986).

37. J.E. Mandula and M. Ogilvie, Phys. Lett. 185, 127(1987).

38. V.M. Bannur, S.A. Barve, L.S. Celenza, V.K. Mishra and C.M. Shakin, Phys. Rev. D34, 3530(1986).

39. J. Sakurai, Advanced Quantum Mechanics, (Addison-Wesley, New York, 1967).

40. R. Casalbuoni, S. De Curtis, D. Dominici and R. Gotto, Phys. Lett. 140B, 357(1984); ibid. 150B, 295(1985).

41. T. Hatsuda and T. Kunihiro, Phys. Rev. Lett. 55, 158(1985).

42. C.D. Roberts and R.T. Cahill, Flinders Univ. of S. Australia preprint: FIAS-R- 164(1986); Aust. J. Phys. 40, 499(1987); Phys. Rev. D32, 2419(1985); J. Praschifka, C.D. Roberts and R.T. Cahill, Phys. Rev. D36, 209(1987); C.D. Roberts, R.T. Cahill and J. Praschifka, Flinders Univ. of S. Australia preprint: FPPG-R- 3-87(1987) - unpublished.

43. R. Fukuda and T. Kugo, Nucl. Phys. B117, 250(1976).

44. V.M. Bannur, L.S. Celenza and C.M. Shakin, Brooklyn College Report: BCCNT 87/101/170 - submitted to Phys. Rev. Lett..

45. V.M. Bannur, L.S. Celenza, C.M. Shakin and Hui-Wen Wang, Brooklyn College Report: BCCNT 87/102/171 - submitted to Phys. Rev. D.

46. L.S. Celenza, Chueng-Ryong Ji and C.M. Shakin, Phys. Rev. C37, 265(1988).

47. W. Weise, in Quarks and Nuclei, edited by W. Weise (World Scientific, Singapore, 1985).

48. C. DeTar and J. Kogut, Phys. Rev. Lett. 59, 399(1987).

49. V.M. Bannur, L.S. Celenza and C.M. Shakin, Brooklyn College Report: BCCNT 87/071/168 - submitted to Phys. Rev. D.

50. R.B. Thayyullathil, Ph.D. Thesis, City University of New York, 1985.

51. S.A. Barve, Ph.D. Thesis, City University of New York, 1987.

52. L.S. Celenza, C.M. Shakin and R.B. Thayyullathil, Phys. Rev. D33, 198(1986).

53. L.S. Celenza, V.K. Mishra and C.M. Shakin, Ann. of Phys. 178, 248(1987).

54. R. Van Royen and V.F. Weisskopf, Nuovo Cimento 50, 617(1967).

55. V.M. Bannur, S.A. Barve, L.S. Celenza and C.M. Shakin, Brooklyn College Report: BCCNT 86/121/161 (unpublished).

56. M.C. Birse and M.K. Banerjee, Phys. Lett. 136B, 284(1984); Phys. Rev. D31, 118(1985).

57. V.M. Bannur, L.S. Celenza and C.M. Shakin, Brooklyn College Report: BCCNT 87/091/169 - submitted to Phys. Rev. D.

58. L.S. Celenza, C.M. Shakin and Hui-Wen Wang, Brooklyn College Report: BCCNT 87/111/172(1987) -submitted to Phys. Rev. Lett..

59. G.C. Wick, Phys. Rev. 96, 1124(1954); R.E. Cutkosky, Phys. Rev. 96, 1135(1954).

60. C. Itzykson and J.B. Zuber, Quantum Field Theory, (McGraw-Hill, New York, 1980).

61. Chueng-Ryong Ji, Phys. Lett. 167B, 16(1986).

62. J.D. Bjorken and S.D. Drell, Relativistic Quantum Fields, (McGraw-Hill, New York, 1965).

63. S.U. Chung, CERN preprint (1971) - unpublished.